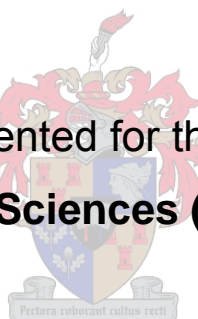


**SYNTHESIS AND CHARACTERIZATION OF  
URETHANE-ACRYLATE  
GRAFT COPOLYMERS**

**By**

**Abubaker Alshuiref**

Thesis presented for the degree of  
**Master of Natural Sciences (Polymer Science)**



**at the**

**University of Stellenbosch**

**Promoter: Prof. R.D. Sanderson**

**Mentor : Dr. S. Seboa**

**Stellenbosch**

**December 2006**

## DECLARATION

**I, the undersigned, hereby declare that the work contained in this thesis is my own original work and has not previously in its entirety or in part been submitted at any university for a degree.**

**Signature:.....**

**Date:.....**

## ABSTRACT

Polyurethanes (PUs) are finding increasing application and use in many industries due to their advantageous properties, such as a wide range of flexibility combined with toughness, high chemical resistance, excellent weatherability, and very low temperature cure. PUs do however have some disadvantages, for instance, PU is considered an expensive polymer, especially when considered for solvent based adhesives. A motivation for this study was to consider a largely unstudied area of PU chemistry by combining PUs with polyacrylates. Polyacrylates are well known adhesives and can carry specific functionality, but have the disadvantage that their flexible backbones impart limited thermal stability and mechanical strength. In this study PU was incorporated into acrylates in an effort to obtain acrylate-g-urethanes with good properties. The mode of incorporation chosen was urethane macromonomers (UMs), a hardly mentioned substance in literature, yet one deserving investigation.

UMs having different urethane chain lengths (X) were synthesized by the polyaddition polymerization of toluene diisocyanate (TDI) and ethylene glycol (EG) by the pre-polymer method, which was terminated by 2-hydroxy ethyl methacrylate (HEMA) and isopropanol. The UMs were characterized by Fourier-transform infrared spectroscopy (FTIR), proton NMR ( $^1\text{H}$  NMR), carbon NMR ( $^{13}\text{C}$  NMR), gel permeation chromatography (GPC), thermogravimetric analysis (TGA) and dynamic mechanical analysis (DMA).

Various percentages of the respective UMs (0-40 wt % according to acrylate monomers) were then incorporated into methyl methacrylate (MMA) and into normal butyl methacrylate (n-BMA) backbones via solution free radical copolymerization. The resulting methyl methacrylate-urethane graft copolymers (PMMA-g-urethane) and normal butyl methacrylate-urethane graft copolymers (n-PBMA-g-urethane) were characterized by GPC,  $^1\text{H}$  NMR and  $^{13}\text{C}$  NMR, FTIR, TGA, and DMA. Phase separation between the urethane segment and acrylate segment in the yield of graft copolymerization products was investigated by DMA and transmission electron microscopy (TEM).

As the concentration of the UMs in the free radical copolymerization feed increased, lower yields of both graft copolymers PMMA-g-urethane and n-PBMA-g-urethane were

observed and more UM was incorporated into the PMMA and n-PBMA backbones. It also was found that the thermal stability of the PMMA-g-urethane and n-PBMA-g-urethane copolymers increased with increasing UM concentration.

DMA results showed that in most graft copolymer products the two respective component parts of PMMA-g-urethane or n-PBMA-g-urethane were completely compatible as only one  $T_g$  was observed. Two glass transitions, at temperatures of 22.0 and 76.0 °C, corresponding to the n-PBMA and urethane moieties, were observed when the chain length of the UMs was increased from X=4 to X=32 [the amount of this UM used in the copolymerization feed was increased to 40%, and microphase separation was indicated].

## Opsomming

Poli-uretane (PUs) bevind 'n toename in aplikasies en gebruike in baie industrieë as gevolg van hul goeie inherente eienskappe, soos 'n wye reeks van buigbaarheid wat gekoppel is aan sterkheid, hoë chemiese weerstand, uitstekende weerbestandheid, en 'n lae kruissings temperatuur. PUs het ook 'n paar negatiewe eienskappe, byvoorbeeld, poli-uretane word beskou as 'n baie duur polimeer, veral in konsederasie vir die gebruik in oplosmiddel gebaseerde gomme. 'n Motivering vir hierdie studie was om 'n groot ongestudeerde area van PU chemie in ag te neem deur PUs met poli-akriëlate te kombineer. Poli-akriëlate is wel bekende gomme met spesifieke funksionaliteite, maar het die negatiewe eienskap waarin hul buigbare ruggraat beperkte termiese stabiliteit en meganiese sterkte meebring. PU was in hierdie studie in akriëlate geïnkorporeer in 'n poging om akriëlaat-g-uretaan ko-polimere met goeie eienskappe te verkry. Die tipe van inkorporasie wat gekies was is die van uretaan makro-monomere (UMs), 'n min bekende skrifstuk in die literatuur, hoewel een wat van meer opvolging toekomstig is.

UMs met verkillende uretaan kettinglengtes ( $X$ ) was gesintetiseer deur die poli-addisie polimerisasie van toluendiisosiannaat (TDI) en etileenglikol (EG), wat met 2-hidroksie etiel metakrilaat (HEMA) en isopropanol getermineer was. Die UMs was deur middel van Fourier-transformasie infrarooi (FTIR) spektroskopie, kern magnetiese resonansie (KMR) spektroskopie, gas-fase permeasie chromatografie (GPC), termogravimetriese analise (TGA) en dinamiese meganiese analise (DMA) gekarakteriseer.

Verskeie persentasies van die gesintetiseerde UMs (0-40 wt%) was met MMA en n-BMA geko-polimeriseer. Hierdie gevormde ko-polimere, naamlik PMMA-g-uretaan en n-PBMA-g-uretaan, was ook deur middel van GPC, KMR, FTIR, TGA en DMA gekarakteriseer. Fase-seperasie tussen die uretaan en akrilaat komponente was deur middel van DMA en Transmissie elektron mikroskopie (TEM) gekarakteriseer.

Daar was bevind dat die ko-polimeer opbrengste afneem met 'n toename in massa UMs wat geïnkorporeer was tydens ko-polimerisasie, asook met 'n toename in die kettinglengte van die UMs. Daar was ook bevind dat die termiese stabiliteit van die ko-polimere toeneem met 'n toename in UM inkorporasie.

DMA resultate het bevestig dat die meeste ko-polimeer produkte net een Tg wys, wat daarop aangedui het dat die twee akrilaat en uretaan komponente heeltamaal mengbaar met mekaar is. Daar was egter twee Tg's in die n-PBMA-g-uretaan ko-polimeer teenwoordig toe die UMs met UM kettinglengte van  $X=32$  se konsentrasie tydens ko-polimerisasie na 40% verhoog was. Die twee Tg's van 22.0°C en 76.0°C wat ooreenstem van die n-PBMA en uretaan komponente, was wel 'n indikatie van mikrofase seperasie.

## **Acknowledgements**

I would like to thank the following people for contributing to this study.

**Prof. R.D. Sanderson**, my promoter, for his fruitful advice, guidance and encouragement throughout this study.

**Dr. S. Seboa**, for his advice and guidance throughout this study.

**Dr. Margie Hurndall**, for taking the time to edit my thesis.

**Centre of Macromolecules and Materials Science (Libya)** for the financial support of this research.

**Plascon Research Centre**, for the use of their analytical laboratory.

All the staff and students at Polymer Science for their assistance and encouragement.

**Dedicated to my wife and my parents**

## TABLE OF CONTENTS

### CHAPTER 1: INTRODUCTION

1.1. INTRODUCTION	1
1.2. OBJECTIVES	3
1.3. REFERENCES	4

### CHAPTER 2

#### HISTORICAL AND THEORETICAL BACKGROUND

2.1. INTRODUCTION	5
2.3 POLYURETHANE APPLICATIONS	6
2.3.1 POLYURETHANE THERMOPLASTIC ELASTOMERS	6
2.3.2 POLYURETHANE COATINGS	8
2.3.3 POLYURETHANE ADHESIVES	9
2.3.4 POLYURETHANE FOAMS	9
2.4 METHODS OF PREPARATION OF POLYURETHANES	9
2.4.1 THE SOLUTION PROCESS	9
2.4.2 THE MELT-DISPERSION PROCESS	10
2.4.3 THE PRE-POLYMER PROCESS	11
2.4.4 KETIMINE AND KETAZINE PROCESS	11
2.5 RAW MATERIALS	12
2.5.1 ISOCYANATES	12
2.5.1.1 Introduction	12
2.5.1.2 Reactivity of the isocyanate group	12
2.5.1.3 Aromatic isocyanates	13
2.5.1.4 Aliphatic isocyanates	14
2.5.1.5 General reactions of isocyanates	14
i) Reaction with alcohol	15
iii) Reaction with water	16
iv) Reaction with carboxylic compounds	16
i) Dimerization	17
ii) Trimerization	18

2.5.2 POLYOLS	18
<b>2.6. POLYACRYLATES</b>	<b>19</b>
<b>2.6.1 INTRODUCTION</b>	<b>19</b>
2.6.2 PREPARATION OF POLYACRYLATES	20
2.6.2.1 Free radical polymerization	20
2.6.3 Polymerization techniques	22
2.6.3.1 Solution polymerization	22
2.6.3.2 Emulsion polymerization	22
2.6.4 APPLICATIONS OF POLYMETHACRYLATES	23
<b>2.7 URETHANE ACRYLATE OLIGOMERS</b>	<b>23</b>
<b>2.8 GRAFT COPOLYMERIZATION</b>	<b>24</b>
2.8.1 SYNTHETIC ROUTES TO GRAFT POLYMERS	26
2.8.1.1 "Grafting from"	26
2.8.1.2 "Grafting onto"	27
2.8.1.3 "Grafting through"	27
<b>2.9 MACROMONOMERS</b>	<b>28</b>
2.9.1 INTRODUCTION	28
2.9.2 SYNTHESSES OF MACROMONOMERS	29
2.9.2.1 The initiation method	29
2.9.2.2 The termination method	30
2.9.2.3 Functional end-group transformation	30
2.9.2.4 Macromonomer by polyaddition polymerization	30
2.9.3 FREE RADICAL POLYMERIZATION OF MACROMONOMERS	31
<b>2.10 GRAFT AND BLOCK COPOLYMERIZATION OF POLYURETHANE</b>	<b>31</b>
<b>2.11 REFERENCES</b>	<b>32</b>
<b>CHAPTER 3</b>	
<b>EXPERIMENTAL WORK</b>	
<b>3.1 INTRODUCTION</b>	<b>37</b>
<b>3.2 SYNTHESIS OF URETHANE MACROMONOMERS</b>	<b>37</b>
3.2.1 RAW MATERIALS	37
3.2.2 EXPERIMENTAL SETUP	38
3.2.3 POLYURETHANE MACROMONOMER FORMULATIONS	38
3.2.4 EXPERIMENTAL PROCEDURE	39

3.2.5. REACTION SCHEME OF THE SYNTHESIS OF URETHANE MACROMONOMERS	40
<b>3.3 SYNTHESIS OF ACRYLATE-URETHANE GRAFT COPOLYMERS</b>	<b>41</b>
3.3.1 INTRODUCTION	41
3.3.2 EXPERIMENTAL	41
3.3.2.1 Solvent	41
3.3.2.2 Materials	41
3.3.2.3 Acrylate-urethane copolymer formulations	42
3.3.2.4 Experimental procedure	44
3.3.2.4 Reaction scheme for graft copolymerization	45

## **CHAPTER 4**

### **ANALYTICAL METHODS**

<b>4.1 INTRODUCTION</b>	<b>46</b>
<b>4.2 FOURIER-TRANSFORM INFRARED SPECTROSCOPY (FTIR)</b>	<b>46</b>
<b>4.3 NUCLEAR MAGNETIC RESONANCE SPECTROSCOPY (NMR)</b>	<b>46</b>
4.3.1 PROTON NMR ( $^1\text{H}$ NMR)	46
4.3.2 CARBON NMR ( $^{13}\text{C}$ NMR)	47
<b>4.4 GEL PERMEATION CHROMATOGRAPHY (GPC)</b>	<b>47</b>
4.4.1 INTRODUCTION	47
4.4.2. GEL PERMEATION CHROMATOGRAPHY COUPLED WITH MULTIPLE DETECTORS	47
<b>4.5 DYNAMIC MECHANICAL ANALYSIS (DMA)</b>	<b>48</b>
<b>4.6. DYNAMIC THERMOGRAVIMETRY (TGA)</b>	<b>49</b>
<b>4.7. TRANSMISSION ELECTRON MICROSCOPY (TEM)</b>	<b>49</b>
<b>4.8 REFERENCES</b>	<b>49</b>

## **CHAPTER 5**

### **RESULTS AND DISCUSSION**

<b>5.1. FOURIER-TRANSFORM INFRARED SPECTROSCOPY</b>	<b>51</b>
5.1.1 NCO CONTENT	51
5.1.2 CHARACTERIZATION OF THE URETHANE MACROMONOMERS	51
5.1.3 PMMA AND N-PBMA HOMOPOLYMERS	53

5.1.4 ACRYLATE-G-URETHANE COPOLYMERS	54
5.1.4.1 PMMA-g-urethane copolymers	54
5.1.4.2 n-PBMA-g-urethane copolymers	55
5.1.5 EFFECT OF THE UM CONTENT ON COPOLYMERIZATION	56
<b>5.2. <sup>1</sup>H NMR ANALYSIS</b>	<b>57</b>
5.2.1 <sup>1</sup> H NMR OF THE URETHANE MACROMONOMERS	57
5.2.2 <sup>1</sup> H NMR OF PMMA AND N-PBMA HOMOPOLYMERS	58
5.2.3 <sup>1</sup> H NMR OF ACRYLATE-URETHANE GRAFT COPOLYMERS	59
5.2.3.1 PMMA-g-urethane copolymers	59
5.2.3.2. n-PBMA-g-urethane graft copolymers	60
5.2.3.3 Spectroscopic evaluation of the % UM in the graft copolymers	61
<b>5.3 <sup>13</sup>C NMR ANALYSIS</b>	<b>63</b>
5.3.1 <sup>13</sup> C NMR OF URETHANE MACROMONOMERS	63
5.3.2 <sup>13</sup> C NMR OF PMMA AND N-PBMA HOMOPOLYMERS	64
5.3.3 <sup>13</sup> C NMR OF ACRYLATE-URETHANE GRAFT COPOLYMERS	65
5.3.3.1 <sup>13</sup> C NMR of PMMA-g-urethane copolymers	66
5.3.3.2 <sup>13</sup> C NMR of n-PBMA-g-urethane copolymers	67
<b>5.4 GEL PERMEATION CHROMATOGRAPHY</b>	<b>68</b>
5.4.1 URETHANE MACROMONOMERS	68
5.4.2 SYNTHESIS OF ACRYLATE-G-URETHANE COPOLYMERS	69
5.4.2.1 Extraction of unreacted and unreactive UMs	70
5.4.2.2 Different methods used to optimize the structure of UMs	71
5.4.2.3 GPC analysis of acrylate-g-urethane copolymers	73
5.4.2.4 Number average molecular weight, weight average molecular weight and polydispersity of the graft copolymers	75
5.4.2.5 Yield of graft copolymers	77
<b>5.5 THERMOGRAVIMETRIC ANALYSIS (TGA)</b>	<b>78</b>
5.5.1 THERMAL STABILITY OF URETHANE MACROMONOMERS	78
5.5.2 THERMAL STABILITY OF ACRYLATE-URETHANE GRAFT COPOLYMERS	79
6.5.2.1 Thermal stability for PMMA-g-urethane copolymers	80
5.5.2.2 Thermal stability of n-PBMA-g-urethane copolymers	81
5.5.2. DYNAMIC MECHANICAL ANALYSIS	83
5.5.2.1. Introduction	83
5.5.2.2. Urethane macromonomers	84
5.5.2.3. PMMA-g-urethane copolymers	85
5.3.2.4. n-PBMA-g-urethane copolymers	87

<b>5.6 REFERENCES</b>	<b>89</b>
-----------------------	-----------

## **CHAPTER 6 CONCLUSIONS AND REMMENDATION**

<b>6.1 CONCLUSIONS</b>	<b>93</b>
------------------------	-----------

<b>6.2. RECOMMENDATION AND FUTURE WORK</b>	<b>95</b>
--	-----------

<b>APPENDIX A: CALCULATION OF THE MOLECULAR WEIGHT OF PMMA AND N-PBMA HOMOPOLYMERS</b>	<b>98</b>
--	-----------

<b>APPENDIX B: ARTICLE SUBMITTED TO POLYMER JOURNAL</b>	<b>100</b>
---	------------

## LIST OF SCHEMES

### CHAPTER 2: HISTORICAL AND THEORETICAL BACKGROUND

<b>SCHEME 2.1:</b> FORMATION OF POLYURETHANE.	5
<b>SCHEME 2.2:</b> MELT DISPERSION PROCESS.	10
<b>SCHEME 2.3:</b> THE KETIMINE AND KETAZINE PROCESS.	11
<b>SCHEME 2.4:</b> RESONANCE STRUCTURES OF THE ISOCYANATE GROUP.	12
<b>SCHEME 2.5:</b> RESONANCE STRUCTURES OF THE AROMATIC ISOCYANATE.	13
<b>SCHEME 2.6:</b> TDI ISOMERS.	13
<b>SCHEME 2.7:</b> 4,4'-DIPHENYLMETHANE DIISOCYANATE (MDI).	14
<b>SCHEME 2.8:</b> HEXAMETHYLENE DIISOCYANATE.	14
<b>SCHEME 2.9:</b> FORMATION OF CARBAMIC ACID DERIVATIVE.	14
<b>SCHEME 2.10:</b> URETHANE LINKAGE FORMATIONS VIA REACTION BETWEEN AN ALCOHOL AND AN ISOCYANATE.	15
<b>SCHEME 2.11:</b> UREA LINKAGE FORMATION VIA REACTION OF AN ISOCYANATES WITH AN AMINE.	15
<b>SCHEME 2.12:</b> REACTION BETWEEN WATER AND ISOCYANATE.	16
<b>SCHEME 2.13:</b> REACTION OF CARBOXYLIC ACID WITH ISOCYANATE.	16
<b>SCHEME 2.14:</b> FORMATION OF ALLOPHANATE AND BIURET.	17
<b>SCHEME 2.15:</b> DIMERIZATION OF ISOCYANATE.	18
<b>SCHEME 2.16:</b> TRIMERIZATION OF ISOCYANATE.	18
<b>SCHEME 2.17:</b> GENERAL FORMULA OF AN ACRYLATE ESTER.	19

### CHAPTER 3

#### EXPRMAENTALWORK

<b>SCHEME 3.1:</b> FORMATION OF URETHANE MACROMONOMERS (WHEN HEMA REACTS AT ONE SIDE AND ISOPROPANOL AT THE OTHER SIDE OF THE UM).	<b>40</b>
<b>SCHEME 3.2:</b> FORMATION OF ACRYLATE-URETHANE GRAFT COPOLYMER.	52

## LIST OF FIGURES

### CHAPTER 2

#### HISTORICAL AND THEORETICAL BACKGROUND

<b>FIGURE 2.1:</b> THE ALTERNATING STRUCTURE OF POLYURETHANE ELASTOMERS	7
<b>FIGURE 2.2:</b> TEM IMAGE OF OSMIUM TETROXIDE TAINTED TPU	8

### CHAPTER 5

#### RESULTS AND DISCUSSION

#### FIGURE

FIGURE 5.1: FTIR SPECTRA SHOWING THE PRESENCE AND ABSENCE OF NCO GROUPS (A) BEFORE ADDITION OF ISOPROPANOL + HEMA, (B) AFTER ADDITION OF ISOPROPANOL + HEMA. ....	52
FIGURE 5.2: FTIR SPECTRUM OF PMMA	
FIGURE 5.3: FTIR SPECTRUM OF N- PBMA .....	53
FIGURE 5.4: FTIR SPECTRA OF COMPARISON BETWEEN PMMA-G-URETHANE HAVING CHAIN LENGTH X=4, URETHANE MACROMONOMER, AND PMMA HOMOPOLYMER.	55
FIGURE 5.5: FTIR SPECTRA FOR COMPARISON BETWEEN N-PBMA-GRAFT- URETHANE HAVING CHAIN LENGTH X=32, URETHANE MACROMONOMER, AND N- PBMA HOMOPOLYMER. ....	56
FIGURE 5.6: FTIR SPECTRA COMPARING PMMA	
FIGURE 5.7: FTIR SPECTRA COMPARING N-PBMA.....	57
FIGURE 5.8: $^{13}\text{C}$ NMR SPECTRUM OF UM OF CHAIN LENGTH X=12, DISSOLVED IN DMSO. .....	64
FIGURE 5.9: $^{13}\text{C}$ NMR SPECTRUM OF PMMA	
FIGURE 5.10: $^{13}\text{C}$ NMR SPECTRUM OF N-PBMA DISSOLVED IN $\text{CDCl}_3$ .	DISSOLVED IN $\text{CDCl}_3$ .
FIGURE 5.11: $^{13}\text{C}$ NMR SPECTRUM OF PMMA-G-URETHANE COPOLYMER DISSOLVED IN $\text{CDCl}_3$ . ....	66
FIGURE 5.12: $^{13}\text{C}$ NMR SPECTRUM OF N-PBMA-G-URETHANE COPOLYMER DISSOLVED IN $\text{CDCl}_3$ . ....	67
FIGURE 5.13: TGA CURVES OF N-BMA COPOLYMERIZED WITH DIFFERENT AMOUNTS OF UMS OF VARIOUS CHAIN LENGTHS. ....	82
FIGURE 5.14: $\text{TAN } \delta$ CURVES OF UM OF DIFFERENT CHAIN LENGTHS.....	84

FIGURE 5.15: TAN  $\delta$  CURVES OF PMMA-G-URETHANE COPOLYMERS CONTAINING  
DIFFERENT AMOUNTS OF UM OF CHAIN LENGTH X=12..... 85

## LIST OF TABLES

### CHAPTER 3

#### EXPERIMENTAL WORK

<b>TABLE 3.1:</b> REAGENTS USED FOR PU FORMULATIONS .....	38
<b>TABLE 3.2:</b> FORMULATIONS USED FOR THE PREPARATION OF POLYURETHANE MACROMONOMERS .....	38
<b>TABLE 3.3:</b> FORMULATIONS FOR THE PREPARATION OF PMMA-URETHANE GRAFT COPOLYMERS.....	42
<b>TABLE 3.4:</b> FORMULATIONS FOR THE PREPARATION OF N-PBMA-URETHANE GRAFT COPOLYMERS.....	43
<b>TABLE 3.5:</b> EFFECT OF THE CONCENTRATION OF INITIATOR ON YIELD OF GRAFT COPOLYMERS.....	44

### CHAPTER 5

#### RESULTS AND DISCUSSION

<b>TABLE 5.1:</b> FTIR PEAK ASSIGNMENT OF THE UMS.....	53
<b>TABLE 5.2:</b> FTIR PEAK ASSIGNMENTS OF THE PMMA AND N-PBMA HOMOPOLYMERS .	54
<b>TABLE 5.3:</b> <sup>1</sup> H NMR DATA FOR PMMA AND N-PBMA HOMOPOLYMER (SOLVENT CDCL <sub>3</sub> )	59
<b>TABLE 5.4:</b> PERCENTAGE UM INCORPORATED INTO THE GRAFT COPOLYMERS, AS DETERMINED BY NMR .....	62
<b>TABLE 5.5:</b> <sup>13</sup> C NMR DATA FOR PMMA AND N-PBMA HOMOPOLYMERS .....	65
<b>TABLE 5.6:</b> NUMBER AVERAGE MOLECULAR WEIGHT, AND POLYDISPERSITY ( $M_N/M_W$ ) OF THE UMS OF DIFFERENT CHAIN LENGTHS, AS DETERMINED BY GPC.....	69
<b>TABLE 5.7:</b> YIELD COMPARISONS BETWEEN THE THREE DIFFERENT METHODS USED TO SYNTHESIZE UMS .....	73
<b>TABLE 5.8:</b> NUMBER AVERAGE MOLECULAR WEIGHT, WEIGHT AVERAGE MOLECULAR WEIGHT AND POLYDISPERSITY ( $M_N/M_W$ ) FOR PMMA-G-URETHANE COPOLYMERS	76
<b>TABLE 5.9:</b> NUMBER AVERAGE MOLECULAR WEIGHT (MN), WEIGHT AVERAGE MOLECULAR WEIGHT (MW) AND POLYDISPERSITY ( $M_N/M_W$ ) FOR N-PBMA-G- URETHANE COPOLYMERS.....	77
<b>TABLE 5.10:</b> TG VALUES OF UMS OF DIFFERENT CHAIN LENGTHS, AS DETERMINED BY DMA. ....	85

<b>TABLE 5.11:</b> TG VALUES OF PMMA-G-URETHANE COPOLYMERS AS DETERMINED BY DMA.....	86
<b>TABLE 5.12:</b> TG VALUES OF N-PBMA-G-URETHANE COPOLYMERS AS DETERMINED BY DMA.....	88

## LIST OF ABBREVIATIONS

<b>AIBN</b>	2,2' Azobis (isobutyronitrile)
<b>BA</b>	Butylacrylate
<b>DMA</b>	Dynamic mechanical analysis
<b>DMF</b>	Dimethylformamide
<b>DSC</b>	Differential scanning calorimetry
<b>EG</b>	Ethylene glycol
<b>FTIR</b>	Fourier transforms infrared spectroscopy
<b>g</b>	Graft copolymer
<b>GPC</b>	Gel permeation chromatography
<b>HDI</b>	Hexamethylene diisocyanate
<b>HEA</b>	2-hydroxyethyl acrylate
<b>HEMA</b>	2-hydroxyethylmethacrylate
<b>MDI</b>	Methylene diphenldiisocyanate
<b>MEK</b>	Methylethylketone
<b>MeOH</b>	Methanol
<b>MMA</b>	Methylmethacrylate
<b>Mn</b>	Number average molecular weight
<b>Mw</b>	Weight average Molecular weight
<b>n-BMA</b>	n-Butylmethacrylate
<b>TGA</b>	Thermal gravimetric analysis
<b>TDI</b>	Toluene diisocyanate
<b>TEM</b>	Transmission electron microscopy
<b>THF</b>	Tetrahydrofuran
<b>PU</b>	Polyurethane
<b>UMs</b>	Urethane macromonomers
<b>X</b>	Urethane chain length

## **Chapter 1**

### **Introduction and Objectives**

#### **1.1. Introduction**

Properties and applications of polymers can be extended by copolymerizing with other polymers to give new materials with tailored properties and performances [1]. Thus, in recent years there has been much focus on exploring the potential of different copolymers, and particularly on combining the useful properties of each of the components while minimizing their undesired characteristics.

Polyurethanes are finding increasing application and use in many industries [2-5] due to their advantageous properties, such as a wide range of flexibility combined with toughness, high abrasion resistance, high chemical resistance, high acid etch resistance, excellent weatherability, and very low temperature cure. These features make PU one of the most widely used and one of the fastest growing types of polymers in the world. PUs do however have some disadvantages, for instance: PU is considered an expensive polymer, especially the isocyanate component, and PU production presents many problems, especially with respect to the high reactivity of the isocyanate group towards impurities such as water, etc. [6]. Today, however, side reactions have been largely reduced, from being a problem to now being under control. A motivation for this study was to use low cost PUs as grafts in polyacrylates to study property improvements that may in future impact on binder or adhesive product properties.

Historically, polyacrylates have found extensive use as adhesives and coatings [7]. Most polyacrylates generally have a low glass transition temperature ( $T_g$ ), which makes them suitable to handle, process, and purify. In addition, the wide range of available acrylate monomers allows the physical properties of their polymers to be tailored. Polyacrylates are less expensive than PUs. However, a problem associated with polyacrylates is that their flexible backbones impart limited thermal stability and mechanical strength. Thus, in this study PUs were incorporated into acrylates to enhance the overall properties of the graft copolymers.

Vinyl monomers have been incorporated into unsaturated polyurethanes in the aqueous phase using conventional polymerization techniques. Monomer and free radical initiators are added to the aqueous phase and grafting is carried out at a suitable temperature. Both anionic and cationic polyurethanes containing unsaturated polyester polyols in their backbone have been used and acrylate monomers grafted onto the main chain [8]. On the other hand, polyurethane ionomeric dispersions have been modified by block copolymerization in which NCO-terminated urethane prepolymers containing ionic groups are first capped with reactive diluents, such as 2-hydroxyethyl acrylate (HEA), via polyaddition. The potential ionic groups are then neutralized and terminal HEA moieties are polymerized with acrylate monomers, via free radical polymerization, to yield acrylate modified polyurethane dispersions [9].

Block copolymerization of polyurethanes has been carried out by crosslinking polyurethane dispersions using difunctional amines as chain extenders. Suitable vinyl monomers and an initiator are added and polymerized to obtain crosslinked aqueous polyurethanes by emulsion polymerization [10-12].

Graft copolymerization by the free radical mechanism is an interesting method for the preparation of polymeric systems with specific properties. Graft copolymers form an important class of polymeric materials. They have a wide range of applications deriving from the possibility to tailor their properties through the combination of monomers that form the backbone and the side chains. For example thermoplastic elastomers can be obtained by combining a soft polymer with hard polymer also impact resistant polymer also obtained by grafted a hard polymer backbone with soft polymer segments [13]. Graft copolymers can be prepared by three main methods: (a) "grafting from", when the polymerization of a second monomer is initiated by sites located on the main polymer chain; (b) "grafting onto", when a polymeric species reacts with functional groups located on the chain of another polymer; and (c) "grafting through", when a macromonomer is copolymerized with a small-molecule comonomer [14].

The macromonomer technique is the simplest way to prepare graft copolymers. Macromonomers are polymers end-capped with a polymerizable end group able to copolymerize with low molecular weight monomers, so the macromonomers can either homopolymerize to give a regular comb polymer or copolymerize with a conventional

monomer to give a graft copolymer. These end-functional polymers can be prepared by modifying polymer end groups or, most conveniently, by using functional initiators in living/controlled polymerizations.

The macromonomer method is generally the most efficient method for producing well defined graft copolymers [15]. There are several reasons for this: the wide variety of macromonomers and comonomers available makes possible the synthesis of graft copolymers with properties that can be selected and the length of their branches can be controlled since the molecular weight of the macromonomer and its distribution can also be preselected.

In this study, graft copolymerization will be achieved via solution free radical copolymerization between vinyl-terminated urethane macromonomers (UMs) which will be synthesized by polyaddition polymerization, and vinyl monomers such as methyl methacrylate (MMA) and normal butyl methacrylate (n-BMA).

## **1.2. Objectives**

The overall objective of this study was the synthesis and characterization of acrylate-g-urethane copolymers using the macromonomer technique. Specific objectives included the following:

- Synthesize linear UMs by the polyaddition polymerization of toluene diisocyanate (TDI) and ethylene glycol (EG) via the pre-polymer method, followed by termination with 2-hydroxy ethyl methacrylate (HEMA) and isopropanol to yield UMs having different urethane chain lengths and being predominantly monofunctional. Three different methods were used to synthesize these UMs to optimize its structure.
- Characterize the urethane macromonomers by FTIR,  $^1\text{H}$  NMR,  $^{13}\text{C}$  NMR, GPC, TGA and DMA.
- Incorporate various percentages of the respective UMs into methyl methacrylate and various percentages of UMs into normal butyl methacrylate, in solution polymerization via free radical copolymerization. The percentages of urethane

macromonomer to be incorporated are between 0% and 40% by weight (according to MMA and n-BMA monomers).

- Characterize the obtained methyl methacrylate–urethane graft copolymers and normal butyl methacrylate–urethane graft copolymers thus obtained by  $^1\text{H-NMR}$  and  $^{13}\text{C-NMR}$ , FTIR, TGA, GPC, and DMA.
- Investigate the possible phase separation between the urethane segment and acrylate segment in the graft copolymerization products by using DMA and TEM.
- Investigate the thermal dependence and mechanical properties of the graft copolymers as a function of UM chain length and percentage incorporation.

### 1.3. References

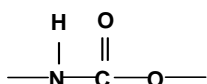
1. S. Al-Malaika and W. Kong, *Polymer Degradation and Stability* **90** (2005) 197.
2. G. Oertel, Ed. *Polyurethane Handbook*, 2nd ed. Hanser, New York, 1993.
3. D. Dounis and G. Wilkes, *Polymer* **38** (1997) 2819.
4. M. Mahkam and N. Sharifi, *Polymer* **80** (2003) 199.
5. K. Weiss, *Progress in Polymer Science* **22** (1997) 203.
6. S. Seboa, MSc thesis, University of Stellenbosch, Dec. 2002.
7. B. Elvers, S. Hawkins, G. Schulz, *Ullmann's Encyclopedia of Industrial Chemistry*, John Wiley and sons, **21A** (1992) 158.
8. S. Tanaka, M. Uno, S. Teramachi and Y. Tsukahara, *Polymer* **36** (1995) 2219.
9. J. Rosthauser and K. Nachtkamp, *Advances in Urethane Science* **23** (1987) 10121.
10. S. Shim, H Jung and K Lee, *Journal of Colloid and Interface Science* **279** (2004) 664.
11. B. Kim and J. Lee, *Polymer* **37** (1996) 469.
12. H. Li and E. Ruckentein, *Polymer* **36** (1995) 2281.
13. C. Nair, P. Chaumont and D. Charmot, *Polymer* **40** (1999) 2111.
14. T. Schunk and T. Long, *Journal of Chromatography A* **692** (1995) 221.
15. V. Langlois, K. Vallee-Rehel, J. Peron, A. Borgne, M. Walls and P. Guerin, *Polymer Degradation and Stability* **76** (2002) 411.

## Chapter 2

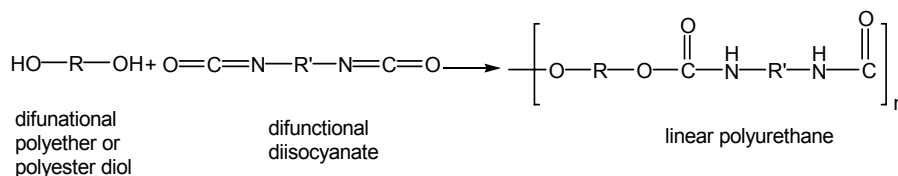
### Historical and theoretical background

#### 2.1. Introduction

Polyurethanes is the collective name for an extensive group of polymers with very different compositions and a variety of property profiles, all of which have the urethane group in common. A urethane group is essentially a carbamic acid ester, i.e. an ester-amide derivative of carbonic acid, and characterized by the following linkage:



There are a number of methods available for the preparation of polyurethanes, but the most widely used is the condensation reaction of di- or poly-functional hydroxyl compounds, such as hydroxyl-terminated polyethers or polyesters, with di- or poly-functional isocyanates. This condensation polymerization does not eliminate any by-product like conventional polycondensation does. Linear polyurethanes are produced when only difunctional reactants are used, as shown in Scheme 2.1.



**Scheme 2.1: Formation of polyurethane.**

If the functionality of the hydroxyl or isocyanate component is increased to three or more, then branched or crosslinked polymers are formed. By altering the R and R' groups, the properties of the PU (such as molecular weight, degree of crosslinking, effective intermolecular forces, chain stiffness and crystallinity) can be changed to better suit the desired end-use/s.

#### 2.2 History and development of polyurethanes

The above urethane-producing reaction was well-known in the nineteenth century, but only as a laboratory curiosity. It was not until the late 1930s that the commercial potential of polyurethanes as fibers, adhesives, coatings and foams began to be

recognized by Otto Bayer and others, as reported by Asha et al. [1]. In fact, the discovery of polyurethanes was made by Otto Bayer and coworkers at I. G. Farben Industries, Germany, in 1937, as reported by K. Mequanint [2].

Further research in the area demonstrated that when an aliphatic isocyanate reacted with a glycol, a new material with interesting properties for the production of plastics and fibers could be made. Du Pont and ICI soon recognized the desirable elastic properties of polyurethanes. The industrial-scale production of polyurethane started in 1940 [3]. Market growth of these materials increased after World War II. It was however only in the 1950s that the first polyurethane coatings were developed, when TDI was manufactured on a large scale [4]. Fast progress followed in the 1970s, when polyurethane coatings were introduced for motor vehicle applications [5, 6].

Despite some business depressions, the world's polyurethane market has shown remarkable growth through the 1980s and 1990s, reaching about 6.6 million tons of isocyanates and polyols in 1995 [7]. Polyurethane nanocomposites form now one of the most important fields in PU research, as evidenced by many papers [8-12].

### **2.3 Polyurethane applications**

Polyurethanes are widely used in many industries [13-19] due to their diversity of physical properties, such as a wide range of flexibility combined with toughness, high abrasion resistance, high chemical resistance, high acid-etch resistance, excellent weatherability, and very low temperature cure, which makes them one of the most widely used polymers in different applications. Polyurethanes are used in applications ranging from construction materials to taxidermy stuffing. They are also used for highly elastic foams (cushions, car seats), rigid foams (insulation material), adhesives, coatings, plastics and elastomers (see Section 2.3.1).

#### **2.3.1 Polyurethane thermoplastic elastomers**

Polyurethane elastomers are important members of the family of thermoplastic elastomers [20]. Although the consumption of polyurethane elastomers is lower than that of polyurethane foams, they are used for a variety of unique applications that cannot be met by other polymers. Their advantageous properties include high hardness for a given modulus, excellent mechanical and elastic properties, extremely high abrasion

*Chapter 2: Historical and background*

---

resistance, chemical resistance, and blood and tissue compatibility. Generally, polyurethane block copolymers have a low glass transition "soft" segment (SS) and a rigid "hard" segment (HS), which often has a high T<sub>g</sub>, but can also show crystallinity. The soft segment is typically a polyester- or polyether- diol, with a molecular weight of between 550 and 4000. The hard segment normally includes the reaction product of a diisocyanate (aromatic or aliphatic) and diol or diamine (the chain extender) [21-23]. The combination of this soft polyol segment and a hard segment forms an (AB)<sub>n</sub> type block copolymer. By varying the structure and molecular weight of the segments, and the ratio of the soft-to-hard segments, a broad range of physical properties can be obtained [24].

Polyurethane elastomers usually exhibit a two-phase microstructure, which arises from the chemical incompatibility between the soft and the hard segments, as shown in Figure 2.1 [25].

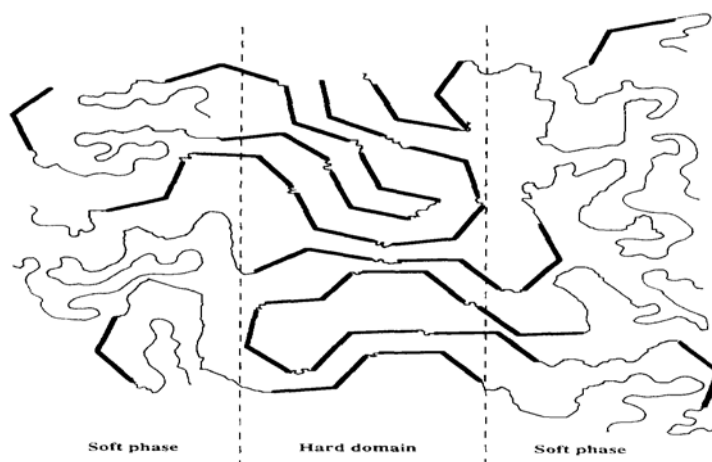


**Figure 2.1: The alternating structure of polyurethane elastomers (HS: hard segment; SS: soft segment).**

The rigid segments separate into a glassy or semi-crystalline domain and the polyol soft segments form amorphous or rubbery matrices in which the hard segments are isolated at varying content levels [26-27]. The hard domain in this two-phase microstructure can act as a physical crosslinking point and reinforcing filler, while the soft segment behaves as a soft elastic matrix. This microphase separation which affects physical and mechanical properties depends on the compatibility between the HS and SS, which in turn is affected by:(i) the ratio of SS to HS; (ii) the lengths of the soft and hard segments; (iii) the compositions of both the soft and hard segments; and (iv) finally, compatibility can be affected by anomalous linkage and molecular mass. To rephase, the degree of

phase separation or ability to form domains not only depends on the weight ratio of the hard-to-soft segments, but also on the type of chain extender, the type and molecular weight of the soft segment, the hydrogen bond formation between the urethane linkages, the manufacturing process, and reaction conditions [13, 28-29]. This phase segregation behaviour of polyurethanes has been well established by a variety of characterization techniques, including TEM (see Figure 2.2), SEM, small angle X-ray scattering (SAXS), infrared dichroism, DMA, and DSC [30-33]. Figure 2.2 shows TEM images of thermoplastic polyurethane (TPU) which shows phase segregation behaviour [31].

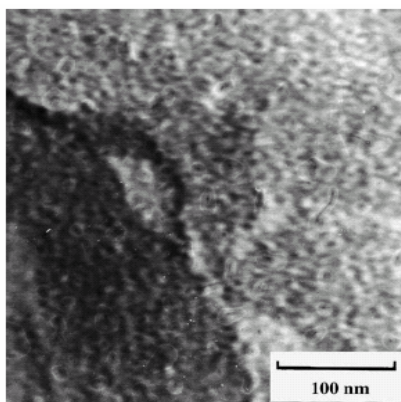


**Figure 2.2: TEM image of osmium tetroxide tained TPU (57% soft segment and 43% hard segment) [31]. (The light regions are hard domains and dark regions are soft domains).**

### 2.3.2 Polyurethane coatings

The polyurethane coatings industry offers a wide range of products for numerous application areas. Polyurethane coatings are available in both one- and two-component forms. A two-component coating will be supplied with the polyol, pigment, solvent and additives together in one pack, and the isocyanate in a second pack, to be added to and mixed with the first pack just before use. When the two components are mixed together the crosslinking reaction begins, causing an increase in the viscosity and molecular chain length. Finally, the viscosity increase is such that the coating becomes unusable. This limit of use is known as the potlife, and is normally expressed either as the time taken for the coating to remain useable or the time taken for a specific viscosity increase [34]. For a one-component coating all the raw materials are supplied, together, in the same pack.

### **2.3.3 Polyurethane adhesives**

Polyurethane adhesives are used in many application areas due to their outstanding properties, their simple and economical processing, and their high strength [35]. Polyurethane adhesive are normally defined as those adhesives that contain a number of urethane groups in the molecular backbone or wherever such groups are formed during use, regardless of the chemical composition of the rest of the chain. Thus, a typical urethane adhesive may contain, in addition to urethane linkages, aliphatic and aromatic hydrocarbons, esters, ethers, amides, urea, and allophanate groups [36].

### **2.3.4 Polyurethane foams**

Polyurethane foams are cellular or expanded materials, synthesized by the reaction of diisocyanate with polyol in the presence of a blowing agent. Depending upon the mechanical properties of the PU foam, it is either categorized as flexible (normally prepared from a polyether), rigid (prepared from a polyester) or semi rigid (prepared from both a polyester and a polyether). The first PU foams obtained, of the rigid kind, were described by Bayer in 1947 [1] and the first flexible soft foams by Hoechstlen in 1952, as reported by Mahmood [37].

## **2.4 Methods of preparation of polyurethanes**

A number of techniques are available to prepare high molecular mass polyurethanes. These include: the melt dispersion process, solution process, pre-polymer process, and ketimine and ketazine process. These are described in more detail below.

### **2.4.1 The solution process**

In this process the reaction between an isocyanate and any hydroxyl-bearing compound occurs at low temperatures (20-120 °C), depending on the nature of the isocyanate used, and whether or not a catalyst is used. The lower reaction temperature means that when a high molecular mass is reached the viscosity of the reaction medium is too high to permit good mechanical agitation and ease of handling. In order to obtain good processing the viscosity must be reasonably low. This is achieved by adding polar, low-boiling solvents such as acetone, methyl ethyl ketone (MEK) or tetrahydrofuran (THF) to the reaction mixture to reduce the viscosity [38]. Besides reducing the viscosity of the mixture, the solvents also act as heat sinks, since the reaction between –NCO and –OH groups are highly exothermic. Reaction progress is measured by determining the



Chapter 2: Historical and background

---

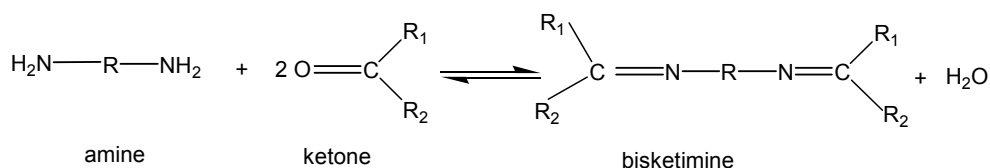
The melt of this preliminary adduct can be diluted with water in the presence of formaldehyde or its derivatives to form a stable dispersion. Reducing the pH causes polycondensation, yielding a high molecular mass PU urea. This process has many advantages, e.g. the reaction can be accelerated by increasing the temperature, no solvent is used, and a high volume-time yield is possible [39-40].

### 2.4.3 The pre-polymer process

Most polyurethane dispersions are produced by this method. In this process the polyol component and excess isocyanate and short diol extender are reacted to give a polyurethane pre-polymer chain, with excess –NCO content. This can be confirmed by the disappearance of the –OH peak of the polyol component, as determined by infrared spectroscopy, or by the volumetric titration value. Then excess –NCO in the pre-polymer can be extended by adding diamines or glycols in the presence of water, to form a high molecular mass PU dispersion. The effect of the phase-inversion temperature on the mechanical and morphological properties has been studied by several researchers [41-42].

### 2.4.4 Ketimine and ketazine process

In this process all the reactants, including the chain extender, are charged in the presence of ketones as solvents. Ketones react reversibly with amines (extenders) to form ketimine or ketazine, as shown in Scheme 2.3. The highly reactive aliphatic diamine, ethylene diamine, reacts slowly with the isocyanate group if the medium is acetone. Addition of water results in dispersion and release of the amine, and polyaddition occurs. This process requires only very small quantities of solvent or no solvent at all [43].



**Scheme 2.3: The ketimine and ketazine process.**

## 2.5 Raw materials

Urethanes can be synthesized from various monomers, the most important two being the isocyanate component and the hydroxyl component. These components will be discussed in greater detail below

### 2.5.1 Isocyanates

#### 2.5.1.1 Introduction

Isocyanates, esters of isocyanic acid, were first synthesized by Wurtz in 1848 (as reported by Chen and Hsu [42]). These compounds have one or several –NCO groups. Isocyanates are generally characterized by high and versatile reactivity. Aliphatic and aromatic monoisocyanates are widely used as building blocks for agricultural chemicals. Their use is mainly prompted by the unique capability of the isocyanate to undergo nucleophilic addition reactions.

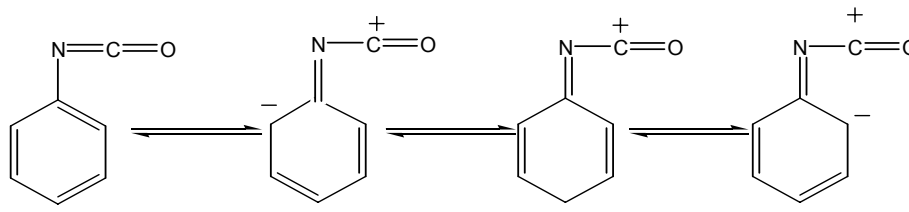
#### 2.5.1.2 Reactivity of the isocyanate group

The high energy content and polarizability of the double bonds in an isocyanate molecule permit multiple reactions. The reactivity of an isocyanate toward nucleophilic agents is mainly due to the pronounced positive character of the C atom in the cumulative double bond sequence consisting of nitrogen, carbon and oxygen, especially in aromatic systems [5]. The electronic structure of the isocyanate group can be represented by several resonance structures, which are illustrated in Scheme 2.4.



**Scheme 2.4: Resonance structures of the isocyanate group.**

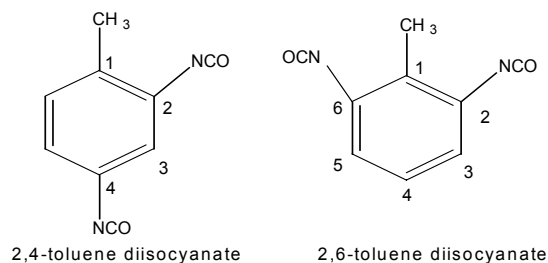
From the resonance structures, the positive charge at the C atom becomes obvious. On the other hand, the negative charge can be delocalized onto the oxygen atom, the nitrogen atom, and the R group. If R is an aromatic group, then the negative charge can be delocalized as illustrated in Scheme 2.5. This explains why an aromatic isocyanate has a distinctly higher reactivity than an aliphatic isocyanate [43]. Furthermore, the reactivity of an isocyanate group can vary significantly even for the same class of isocyanates. The structure, substituents, and steric effect can all influence reactivity [44, 45].



**Scheme 2.5: Resonance structures of the aromatic isocyanate.**

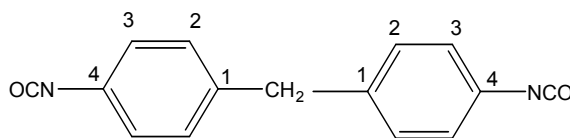
### 2.5.1.3 Aromatic isocyanates

More than 90% of polyurethanes are still produced from aromatic polyisocyanates [35]. The most commonly used aromatic isocyanates are TDI, and 4,4'-methylenediphenyl diisocyanate (MDI). TDI consists of a mixture of 80% 2,4- and 20% 2,6-toluene diisocyanate isomers (Scheme 2.6). The commercially available TDI is a mixture of these two isomers, in various ratios, although the pure 2,4- compound is also available commercially. TDI is a colorless liquid with a boiling point of 120 °C at 10 mm Hg .



**Scheme 2.6: TDI isomers.**

Temperature has a big influence on the reactivity of the NCO groups in their various ortho and para positions. At 25 °C NCO groups in the para position are eight to ten times more reactive than NCO groups in the ortho position. As the temperature increases, the reactivity of the ortho NCO increases at a far greater rate than that of the para NCO group, until their reactivities are equal at 100 °C [46]. The difference in reactivity at low temperature allows for polymer synthesis with an "ordered arrangement". TDI is used in the production of amongst other items, flexible foams, coatings, sealants, elastomers, adhesives [45]. MDI is a solid with a melting point of 37 °C. It tends to dimerize at room temperature, and should therefore be stored below 0 °C as a solid, or between 40-45°C as a liquid, to minimize the dimerization. MDI is normally produced as the 4,4' isomer (Scheme 2.7) (98%); the 2,4'- and 2,2'- isomers are present in trace amounts. MDI is used in the production of rigid foams, elastomers, and some coatings [42].



**Scheme 2.7: 4,4'-Diphenylmethane diisocyanate (MDI).**

There are other aromatic diisocyanates which have some important applications, such as 1,5-diisocyanatonaphthalene (NDI), toluidine diisocyanate (TODI) and p-phenylene diisocyanate (PPDI) [4].

#### 2.5.1.4 Aliphatic isocyanates

Aliphatic isocyanates can be made from the corresponding aliphatic diamines via the phosgenation process. Cyclic aliphatic diamines are, in many cases, available through ring hydrogenation of the corresponding aromatic amines, such as the hydrogenation of diamino diphenyl methane (MDA) to give diamino dicyclohexyl methane [46]. The most important aliphatic isocyanates are 1,6-hexamethylene diisocyanate (HDI) (Scheme 2.8) and 4,4-diisocyanate dicyclohexylmethane (H<sub>12</sub>MDI).



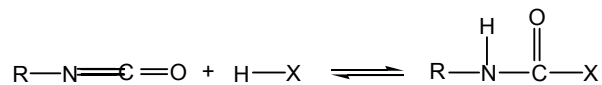
**Scheme 2.8: Hexamethylene diisocyanate.**

These aliphatic isocyanates, or their modified forms, are widely used in the coatings industry [17]. HDI is a colorless liquid and with a boiling point of 127 °C at 1.33 kPa. HDI is less reactive than TDI and MDI. The reactivity of HDI can be increased by tertiary amines or tin compounds, to equal to or better than the NCO reactivity in TDI [41].

#### 2.5.1.5 General reactions of isocyanates

##### 1) Nucleophilic addition reactions

The most important reaction of isocyanates is the formation of carbamic acid derivatives (Scheme 2.9) by addition of nucleophilic reactants across the C=N double bond.



**Scheme 2.9: Formation of carbamic acid derivative.**

*Chapter 2: Historical and background*

---

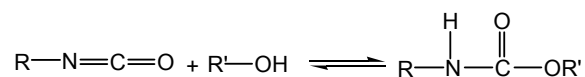
With increasing nucleophilic character of HX, the reaction proceeds at lower temperatures [35]. However, the above reaction product decomposes at higher temperatures to regenerate the starting material, i.e. free –NCO, since the reaction is a genuine equilibrium [2].

**2) Primary reactions**

Primary reactions require only low temperatures compared to the secondary reactions. Primary reactions are based on the relative reaction velocity.

i) Reactions with alcohols

The reaction between an alcohol and an isocyanate (Scheme 2.10) is an exothermic reaction [35].

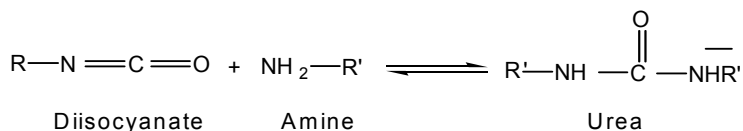


**Scheme 2.10: Urethane linkage formations via reaction between an alcohol and an isocyanate.**

These reactions are usually catalyzed by bases, mainly tertiary amines or organic metal organics such as organo tin compounds. Reactivity is influenced by the structure of the catalyst. For example, in using the amine catalysts, the reactivity decrease respectively from primary to secondary to tertiary amine due to the neighbouring methyl group causing steric hindrance. Hydroxylated compounds with tertiary amino groups (like triethanolamine) exhibit a catalytic effect [47].

ii) Reactions with amines

Reactions of isocyanates with amines to form polyureas (Scheme 2.11) are very fast and do not require catalysis.



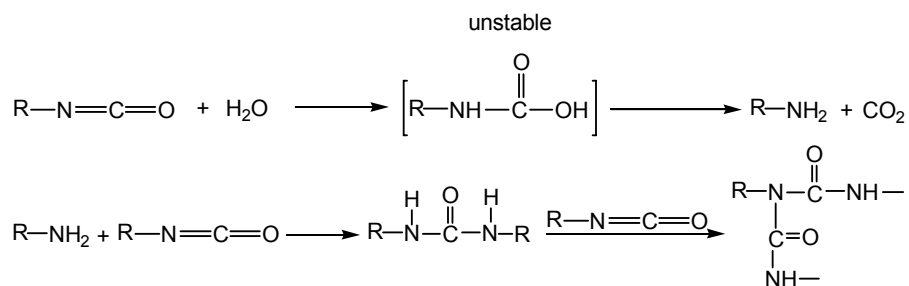
**Scheme 2.11: Urea linkage formation via reaction of an isocyanate with amines.**

Chapter 2: Historical and background

Aliphatic amines react more quickly than aromatic amines. The highly reactive aliphatic amines are used as chain extenders for polyurea.

iii) Reaction with water

The reaction between an isocyanate and water is a special case of an alcohol/isocyanate reaction. In this reaction, the primary product is the carbamic acid. It is not stable and will decompose to the corresponding amine and carbon dioxide. The amine formed will then react immediately with the isocyanate group in the system to form a branched polyurethane structure, as illustrated in Scheme 2.12.

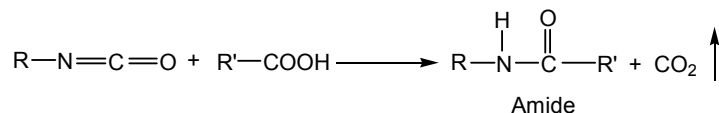


**Scheme 2.12: Reaction between water and isocyanate.**

This reaction is very important for the formation of polyurethane foam, since the carbon dioxide acts as a blowing agent. However, this reaction can also create problems in the storage of isocyanate. Moreover, to obtain high molecular weight, linear, thermoplastic polyurethane, it is essential to completely exclude water from the reaction system [48-49].

iv) Reaction with carboxylic compounds

The reaction of isocyanates with carboxylic acids gives intermediate carbamyl anhydrides. These are generally not stable and decompose at a certain temperature to form amides and CO<sub>2</sub>, as shown in Scheme 2.13.



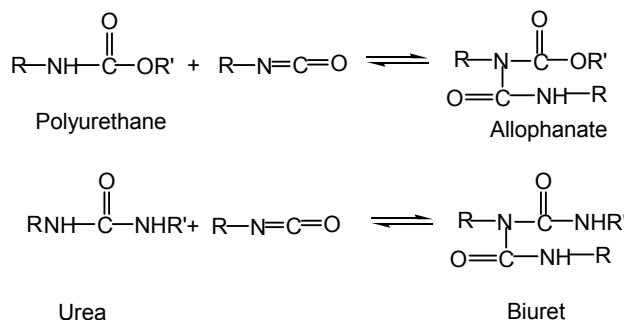
**Scheme 2.13: Reaction of carboxylic acid with isocyanate.**

**3) Secondary reactions**

The urethane and urea formed from the primary reactions still contain active hydrogen. Although the reactivities of these compounds are lower than the starting reagents,

Chapter 2: Historical and background

alcohol and amine, they are still capable of nucleophilic attack by the isocyanate, which results in an allophanate and a biuret. Allophanates are usually formed between 120 °C and 150 °C, and biurets between 100 °C and 150 °C [49]. Due to their low thermal stability, allophanates and biuret will dissociate into the starting components above 150 °C, as shown in Scheme 2.14



**Scheme 2.14: Formation of allophanate and biuret.**

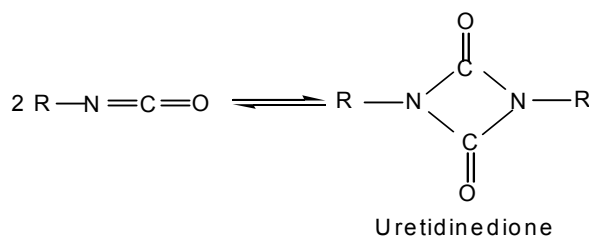
The formation of allophanates and biuret can result in the polyurethane crosslinking. Since these bonds dissociate at elevated temperatures, a small amount of excess isocyanate functionality is often used in the polymerization to promote crosslinking while the polymer can still be melt processed.

#### 4) Self-addition reactions

The highly unsaturated character of the NCO groups allows, under specific conditions, dimerization.

##### i) Dimerization

The dimerization reaction is shown in Scheme 2.15. Dimerization is limited to aromatic isocyanates and it is inhibited by ortho substituents [50]. For example, 2,4- and 2,6-TDI dimerize very slowly due to the hindering effect of the methyl group attached to the aromatic radical, while MDI dimerizes reasonably at room temperature, even without a catalyst. Moreover, dimerization is also a readily reversible reaction above 150 °C. However, the isocyanates, which can be formed by heating both aliphatic and aromatic isocyanates, are very stable and the dimerization reaction cannot be easily reversed [51].

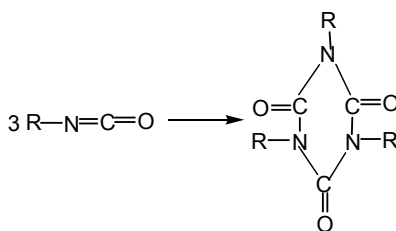


**Scheme 2.15: Dimerization of isocyanate.**

The dimerization reactions proceed at ambient temperature in highly polar solvents, such as DMF, with alkaline catalyst. The product depolymerizes readily and hence the reaction is of no technical use. Due to this splitting, dimerization of aromatic isocyanate is restricted to only thermal crosslinking applications [52].

### ii) Trimerization

Trimerization of isocyanate to form stable isocyanate rings, as shown in Scheme 2.16, is more valuable than dimerization. Trimerization is usually catalyzed by strong bases. After a given degree of trimerization, the reaction has to be terminated with *o/p*-toluene-sulphonic acid–methyl ester to avoid brittle polycyclic and crosslinked structures [52].



**Scheme 2.16: Trimerization of isocyanate.**

Aliphatic and cycloaliphatic isocyanates can either be trimerized alone or mixed with aromatic polyisocyanates. The isocyanates are mainly used for light-stable and weather-resistant coatings [52].

### **2.5.2 Polyols**

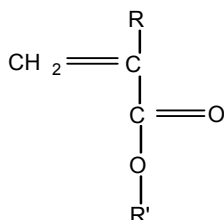
Polyols commonly include hydroxy-terminated polyesters and polyethers, polyolefins and glycols. The properties of any polyurethane depend on the chemical composition and the molecular mass of the polyol used for its production. Typically, long-chain, high molecular weight polyols are preferable in elastomer synthesis.

## 2.6. Polyacrylates

### 2.6.1 Introduction

Acrylic acid and acrylate esters have been known since the middle of the nineteenth century. A systematic investigation of acrylate esters was published as long ago as 1901 by Von Pechmann and Rohm [53]. A process for the industrial production of acrylate esters was developed in 1928 by H. Bauer and H Rohm [54]. Polymethylmethacrylate has been produced by solution polymerization since 1927 by Rohm and Hass. Emulsion polymers were first developed on an industrial scale in 1930 by H. Fikentescher [53]. The use of polyacrylate in many fields of applications increased rapidly with the development of new methods for producing acrylic acids and acrylate esters.

Acrylate and methacrylate esters are derivatives of the corresponding acids. They are the simplest members of the family of polyunsaturated carboxylic acids. Polyacrylates, formed by a head-to-tail addition process, have a hydrocarbon backbone with a pendent ester group. Polymethacrylates also have a pendent and methyl group on the same carbon atom. The acrylate polymers are characterized by having hydrogen adjacent to the carbonyl group (C=O in Scheme 2.17), and therefore have more rotational freedom than the methacrylate. The substitution of methyl (CH<sub>3</sub>) for the hydrogen atom, producing a methacrylate polymer, restricts the freedom of rotation of the polymer and thus produces harder polymers with higher tensile strength and lower elongation than the acrylate counterpart [54]. A list of commercially important acrylic monomers is given in Table 2.1.



**Scheme 2.17: General formula of an acrylate ester.**

where, R = H for acrylate or R= CH<sub>3</sub> for methacrylate, and R' is an alkyl group.

**Table 2.1: Commercially important acrylate and methacrylate monomers**

Acrylates	Methacrylates
n-Butyl acrylate	n-Butyl methacrylate
Ethyl acrylate	Cyclohexyl methacrylate
2-Ethylhexyl acrylate	2-Ethylhexyl methacrylate
Methyl acrylate	Ethylhexyl methacrylate
	Isobutyl methacrylate
	Laurylmethacrylate
	Methyl methacrylate
	Stearyl methacrylate

### 2.6.2 Preparation of polyacrylates

Acrylates can be polymerized very easily because their carbonyl groups are adjacent to a vinyl group. Polyacrylates are produced almost exclusively by radical polymerization. Conventional radical formers (e.g. peroxides and other per compounds) or azo compounds are used as initiators (controlled free radical reactions are also possible).

#### 2.6.2.1 Free radical polymerization

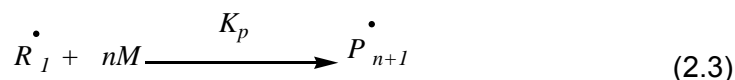
Generally, free radical polymerization comprises four types of reactions: the initiation reaction, propagation reaction, termination reaction, and chain transfer to small molecules, as described in detail below:

1) Initiation reaction, which continuously generates radicals during polymerization



where  $I$  = initiator,  $K_d$  = rate of decomposition,  $R^{\bullet}$  = radical fragment,  $K_i$  = rate of initiation,  $in$  = initial radical.

2) Propagation reaction, which is responsible for the growth of the polymer chain by

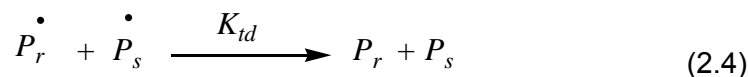


Chapter 2: Historical and background

---

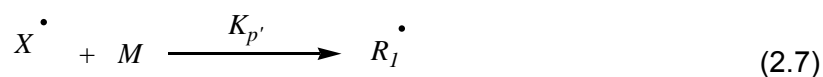
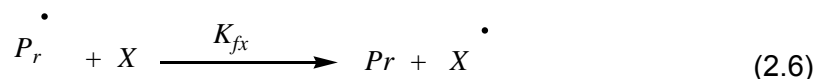
where  $R_1$  = radical fragment,  $M$  = monomer,  $K_p$  = rate of propagation  $n$  = number of monomers (repeat units) and  $P^\cdot$  = polymer chain radical.

3) Termination reactions between two radical centers. These are disproportionation (Eq. 2.4) and combination (Eq. 2.5)



where  $P_r$  is a polymer molecule of chain length  $r$  and does not have a radical center while a polymer radical (macro radical) of chain length  $r$  has the symbol  $P_r^\cdot$ .

4) Chain transfer to small molecules, which causes the termination of growth of polymer radicals, while simultaneously generating small transfer radicals. Chain-transfer reactions do not give a net consumption of radicals, and if the transfer radicals are as reactive as the polymer radical (or more reactive) these reactions should not affect the polymerization rate or monomer consumption rate. Chain-transfer reactions to small molecules reduce the size of polymer radicals and therefore increase bimolecular termination rates when these reactions are diffusion controlled.



where  $X$  may be a monomer or a solvent molecule, or a chain-transfer agent. When  $X$  is a polymer molecule, polymer molecules with long-chain branches are formed.

Since polymer molecules with high molecular masses are produced from the very start of polymerization, the reacting solution can be quite viscous over most of the monomer conversion range. The high viscosities not only cause problems in mixing and heat removal, but can also affect reaction rates [53].

### **2.6.3 Polymerization techniques**

Acrylic polymers are generally produced by two techniques: solution polymerization and emulsion polymerization. The choice of process depends upon the desired properties and the planned application of the subsequent polymer.

#### **2.6.3.1 Solution polymerization**

Solution polymerization involves heating the monomer and initiator in the presence of solvent. At the end of the polymerization the solvent may be removed by distillation or a spray-drying technique. Aromatic hydrocarbons such as benzene and toluene are used as suitable solvents for the polymerization of acrylates of long-chain alcohols, while esters and ketones can be used for the polymerization of acrylates of short-chain alcohols. If the solvent boils at the temperature used for polymerization, a large amount of the heat of polymerization can be removed by evaporative cooling. The solvent may act as modifier in solution polymerization, hence it is very important to take this into consideration when choosing a solvent. The lower the transfer constant is, the higher is the molecular mass of the polymers, and the higher the viscosity will be. The latter has a negative effect on the mixing of the reactor contents and the removal of the heat of polymerization [54].

Soluble azo compounds, peroxides, or hydroperoxides are used as initiators, in concentrations of 0.01-2.00 wt % relative to the monomer [53].

Solution polymerization can be carried out by two methods: (i) the all-in-one, or 'one-shot', process, which involves charging all the monomer, solvent initiator and modifier into the reaction vessel and heating to the reaction temperature, and (ii) The 'drip-feed', or continuous process, which involves feeding the monomer and initiator separately into the solvent at the reaction temperature. Factors influencing solution polymerization include reaction temperature, monomer concentration, type of solvent, concentration of initiator and chain-transfer agents [53].

#### **2.6.3.2 Emulsion polymerization**

The basic components of an emulsion polymerization are water, acrylic monomer, surfactant, initiator, modifier and buffer. Emulsion polymerization of acrylic polymers provides both product property and process advantages [55]. The characteristic

properties of a polymer are influenced by the conditions of polymerization, such as catalyst, reaction time and temperature, and monomer concentration. All of these factors can be adjusted to change the molecular weight of the polymer and ultimately the polymer properties.

Acrylic emulsions are used in large volumes for many products, such as coatings, sealants and adhesives, and as cement modifiers. Polymer composition and structure can be tailored to meet the required application. Emulsions are easier to handle and are non-hazardous compared with solution polymers.

#### **2.6.4 Applications of polymethacrylates**

Polyacrylates are used in many applications, such as coatings, textiles, papers, oil additives, paints, and adhesives [55]. Polymethacrylates can be soft or hard, for example: polymethyl methacrylate is a hard polymer and because of its high hardness, tends to be used for making shaped objects while polybutyl methacrylate is much softer and tends to find use in applications that require flexibility or extensibility. The ease of handling polyacrylates and the ease of copolymerizing softer acrylates with harder methacrylate, styrene, vinylacetate, and polyurethane, allows the manufacture of products that range from soft rubbers to hard film-forming polymers.

#### **2.7 Urethane acrylate oligomers**

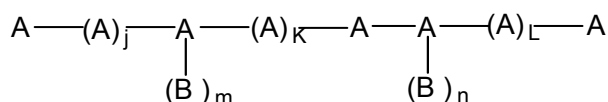
Coatings which consist of an oligomer, a monomer and a photo-initiator can be cured by UV. The most commonly used UV-curable formulations contain unsaturated acrylates. The main types of acrylic oligomers include epoxy acrylates, polyester acrylates, polyether acrylates, urethane acrylates and silicone acrylates. Among the oligomers used for UV-curable coatings, the urethane acrylate oligomers (UAO) offer a wide range of excellent application properties, such as high impact and tensile strength, abrasion resistance and toughness, combined with excellent resistance to chemicals and solvents [56]. Hence urethane acrylates are used extensively in wood coatings, overprint varnishes, printing inks and adhesives applications.

Urethane acrylate oligomers are commercially available with molecular weights ranging from 600 to 6000 g/mol and functionalities ranging from 2 to 6 [57, 58]. They provide either a hard or flexible coating depending on molecular weight, functionality and chemical structure [59]. Polyurethane derivatives are obtained by the reaction of a polyol

with a diisocyanate, whereas polyurethane acrylate (PUA) oligomers are generally prepared by a two-step synthesis [60]. An excess of diisocyanate can react with a polyol, and only then with an hydroxyl-terminated acrylate [61]. In another procedure described by Nocii et al. a diisocyanate in excess first reacts with a monoalcohol acrylate and then with the polyol, as reported by Burel et al. [62]. Finally, as recently described by Chen et al. [63], a one-step synthesis can also be performed by exothermic control or by using 2-methyl-2-propenoyl isocyanate (MPI). Most of these urethane acrylate macromonomers are multi functional, i.e. at least difunctional and give crosslinked coatings.

## 2.8 Graft Copolymerization

A graft copolymer is a polymer comprising a main chain (polymer backbone) and one or more species connected to the main chain, as side chains, having constitutional or configurational features that differ from those in the main chain. In principle, graft copolymerization is a process in which side chain grafts are covalently attached to the main chain, to form a branched copolymer [64]. The simplest case of a graft copolymer is represented by the structure in Scheme 2.18, where A is the main polymer chain, (I, K, L) are repeat units, and  $B_n$  and  $B_m$  are the side chain grafts made from monomer B.



**Scheme 2.18: Representation of a graft copolymer.**

The extent of polymerization in  $B_n$  and  $B_m$  grafts is called the degree of grafting (grafting yield) which is gravimetrically determined as a percentage of the mass increase [65]. Both the backbone and side chain grafts can be either homopolymers or copolymers, with different chemical compositions. Branching in one or more stages and crosslinking may occur and these branches are usually randomly distributed along the polymer backbone [66].

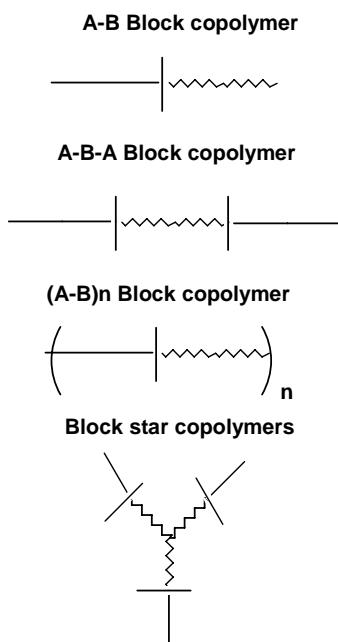
Linear block copolymers comprise chemically different segments, much like grafts. They can be arranged as a copolymer of two differing monomeric units, such as A-B, with only two distinct segments, or in a triblock fashion, such as A-B-A, with three segments, or as

Chapter 2: Historical and background

---

multiblocks of the structure  $(A-B)_n$ , comprising many segments, as shown in Scheme 2.19.

In block copolymers, like graft copolymers, both A and B sequences may be homopolymer or copolymer, as long as the A sequence is different from the B sequence. Another, less common configuration is the star block copolymer, with arms that radiate from a central core of a chemical makeup that is different to that of the arms [67].



**Scheme 2.19: Representation of block copolymers.**

Graft copolymerization takes place as a result of the formation of active sites on the polymer backbone. The active sites may be functional groups, free radicals or ionic groups, which initiate the polymerization reaction. The formation of active sites on the polymer backbone can be carried out by several methods, such as synthetically, or by postmodification with plasma treatment, ultraviolet or light radiation, decomposition of chemical initiator and high energy radiation [68]. The free radical polymerization method is the oldest and most widely used procedure for the synthesis of graft polymers because it is relatively simple. [67]. However, it usually yields heterogeneous materials that are difficult to characterize.

Graft copolymers are often prepared in order to modify polymer properties [69]. This is because the main chains are usually thermodynamically incompatible. Most graft copolymers can be classified as multiphase polymers in solid state, similar to polymer blends, block copolymers, and polymer networks. Microphase-separated graft copolymers can display many of the unique thermal and mechanical properties observed in block copolymers, including thermoplastic elasticity. Since the morphology of heterophase polymers can be affected by the casting solvent and the nature of its interaction with the polymers blocks, the physical properties are also expected to depend on the casting solvent [70]. Newer areas of interest are nanophase-separated graft copolymer systems, as in the present study. This occurs when the grafts are too short to form a large domain which can (in this later case) change bulk properties to portray both phases independently.

### **2.8.1 Synthetic routes to graft polymers**

The preparation of graft polymer structures has been achieved by three different methods, generally described as "grafting through", when a macromonomer is copolymerized with a small-molecule comonomer; "grafting from", when the polymerization of a second monomer is initiated by sites located on the main polymer chain; and "grafting onto", when a polymeric species reacts with functional groups located on the chain of another polymer. These synthetic routes have been adapted from techniques mostly used to prepare comb-branched polymers [71]. These three different methods will be discussed in detail below.

#### **2.8.1.1 "Grafting from"**

In the "grafting from" method, after the preparation of the polymer backbone, active sites are produced along the main chain and these are able to initiate the polymerization of the second monomer. Polymerization of the second monomer results in formation of the branches and the final graft copolymers. The number of branches can be controlled by the number of active sites generated along the backbone, assuming that each one of them initiates the formation of one branch. The isolation and characterization of each part of a graft copolymer in this case is almost always impossible, because knowledge of precursor molecular characteristics is limited to the backbone [72-74].

### 2.8.1.2 "Grafting onto"

The "grafting onto" method is most commonly used for the preparation of graft polymers with a tailored structure and topology. In the "grafting onto" method the polymer backbone and the arms are prepared separately, by a living polymerization mechanism. The backbone bears functional groups, distributed along the chain, which can react with living branches. Upon mixing the backbone and the branches in the desired quantity and under the right experimental conditions, a coupling reaction takes place in the final comb-shaped polymers [75-78]. The branching sites can be introduced into the backbone either by a homopolymerization reaction or by copolymerization of the main backbone monomer(s) with a suitable comonomer with the desired functional groups.

### 2.8.1.3 "Grafting through"

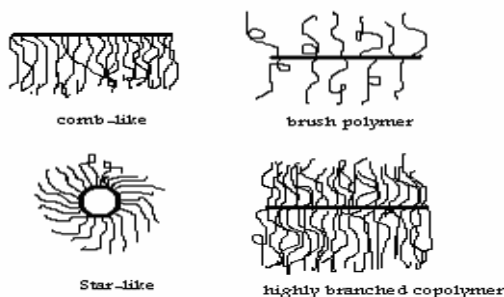
The "grafting through" method of preparation of graft copolymers consists of two steps. Firstly, a linear polymer bearing a terminal vinyl group is prepared. This species is referred to as a macromonomer. The second step consists of the copolymerization of the macromonomer with a suitable comonomer, generally by radical polymerization. In this case, the macromonomer comprises the branch of the copolymer, and the backbone is formed *in situ*. The number of branches per backbone can generally be controlled by the ratio of the molar concentration of the macromonomer and comonomer. Several other factors have also to be considered. Among them, the most important one is the copolymerization behaviour of the macromonomer and the comonomer forming the backbone. Depending on the reactivity ratios of the macromonomer and comonomer, different degrees of randomness can be achieved, with respect to the placement of branches.

Since macromonomer and comonomer incorporation in the graft copolymers can vary in the course of the copolymerization reaction, due to changes in the concentration of the two compounds in the mixture, different kinds of graft copolymers are formed as a function of time. Phase separation can also occur in these systems, due to the formation of the copolymers, leading to increased compositional and molecular weight heterogeneity of the final product. Numerous examples of comb-branched graft copolymers prepared by this approach have been reported [79-86].

## 2.9 Macromonomers

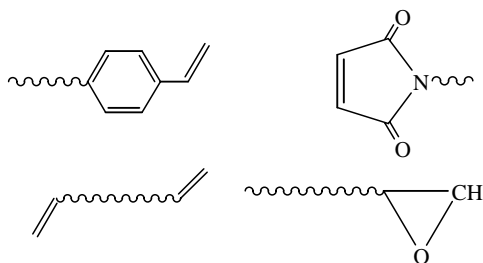
### 2.9.1 Introduction

The term macromonomers is defined as low molecular mass polymers with polymerizable groups either at one or both chain ends [87]. Interest in macromonomers is increasing because of their ability to undergo subsequent homo- and copolymerization reactions to yield numerous types of different polymers. They give comb-like, star-like and brush polymers, having regular and dense branching along their lengths, as a result of subsequent homopolymerization. Graft copolymers with a random distribution of branches can also be obtained by copolymerization of macromonomers with low molecular mass monomers. Macromonomers can be used to design copolymers with multiple types of branched structures (Scheme 2.20) that can be utilized in specific applications. Copolymerization of macromonomers that bear hydrophilic and hydrophobic side chains may result in copolymers that can undergo self-organization.



**Scheme 2.20: Branched architectures of different polymer types.**

The number of polymerizable groups at the chain ends may result in different types of polymers. Network polymer structures can be achieved by copolymerization of macromonomers with two polymerizable groups at the chain ends. Some of the macromonomers with different polymerizable groups are shown in Scheme 2.21 [88].



**Scheme 2.21: Types of macromonomers [88].**

The synthesis and characterization of macromonomers have been widely studied. Their synthesis was realized more than 40 years ago, in 1960. Asami et al. [89] reacted *p*-chlorostyrene with a chlorine end-capped poly (dimethylsiloxane) via a Grignard intermediate. They also made low molecular weight  $\omega$ -unsaturated polymers by using anionic techniques. Ito and Kawaguchi [91] also synthesized macromonomers via a free radical polymerization technique. The free radical polymerization of methyl methacrylate was carried out in the presence of 2-hydroxyethanethiol (HOCH<sub>2</sub>CH<sub>2</sub>SH) as transfer agent. Well-defined macromonomers with different chemical structures were prepared,

## 2.9.2 Syntheses of macromonomers

Macromonomers are synthesized by introducing an appropriate polymerizable end group by one of the following methods: initiation, termination, functional end-group transformation, or polyaddition polymerization.

### 2.9.2.1 The initiation method

In this method, the macromonomers can be synthesized by introducing a suitable polymerizable end group by initiation of living polymerization. In order to yield a macromonomer the initiator's functional group must not react during the course of polymerization. Macromonomers that are prepared by this method are usually characterized by their narrow molecular weight distribution and a controlled degree of polymerization. Polydimethylsiloxane macromonomer with *p*-vinyl benzene at the chain end has been prepared in this way, by reacting *p*-chlorostyrene with  $\omega$ -chlorodimethylsiloxane [88].

### 2.9.2.2 The termination method

The termination method is typically achieved by end-capping of a living polymerization. In other words, with this method a polymerizable group is introduced via termination of a living polymerization system by a suitable functional group in order to provide a macromonomer. The components that impart the functional group to the polymer are termed deactivates. The most common activates include organic halides and esters [88]. Benzyl halides are well known to be efficient deactivates for a styrene living system, with a possible side reaction of the styryl carbanion with *p*-vinyl benzene chloride [88].

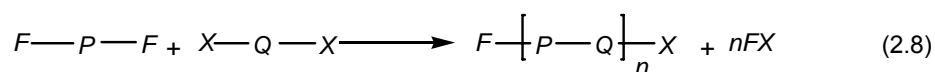
### 2.9.2.3 Functional end-group transformation

In this method we utilize any end-functionalized polymers, such as those obtained from chain-transfer-controlled radical polymerization and polycondensation. It is well known that the main function of the chain transfer agents in free radical polymerization is to control the molecular weight. In addition, an effective transfer agent may result in producing polymers with narrow polydispersity.

Numerous examples of macromonomers have been prepared by this method [90-93], for example, the polyethylene oxide macromonomer

### 2.9.2.4 Macromonomer by polyaddition polymerization

In polyaddition polymerization reactions conventional reactions between two functional groups F and X are used to build up polymer chains. These reactions yield polymers when they are carried out with difunctional molecules, either "FX-type" monomers (with complementary functional groups in one molecule, e.g. hydroxyl-carboxylic acids) or pairs of "FF"-type' and "XX"-type monomers (with the same type of functionality in one molecule, e.g. diols and diisocyanates), as shown in Equation 2.8.



where F and X are appropriate functional groups, P and Q are repeating monomer units, and n is the number-average degree of polymerization.

Polyaddition involving vinyl groups (F in Equation 2.8) is one of the convenient methods by which to prepare macromonomers directly [94]. Other examples of macromonomers

synthesized by this method include nitrogen-containing macromonomers such as polyamideamines [95], polyamines [96], polyguanamines [94] and silicon-containing macromonomers [95].

Linear type vinylurethane macromonomers with difunctionality have been synthesized by reaction of isocyanate-terminated prepolymer with methacrylamide [96, 97]. This vinylurethane macromonomer was then used in dispersion polymerization of styrene and methylmethacrylate [98].

### **2.9.3 Free radical polymerization of macromonomers**

The homopolymerization of macromonomers and copolymerization of macromonomers with comonomer is considered a very specific kinetic behaviour [99]. Thus, homo- and co-polymerization of macromonomers can be considered as the polymerization of two polymers together. Examples of the synthesis and copolymerization of macromonomers can be readily found in literature; an excellent review article on the subject has been prepared by Ito and Kawaguchi [88].

Free radical homopolymerization of macromonomers such as polystyrene and polymethyl methacrylate has been studied by Tanaka et al. [89] in great detail. They found that the overall rate of polymerization of the macromonomers is comparable to that of the monomers. The macromonomer polymerization could however be more difficult than the monomer polymerization. The difficulty arises from the fact that the macromonomers themselves are considered to be polymers. Thus, the viscosity of the solution could be high from the beginning of the polymerization. Secondly, the reactivity of the macromonomer in the polymerization is dependent on the chemical structure of the macromonomer. In the case of macromonomers the chain length could also affect the rate of polymerization due to diffusion. There are also many other aspects that can affect the kinetics of radical polymerization, which can be explained by discussing the initiation, propagation, termination, and chain transfer reactions.

### **2.10 Graft and block copolymerization of polyurethane**

The grafting of vinyl monomers into unsaturated polyurethane is usually accomplished in the aqueous phase using conventional polymerization techniques. Monomer and free radical initiators are added to the aqueous phase and grafting is carried out at a suitable temperature. Both anionic and cationic polyurethanes containing unsaturated polyester

polyols in their backbones have been used to graft acrylate monomers onto the main chain [100].

Polyurethane ionomeric dispersions can be modified by block copolymerization. NCO-terminated urethane prepolymers containing ionic groups are first capped with reactive diluents, such as 2-hydroxyethyl acrylate (HEA), via polyaddition. The potential ionic groups are then neutralized and terminal HEA moieties are polymerized with acrylate monomers, via free radical polymerization. The resulting block copolymers of polyurethane ionomers and polyacrylates are dispersed in water to obtain acrylate-modified polyurethane dispersions [101].

On other hand, graft and block copolymerization of polyurethanes can be made by crosslinking polyurethane dispersions using difunctional amines as chain extenders [102, 103]. For instance, for the crosslinking of polyurethane dispersions by emulsion polymerization, first vinyl-terminated aqueous polyurethane dispersions were prepared from aliphatic diisocyanate, polyol, ionic, diol and hydroxyl acrylate. Then suitable vinyl monomers and an initiator were added, and polymerized, to yield crosslinked aqueous polyurethane [104-106].

## 2.11 References

1. S. Asha, M. Thirumal, A. Kavitha and C. Pillai, *European Polymer Journal* **41** (2005) 5.
2. K. Mequanint, PhD Thesis, University of Stellenbosch, South Africa, Feb. 2001.
3. A. Christ and W. Hanford, U.S. Patent 233639 (1940).
4. F. Schmitt, A. Wenning, J. Weiss, *Progress in Organic Coatings* **34** (1998) 227.
5. K. Mequanint, MSc Thesis, University of Stellenbosch, South Africa, Dec. 1997.
6. W. Shenshen, U.S. Patent 20049099 (1979).
7. www.<http://statusreports-atp.nist.gov/reports/94-00027PDF.PDF>  
(accessed 15/12/2005)
8. S. Zhou, L. Wu, J. Sun and W. Shen, *Progress in Organic Coatings* **45** (2002) 33.
9. S. Moon, J. Kim, C. Nah and Y. Lee, *European Polymer Journal* **40** (2004) 1615.
10. L. Song, Y. Hu, Y. Tang, R. Zhang, Z. Chen and W. Fan, *Polymer Degradation and Stability* **87** (2005) 111.
11. A. Pattanayak and S. Jana, *Polymer* **46** (2005) 3275.

*Chapter 2: Historical and background*

---

12. J. Zheng, R. Ozisik and R. Siegel, *Polymer* **46** (2005) 10873.
13. G. Oertel, Ed. *Polyurethane Handbook*, 2nd ed. Hanser, New York (1993) 18.
14. K. Ito, H. Tsuchida, A. Hayashi, T. Kitano and E. Yamada, *Journal of Polymer* **17** (1985) 827.
15. D. Dounis and G. Wilkes, *Polymer* **38** (1997) 2819.
16. M. Mahkam and N. Sharifi, *Polymer* **80** (2003) 199.
17. K. Weiss, *Progress in Polymer Science* **22** (1997) 203.
18. H. Qi and M. Boyce, *Mechanics of Materials* **37** (2005) 817.
19. Q. Wei, L. Christopher and W. Macosko, *Polymer* **45** (2004) 1981.
20. H. Yeganeh and M. Shamekhi, *Polymer* **45** (2004) 359.
21. B. Briscoe and C. Kelly, *Polymer* **15** (1996) 3405.
22. P. Potschke, J. Piontecka and H. Stutz, *Polymer* **43** (2002) 6965.
23. H. Qi, M. Boyce, *Mechanics of Materials* **37** (2005) 817.
24. Y. Xiu, *Polymer* **33** (1992) 1335.
25. Y. Xiu, D. Wang, C. Hu and J. Li, *Journal of Applied Polymer Science* **48** (1993) 867.
26. G. Woods, *The ICI Polyurethane Book*, 2nd ed, John Wiley and sons, New York (1990) 78.
27. Z. Petrovic and J. Ferguson, *Progress in Polymer Science* **16** (1991) 695.
28. G. Edwardsa, P. Halleyb, G. Kerven and D. Martin, *Thermochimica/Acta* **429** (2005) 13.
29. M. Crawforda, R. Bass and T. Haas, *Thermochimica/Acta* **323** (1998) 53.
30. B. Dickie, *Thermochimica/Acta* **304** (1997) 347.
31. M. Yen and K. Chang, *Journal of Applied Polymer Science* **52** (1994) 1707.
32. D. Randall and S. Lee, *Polyurethane hand Book*, John Wiley and sons, New York (2002) 78
33. P. Thomes, *Water Borne and Solvent Based Surface Coatings*, John Wiley and sons, New York, **Vol. III** (1998) 51.
34. R. Jayakumar and S. Nanjundan, *European Polymer Journal* **41** (2005) 1623.
35. Y. Zhu, Y. Huang, Z. Chi and H. J. Shen, *European Polymer Journal* **30** (1994)1493.
36. D. Chattopadhyay, B. Sreedhar and K. Raju, *Polymer* **47** (2006)3814
37. N. Mahmood, PhD Thesis, University of Halle-Wittenberg, Germany (2005) 9.

38. A. Dombrow, Reinhold Plastics Applications Series, Polyurethanes, New York (1957) 75.
39. R. Register and S. Cooper, *Macromolecules* **23** (1993) 318.
40. D. Dietrich, *Progress in Organic Coatings* **9** (1981) 281.
41. T. Harjunalanen and M. Lahtinen, *European Polymer Journal* **39** (2003) 817.
42. S. Chen and J. Hsu, *Polymer* **34** (1993) 2776.
43. S. Seboa, MSc thesis, University of Stellenbosch, South Africa, Dec. 2002.
44. F. Wang, PhD Thesis, Faculty of the Virginia Polytechnic Institute and State University, April 1998.
45. J. Disteldorf, W. Heubel and E. Wolf, U.S. Patent 4476054 (1984).
46. S. Fukuoka, C. Masazumi and K. Masashi, *Journal of the Chemistry Society* **18** (1984) 399.
47. D. Chattopadhyay, P. Prasad and B. Sreedhar, *Progress in Organic Coatings* **54** (2005) 296.
48. J. Britain and P. Ge, *Journal of Applied Polymer Science* **4** (1960) 207.
49. A. Douglas, W. Zeno and J. Wicks, *Progress in Organic Coatings* **54** (2005) 141.
50. P. Bruins, Polyurethane Technology, John Wiley and sons, New York (1969) 72.
51. H. Orzesek, *Applied Catalysis A: General* **221** (2001) 303.
52. G. Wegener, M. Brandt, L. Duda, J. Hofmann, B. Kleszczewski, D. Koch, R. Kumpf, H. Orzesek, H. Pirkl, C. Six, C. Steinlein and M. Weisbeck, *Applied Catalysis A: General* **221** (2001) 303.
53. B. Elvers, S. Hawkins, G. Schulz, *Ullmann's Encyclopedia of Industrial Chemistry* John Wiley and sons, New York, **21A** (1992) 158.
54. E. Wilks, *Industrial Polymer Handbook*, John Wiley and sons, New York **1** (1988) 578.
55. M. Cunningham, *Progress in Polymer Science* **27** (2002) 1039.
56. B. Lee and H. Kim, *Polymer Degradation and Stability* **91** (2006) 1025.
57. Sartomer Company, Inc. Exton, Pennsylvania USA, [www.sartomer.com](http://www.sartomer.com) (accessed 28/03/2006).
58. RAHN Excellence in Energy Curing, [www.rahn-group.com](http://www.rahn-group.com) (accessed 29/03/2006)
59. G. Xu and W. Shi, *Progress in Organic Coatings* **52** (2005) 110.
60. H. Hanahata, E. Yamazaki and Y. Kitahama, *Polymer Journal* **29** (1997) 818.
61. S. Oprea, S. Vlad, A. Stanciu, C. Ciobanu and M. Macoveanu, *European Polymer Journal* **35** (1999) 1269.

62. F. Burel, L. Lecamp, B. Youssef, C. Bunel and J. Saiter, *Thermochemica/Acta* **326** (1999) 133.
63. J. Chen, J. Pascault and M. Taha, *Journal of Polymer Science. Part A: Polymer Chemistry* **34** (1996) 2889.
64. J. Vermeulen, MSc, University of Stellenbosch, Stellenbosch, December 1999.
65. J. Miroslav, M. Bohumil, L. Toman, P. Vlcek and P. Latalova, *Reactive Functional Polymers* **57** (2003) 137.
66. J. Salager and P. Becker, *Encyclopedia of Emulsion Technology*, **Vol. 3**, John Wiley and sons, New York, 1998.
67. W. David Polk, PhD thesis, University of Stellenbosch, Stellenbosch, July 2001.
68. M. Nasef and S. Hegazy, *Progress in Polymer Science* **29** (2004) 499.
69. H. Battared and G. Treger, *Graft Copolymerization*, Wiley-Interscience, New York, 1967.
70. H. Xie and D. Xie, *Progress in Polymer Science* **24** (1999) 275.
71. T. Schunk and T. Long, *Journal of Chromatography A* **692** (1995) 221.
72. K. Kato, E. Uchida, E. Kang, Y. Uyama and M. Ikada, *Progress in Polymer Science* **28** (2003) 209.
73. K. Beers, S. Gaynor, K. Matyjaszewski and M. Moeller, *Macromolecules* **26** (1998) 9413.
74. G. Carrot, J. Valmalette, C. Plummer, S. Scholz and J. Hilborn, *Colloid Polymer Science* **276** (1998) 853.
75. E. Park, H. Lee, H. Choi, D. Lee, I. Chin, K. Lee, C. Kim and J. Yoon, *European Polymer Journal* **37** (2001) 367.
76. A. Essel and Q. Pham, *Journal of Polymer Science, Part B*, **8** (1970) 723.
77. M. Takaki, R. Asarni and M. Ichikawa, *Macromolecules* **10** (1977) 850.
78. R. Quirk and Q. Zhuo, *Macromolecules* **30** (1997) 1531.
79. T. Altares, P. Wyman, R. Allen and J. Meyersen, *Polymer* **3** (1965) 131.
80. L. Norton, and J. McCarthy, *Macromolecules* **2** (1989) 1022.
81. H. Uyama and S. Kobayashi, *Macromolecules* **24** (1991) 614.
82. R. DeClercq and J. Goethals, *Macromolecules* **25** (1992) 1109.
83. R. Asami, M. Takaki and K. Kyuda, *Polymer* **15** (1983) 139.
84. T. Suzuki and T. Okawa, *Polymer* **2** (1988) 2095.
85. B. Charleux and C. Pichot, *Polymer* **34** (1993) 195.
86. W. Richtering, R. Loffler and B. Wurchard, *Macromolecules* **25** (1992) 3642.

*Chapter 2: Historical and background*

---

87. R. Asami, M. Takaki, and H. Hanahata, *Macromolecules* **16** (1981) 628.
88. K. Ito and S. Kawaguchi, *Advances in Polymer Science* **142** (1999) 129.
89. Y. Tsukahara, K. Tsutsumi, Y. Yamashita and S. Shimada, *Macromolecules* **23** (1990) 5201.
90. V. Percec and H. Wang, *Journal of Polymer Science: Part A: Polymer Chemistry* **28** (1990) 1059.
91. M. Izawa, S. Nunomoto and Y. Kawakami, *Polymer* **25** (1993) 873.
92. T. Uryu, M. Yamanaka, M. Date, M. Ogawa and K. Hatanaka, *Macromolecules* **21** (1988) 1916.
93. J. Hawker and J. Frechet, *Polymer* **33** (1992) 1507.
94. H. Kunisada, Y. Ukai, S. Nishimori and A. Masuyama, *Journal of Polymer Science* **23** (1991) 1455.
95. Y. Nagasaki, R. Ukai, M. Kato and T. Suruta, *Macromolecules* **27** (1994) 7236.
96. K. Lee, S. Shim, H. Jung, S. Kim and S. Choe, *Macromolecules* **38** (2005) 2686.
97. H. Jung, S. Y. Kim, K. Lee, B. H. Lee, S. E. Shim and S. Choe, *Journal of Polymer Science, Part A: Polymer Chemistry* **43** (2005) 3566.
98. B. Charleux, C. Pichot and M. Llauro, *Polymer* **34** (1993) 4352.
99. S. Tanaka, M. Uno, S. Teramachi and Y. Tsukahara, *Polymer* **36** (1995) 2219.
100. F. Herman, M. Norbert, G. Charles, M. George and I. Jacqueline, *Encyclopedia of Polymer Science and Engineering*, Wiley-Interscience, John Wiley and sons, New York, 1986, p 192.
101. J. Rosthauser and K. Nachtkamp, *Advances in Urethane Science* **23** (1987) 10121.
102. S. Shim, H. Jung and K. Lee, *Journal of Colloid and Interface Science* **279** (2004) 664.
103. B. Kim and J. Lee, *Polymer* **37** (1996) 469.
104. H. Li and E. Ruckentein, *Polymer* **36** (1995) 2281.
105. C. Bamford, G. Eastmond and D. Wittle, *Polymer* **10** (1969) 771.
106. J. Liu, H. Zhou, C. Hou and S. Ni, *Polymer* **32** (1991) 321.

## Chapter 3

### Experimental work

#### 3.1 Introduction

The experimental procedures used to synthesize the acrylate–urethane graft copolymers are described in this chapter. The first task (Section 3.2) was to synthesize the UMs with different chain lengths, according to formula 3.1 below:



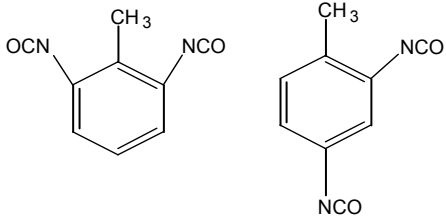
where HEMA is 2-hydroxyethyl methacrylate, EG is ethylene glycol, TDI is toluene diisocyanate (consisting of a mixture of 20% of the 2,6 isomer and 80% of the 2,4 isomer), and  $x$  can be either 4, 8, 12, or 32. The second task (Section 3.3) was to incorporate various percentages of the synthesized UMs into the acrylic monomers (MMA or n-BMA) in solution via free radical copolymerization. The percentages of macromonomer to be incorporated were: 0, 5, 10, 15, 20, 25, 30 and 40% by weight (according to monomer). The acrylate–urethane copolymers were to be characterized by  $^1\text{H-NMR}$  and  $^{13}\text{C-NMR}$ , FTIR, TGA, DSC, GPC, and DMA.

#### 3.2 Synthesis of urethane macromonomers

##### 3.2.1 Raw materials

The raw materials used for the synthesis of the UMs are tabulated in Table 3.1.

**Table 3.1: Reagents used for PU formulations**

Raw material	Chemical structure	Source
<b>Toluene diisocyanate (TDI)</b>	 <p style="text-align: center;">                 2,6 TDI (20%)                  2,4 TDI (80%)             </p>	Bayer
<b>Ethylene glycol (EG)</b>	$\text{HO}-\overset{\text{H}_2}{\text{C}}-\overset{\text{H}_2}{\text{C}}-\text{OH}$	Sigma-Aldrich
<b>2-hydroxyethyl methacrylate (HEMA)</b>	$\text{OH}-\text{CH}_2-\text{CH}_2-\text{O}-\overset{\text{O}}{\parallel}{\text{C}}-\underset{\text{CH}_2}{\text{C}}-\text{CH}_3$	BASF
<b>Isopropanol</b>	$\begin{array}{c} \text{CH}_3 \\   \\ \text{CH}_3-\text{CH}-\text{OH} \end{array}$	Sigma-Aldrich

The following reagents were dried as follows prior to use:

- HEMA and EG were dried over a 3<sup>o</sup>A molecular sieve (the molecular sieve was first dried in a vacuum oven for 24 h at 100 °C)
- MEK was dried over a 3<sup>o</sup>A molecular sieve.

### 3.2.2 Experimental setup

The following equipment was used for UM synthesis: a 250-ml three-neck flask, nitrogen gas inlet, oil bath, reflux condenser, temperature controller unit, magnetic stirrer, bubbler, glass syringe, packed column with molecular sieve, and calcium chloride to prevent any moisture entering the reactor vessel/flask.

### 3.2.3 Polyurethane macromonomer formulations

Formulations for the preparation of the UMs are tabulated in Table 3.2.

**Table 3.2: Formulations used for the preparation of polyurethane macromonomers**

Raw material	UM having X=4 (mass, g)	UM having X=8 (mass, g)	UM having X=12 (mass, g)	UM having X=32 (mass, g)
<b>TDI</b>	33.61	34.98	35.54	21.79
<b>EG</b>	9.58	11.08	11.69	7.53
<b>HEMA</b>	4.01*	2.32*	1.63*	0.41*
<b>Isopropanol</b>	2.78*	1.60*	1.13*	0.29*
<b>Total mass</b>	50	50	50	30
<b>Excess of isopropanol</b>	3.54**	3.66**	3.72**	2.06**
<b>[OH]/[NCO]</b>	1.15	1.15	1.14	1.13

\* The amounts of HEMA, isopropanol, TDI and EG used to synthesize UMs were calculated as mole % according to the formula 3.1 (Section 3.1) at [OH]/ [NCO] mole ratio 1:1, in which HEMA was calculated as 40 mole % in the UM chain end and isopropanol was calculated as 60 mole % in the UM chain end.

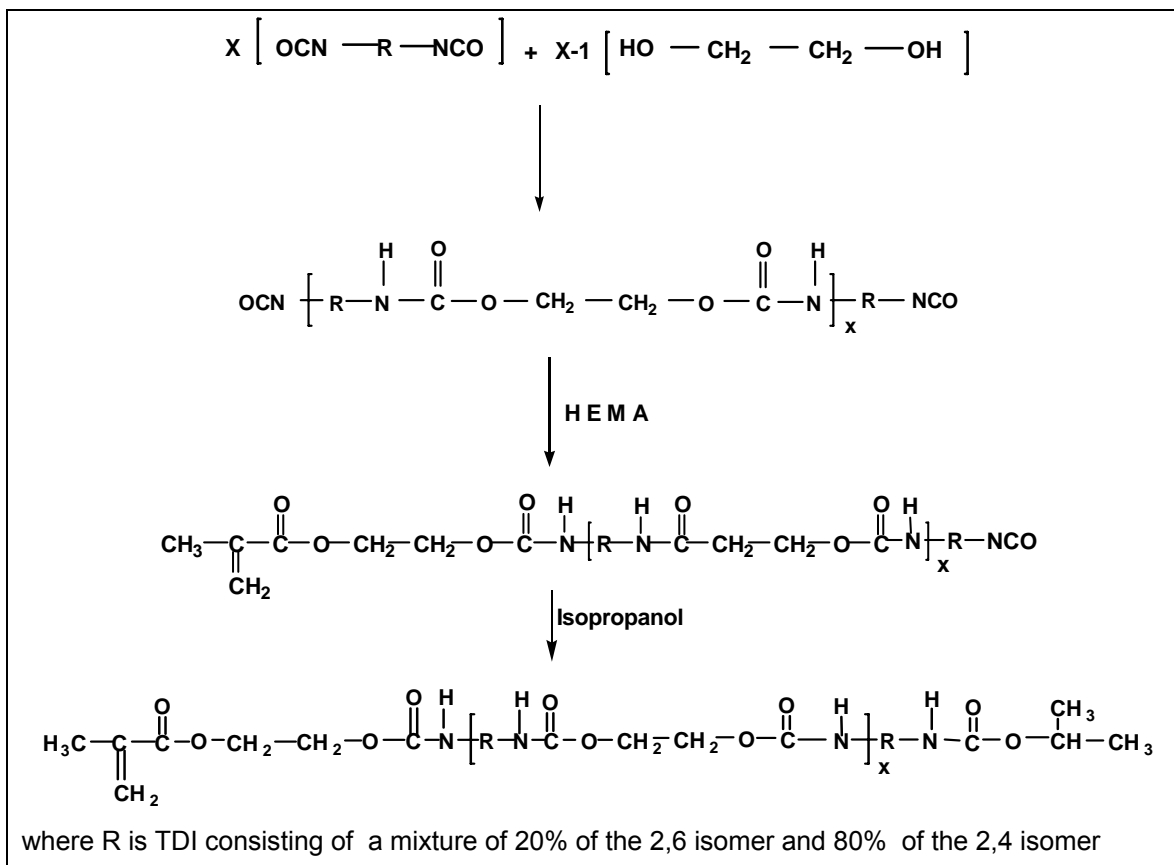
\*\* The excess amount of isopropanol was needed to ensure that all reactive NCO group were fully reacted. If not, then secondary reactions will take place, to ultimately form crosslinked structures (see chapter 2). Thus, the minimum quantities of excess isopropanol were experimentally determined to be 0.15 moles (using FTIR), to ensure that all the NCO groups are fully reacted.

### 3.2.4 Experimental procedure

The TDI and MEK were added to the reaction vessel, and then cooled to below 10 °C in a cold water bath. Thereafter the reactor was sealed, and purged with nitrogen gas. This was followed by addition of the ethylene glycol all at once, under stirring (400-500 rpm). The temperature was increased to 15-18 °C and held for there 30-60 minutes, to form urethane chains with excess isocyanate end groups (prepolymer). The reaction temperature was then increased to 20-30 °C and HEMA was added all at once. The reaction was allowed to run over 60 minutes. Thereafter the reaction temperature was increased again to 30-35 °C and then all the isopropanol was added all at once. This was done to ensure that all the isocyanate was reacted. If some of the isocyanate remained unreacted it could lead to secondary reactions, resulting in crosslinking. The reaction temperature was increased again to 55 °C to ensure all unreacted isocyanate had reacted. Once the absorption peak of the isocyanate group at 2270 cm<sup>-1</sup> in the FTIR spectra was no longer visible, the reaction was considered to be completed. The obtained UMs were then dried in a vacuum oven at 45 °C for 24 hours and then stored in a desiccator until required for use in further polymerization reactions.

### 3.2.5. Reaction scheme of the synthesis of urethane macromonomers

An outline of the synthesis of the UMs is shown in Scheme 3.1.



**Scheme 3.1: Formation of urethane macromonomers (when HEMA reacts at one side and isopropanol at the other side of the UM).**

Three different methods were used to try to optimize the reaction conditions to ensure incorporation of HEMA into the one chain end and isopropanol into the other during UM synthesis. After polyurethane with excess isocyanate was prepared (first step in reaction Scheme 3.1) the temperature was decreased to 10 °C then the following respective procedures were used:

- 1) HEMA was added all at once and the temperature was kept at between 20-25 °C for 45-60 minutes to get a homogenous mixture, followed by the addition of all the isopropanol at once for 45-60 minutes.
- 2) HEMA was added dropwise at 20 °C and the reaction temperature was kept at 20-30 °C for 45-60 minutes, followed by the addition of all the isopropanol at once for 45-60 minutes.

3) HEMA and isopropanol were added in fractions at 20 °C and the reaction temperature was kept at 20-30 °C for 60-90 minutes.

It was found that method 1 was the best, as it gave the highest yield of graft copolymers. This will be discussed in more detail later.

### **3.3 Synthesis of acrylate-urethane graft copolymers**

#### **3.3.1 Introduction**

Most graft copolymers are formed by the reaction of a parent polymer, containing reactive sites (macromonomer technique), with a second type of monomer. In this study UMs were grafted with MMA and with n-BMA respectively. The success of the grafting reactions was determined by characterizing the products by <sup>1</sup>H NMR, <sup>13</sup>C NMR, GPC, FTIR, DMA and TEM.

#### **3.3.2 Experimental**

Various amounts of UMs were copolymerized with various amounts of MMA, and with various amount of BMA, respectively, using solution free radical copolymerization.

##### **3.3.2.1 Solvent**

The choice of a good solvent for the acrylate and UM was done by trail and error. Many different solvents were tried such as benzene, toluene, acetone, acetonitrile, methanol, ethanol, dimethylformamide (DMF), dimethylsulfoxide (DMSO). Complete separation of the UM and acrylate was achieved by using DMF or DMSO. However, DMSO could not readily be used due to the fact DMSO crystallizes at room temperature and needs to be heated before use. Therefore DMF was chosen as the solvent for all the copolymerization reactions of acrylate and UM.

##### **3.3.2.2 Materials**

n-BMA (Aldrich, 99%) and MMA (ICI Chemicals and Polymers, 99.9%) were washed with a 0.3 M potassium hydroxide solution (KOH, Associated Chemical Enterprises, 85%) followed by distillation under reduced pressure to remove the inhibitor. The monomers were stored for 24 hours at 0 °C over molecular sieves (4A°). The following materials were also used: methanol (MeOH, 99.8%), dimethylformamide (DMF, 99.5%), distilled and deionized water (DDI, from a Millipore milli-Q purification system) and silicon

Chapter 3: Experimental work

oil (SA Silicones). 2,2'-Azobis(isobutyronitrile) (AIBN, Delta Scientific, 98%) was recrystallized from methanol. The urethane macromonomers (see Table 3.2) were synthesized as described earlier in Section 3.2.6.

**3.3.2.3 Acrylate-urethane copolymer formulations**

Formulations of the different PMMA-urethane graft copolymers and n-PBMA-urethane graft copolymers are shown below in Tables 3.3 and 3.4, respectively.

**Table 3.3: Formulations for the preparation of PMMA-urethane graft copolymers**

Series number	Reagents	Mass of reagents used in various experiments (1-7)						
		EXP.1* (g)	EXP.2* (g)	EXP.3* (g)	EXP.4* (g)	EXP.5* (g)	EXP.6* (g)	EXP.7* (g)
1	MMA	5.00	4.75	4.50	4.25	4.00	3.75	3.50
	AIBN**	0.05	0.047	0.045	0.042	0.040	0.037	0.035
	UM (X=4)	0.00	0.25	0.50	0.75	1.00	1.25	1.50
	DMF	35.00	35.23	35.20	35.12	35.28	35.45	35.18
2	MMA	5.00	4.75	4.50	4.25	4.00	3.75	3.50
	AIBN**	0.05	0.047	0.045	0.042	0.040	0.037	0.035
	UM (X=8)	0.00	0.25	0.50	0.75	1.00	1.25	1.50
	DMF	35.17	35.47	35.29	35.33	35.46	35.32	35.23
3	MMA	5.00	4.75	4.50	4.25	4.00	3.75	3.50
	AIBN**	0.05	0.047	0.045	0.042	0.040	0.037	0.035
	UM(X=12)	0.00	0.25	0.50	0.75	1.00	1.25	1.50
	DMF	35.24	35.57	35.11	35.08	35.09	35.12	35.35
4	MMA	5.00	4.75	4.50	4.25	4.00	3.75	3.50
	AIBN**	0.05	0.047	0.045	0.042	0.040	0.037	0.035
	UM (X=32)	0.00	0.25	0.50	0.75	1.00	1.25	1.50
	DMF	35.35	35.21	35.44	35.29	35.09	35.19	35.28

\*The concentrations of the UMs were between 0 and 30 wt% (relative to MMA), and the amounts of urethane macromonomer and MMA in all copolymerization feeds were based on 5 g.

**Table 3.4: Formulations for the preparation of n-PBMA-urethane graft copolymers**

Series number	Reagents	Mass of reagents used in various experiments (1-7)						
		EXP.1* (g)	EXP.2* (g)	EXP.3* (g)	EXP.4* (g)	EXP.5* (g)	EXP.6* (g)	EXP.7* (g)
1	n-BMA	5.00	4.75	4.50	4.25	4.00	3.75	3.50
	AIBN**	0.05	0.047	0.045	0.042	0.040	0.037	0.035
	UM (X=4)	0.00	0.25	0.50	0.75	1.00	1.25	1.50
	DMF	35.00	35.23	35.20	35.12	35.28	35.45	35.18
2	n-BMA	5.00	4.75	4.50	4.25	4.00	3.75	3.50
	AIBN**	0.05	0.047	0.045	0.042	0.040	0.037	0.035
	UM (X=8)	0.00	0.25	0.50	0.75	1.00	1.25	1.50
	DMF	35.09	35.34	35.45	35.22	35.38	35.19	35.28
3	n-BMA	5.00	4.75	4.50	4.25	4.00	3.75	3.50
	AIBN**	0.05	0.04	0.04	0.04	0.04	0.03	0.03
	UM (X=12)	0.00	0.25	0.50	0.75	1.00	1.25	1.50
	DMF	35.16	35.29	35.15	35.54	35.32	35.08	35.44
4	n-BMA	5.00	4.75	4.50	4.25	4.00	3.75	3.50
	AIBN**	0.05	0.047	0.045	0.042	0.040	0.037	0.035
	UM (X=32)	0.00	0.25	0.50	0.75	1.00	1.25	1.50
	DMF	35.27	35.11	35.54	35.27	35.36	35.14	35.52

\*The concentrations of the UMs were between 0 and 30 wt% (relative to n-BMA), and the amounts of urethane macromonomer and n-BMA in all copolymerization feeds were based on 5 g.

\*\* The concentration of initiator (AIBN) was varied between 0.7 to 1% by weigh according to n-BMA this is actually considered slightly high, and will affect the molecular weight of graft copolymers. These concentrations of initiator were chosen due to the fact that at low concentration of initiator, the yield of graft copolymer was very low (as can be seen in Table 3.5) because of the high chain transfer constant to DMF, the solvent used.

**Table 3.5: Effect of the concentration of initiator on yield of graft copolymers**

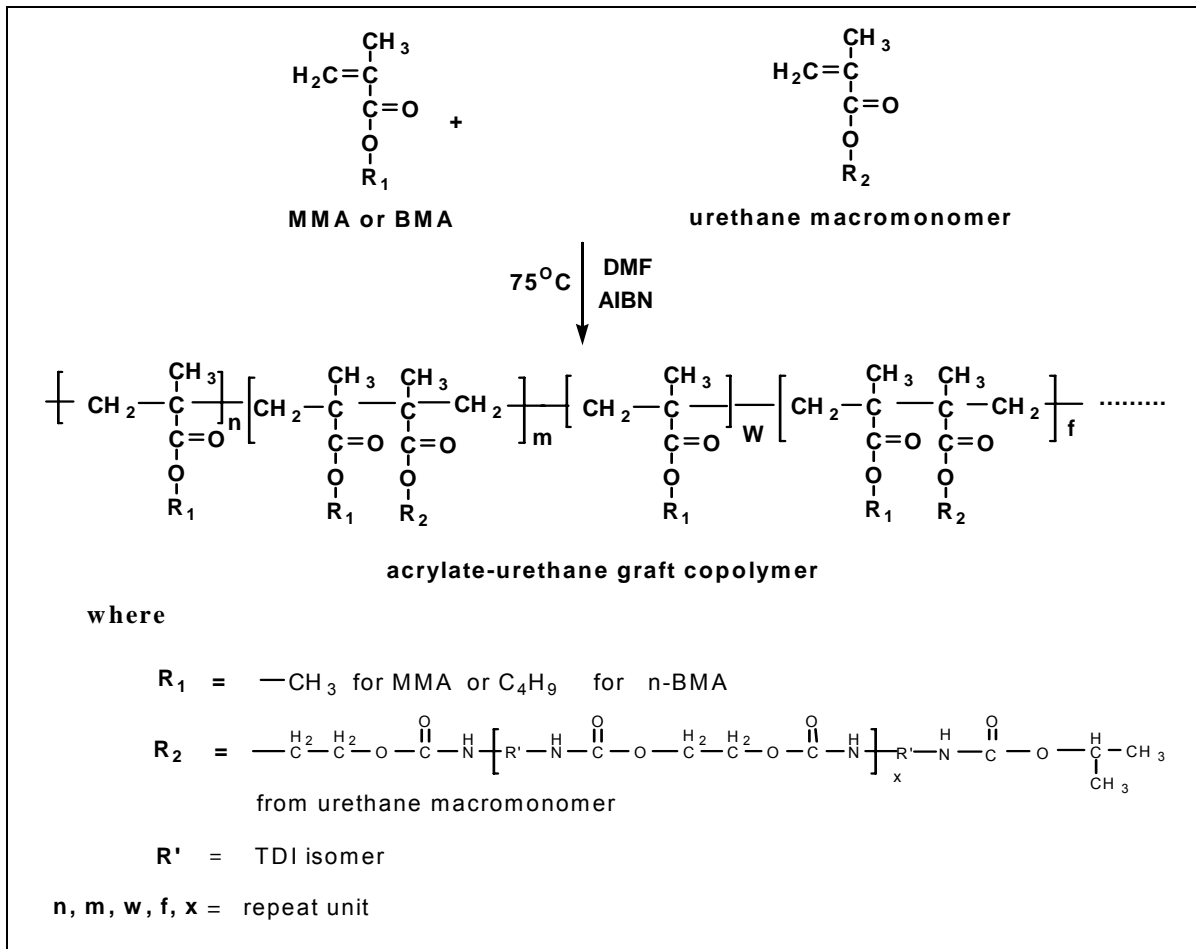
Concentration of AIBN (%)	Feed polymerization			graft yield from PMMA-g-urethane (g)	graft yield from PBMA-g-urethane (g)
	UM (X=8) (g)	MMA (g)	n-BMA (g)		
0.1	0.25	4.75	4.75	1.54	1.92
0.3	0.25	4.75	4.75	2.32	2.81
0.5	0.25	4.75	4.75	2.71	3.15
0.7	0.50	4.50	4.50	3.74	3.94
1	0.50	4.50	4.50	3.85	4.01
1.3	0.50	4.50	4.5	3.18	3.32

### 3.3.2.4 Experimental procedure

Solution free radical copolymerization was carried out in a 250-ml three-neck reactor with magnetic stirring, under a nitrogen atmosphere. Scheme 3.2 shows the synthesis procedure for the graft copolymers. Solution free radical copolymerization was carried out in a 250-ml three-neck reactor with magnetic stirring, under a nitrogen atmosphere. DMF was first introduced into the reactor. MMA or BMA, and AIBN (1% wt relative to the monomer), were then charged into the reactor, followed by the UM. Various concentrations of all the different chain lengths of urethane macromonomers were used: 0, 5, 10, 15, 20, 25, 30 and 40 wt% relative to MMA or n-BMA. The polymerization temperature was 75 °C and the reaction time was 18 hours. The solution of polymer product was poured into 400 ml methanol to precipitate the polymer out of solution. The copolymers were dried overnight in a vacuum oven at 40 °C. Dried samples were analyzed by NMR GPC, TGA, TEM and DMA.

### 3.3.2.4 Reaction scheme for graft copolymerization

The copolymerization of the urethane macromonomer with acrylate monomer is described in Scheme 3.2



Scheme 3.2: Formation of acrylate-urethane graft copolymer.

## Chapter 4

### Analytical Methods

#### 4.1 Introduction

The following analytical techniques were used during the synthesis of the UMs, as well as to characterize the final graft copolymer products:

- Fourier-transform infrared spectroscopy (FTIR)
- Proton NMR spectroscopy ( $^1\text{H}$  NMR)
- Carbon NMR spectroscopy ( $^{13}\text{C}$  NMR)
- Gel permeation chromatography (GPC)
- Thermogravimetric analysis (TGA)
- Dynamic mechanical analysis (DMA)
- Transmission electron microscopy (TEM)

#### 4.2 Fourier-transform infrared spectroscopy (FTIR)

Fourier-transform infrared spectroscopy was used to follow and characterize the emerging and disappearing functional groups during the preparation of the UMs and the graft copolymers that were synthesized [1-3]. During the synthesis of the UMs, FTIR samples were prepared by extracting some polymer (dissolved in MEK) from the reactor. The samples were then run against a MEK background between sodium chloride discs. This was done to monitor the NCO content during the UM synthesis.

Infrared spectra were obtained with a Perkin Elmer 1650 Fourier-transform infrared spectrophotometer, and recorded by averaging 32 scans.

#### 4.3 Nuclear magnetic resonance spectroscopy (NMR)

The structures of UMs and acrylate-urethane graft copolymers were determined by NMR analysis.

##### 4.3.1 Proton NMR ( $^1\text{H}$ NMR)

$^1\text{H}$  NMR spectra were measured on a Varian 300 MHz and 600 MHz instrument using  $\text{CDCl}_3$  or DMSO as solvents, depending on the solubility of the material being analyzed.

DMSO was used as solvent for UM samples and  $\text{CDCl}_3$  as solvent for all graft copolymer samples. All spectra were referenced to tetramethylsilane (TMS) at 0 ppm.

### **4.3.2 Carbon NMR ( $^{13}\text{C}$ NMR)**

$^{13}\text{C}$  NMR spectra were obtained in the same manner as the proton  $^1\text{H}$  NMR spectra, but at a frequency of 600 MHz. Long runs were used (overnight).

## **4.4 Gel permeation chromatography (GPC)**

### **4.4.1 Introduction**

Gel permeation chromatography is widely used to obtain molecular weight and molecular weight distribution data. In the conventional mode, a GPC column is first calibrated with a polystyrene standard, whose molecular weight is known, in order to determine the relationship between elution volume and the molecular weight of the polystyrene standard. Then, the molecular weight of an unknown polymer is determined by comparing the elution volume of this polymer to that of the polystyrene standard, assuming the same elution volume results in the same molecular weight. Therefore, this molecular weight is actually referred to as the molecular weight compared to polystyrene. Obviously, the conventional method cannot yield the absolute molecular weight of a polymer since the elution volume is only directly proportional to the size of the polymer, which in turn is related to the hydrodynamic volume of the polymer. For homopolymers, condensation polymers and strictly alternating copolymers, there is a correlation between elution time and molar mass. Thus, chemically similar polymer standards of known molar mass can be used for calibration.

### **4.4.2. Gel permeation chromatography coupled with multiple detectors**

One must exercise extreme care when analyzing heterogeneous systems such as copolymers and polymer blends by GPC. The dimensional distribution of macromolecules can generally only unambiguously correlate with the MMD within one heterogeneity type. For samples consisting of molecules of different chemical compositions, the distributions obtained represent an average of dimensional distributions of molecules having different compositions and, therefore, cannot be attributed to a certain type of molecule.

In the analysis of binary copolymers, GPC with multiple concentration detectors can be used if the response factors of detectors for the components of the polymer are sufficiently different. The chemical composition of each slice of an elution curve can be determined from the detector signals. Typically, a combination of an ultraviolet index (UV) and a refractive index (RI) is used. The common combination of a RI and a UV detector can only be applied if at least one of the monomers of the copolymer absorbs at a suitable wavelength, and if the UV spectra of both components are sufficiently different. Successful applications of this setup include the analysis of mixtures of polystyrene with PMMA, polybutadiene (PB), polyvinyl chloride or poly butyl methacrylate [4]. A RI detector provides the total elution profile, whereas the UV detector yields the elution profile of an absorbing polymer.

Gel permeation chromatography was used to determine the molecular weights of the UMs prepared in this study. Samples of UMs were dried at 40 °C for 24 h under vacuum and then dissolved in THF.

GPC analyses was carried out using a Waters model 610 pump, Waters model WISP 717 autoinjector, model 410 refractive index detector and model 486 UV detector (at 254 nm). THF was used as solvent at a flow rate of 1.0 ml/min and calibration was done using polystyrene standards.

#### **4.5 Dynamic mechanical analysis (DMA)**

Dynamic mechanical analysis is an increasingly useful technique for the characterization of polymers and viscoelastic properties [5-7]. DMA measures the mechanical properties of a material, such as the modulus (stiffness) and damping (energy dissipation) as a function of temperature and frequency under periodic (oscillatory) stress. The properties that can be obtained by means of the DMA technique are the glass transition temperature ( $T_g$ ), damping characteristics, degree and rate of cure, and polymer morphology. DMA is the study of the movement of polymer chains by the application of a sinusoidally varying total force programmed in MilliNewton (Mn) as applied to the polymer [5]. The total force applied to the polymer is the sum of static force and dynamic force, with chosen frequency. The sample responds to the applied force with oscillating amplitude. The sample also responds to the applied force with a phase lag ( $\delta$ ).

Dynamic mechanical analysis of UMs and acrylate-urethane graft copolymers prepared in this study was carried out on a Perkin Elmer DMA 7e using the thin-film extension mode. The frequency was 1 Hz and the heating rate was 5 °C/min. The sample was a 0.3-mm thick, solution-cast film, which was dried before testing.

#### **4.6. Dynamic thermogravimetry (TGA)**

Thermogravimetric analysis [4, 6, 7] is especially useful for studying polymers and composite materials. It measures the amount, and the rate, of change in the weight of a material as a function of temperature or time, in a controlled atmosphere. TGA measurements are primarily used to determine the composition of materials and to predict their thermal stabilities at temperatures up to 1000 °C. TGA can be used to characterize a material that exhibits weight loss or gain due to decomposition, oxidation or dehydration. Results of TGA analysis provide information on the composition of multi-component systems, the thermal and oxidative stability of materials, their estimated lifetime and decomposition kinetics.

TGA analyses of the UMs and acrylate-urethane copolymers were carried out using a TGA-50 SHIMADZU thermogravimetric instrument with a TA-50WSI thermal analyzer connected to a computer. Samples (10-15 mg) were degraded in nitrogen or air (flow rate 50 ml/min) at a heating rate of 2.5°C/min.

#### **4.7. Transmission electron microscopy (TEM)**

TEM was used to directly visualize the morphology of the urethane-acrylate graft copolymers. Bright-field TEM images were recorded on a JEM 200CX (JEOL Tokyo, Japan) TEM at an accelerating voltage of 120 kV. Prior to analysis, samples of urethane-acrylate graft copolymers were stained with OsO<sub>4</sub>, then embedded in epoxy resin and cured for 24 h at 60 °C. The embedded samples were then ultra-microtomed with a diamond knife on a Reichert Ultracut S ultra-microtome at room temperature. This resulted in sections with a nominal thickness of ~ 100 nm. The sections were transferred from water at room temperature to 300-mesh copper grids, which were then transferred to the TEM apparatus.

#### **4.8 References**

1. J. Fuente, M. Wilhelm, H. Spiess, E. Madruga, M. Fernandez-Garcia and

- M. Cerrada, *Polymer* **46** (2005) 4544.
2. S. Asha, M. Thirumal, A. Kavitha and C. Pillai, *European Polymer Journal* **41** (2005) 23.
3. D. Otts, S. Dutta, P. Zhang, O. Smith, S. Thames and M. Urban, *Polymer* **45** (2004) 6235.
4. B. Elvers, S. Hawkins and W. Russey, *Ullmann's Encyclopedia of Industrial Chemistry*, VCH Publishers, New York, **Vol. B6**, 1993, 9.
5. H. Tan, J. Li, M. Guo, R. Du, X. Xie, Y. Zhong and Q. Fu, *Polymer* **46** (2005) 7230.
6. Y. Chen, S. Zhou, H. Yang, G. Gu and Limin Wu, *Journal of Colloid and Interface Science* **279** (2004) 370.
7. J. Yang and H. Lin, *Journal of Membrane Science* **187** (2001) 159.
8. H. Kumar and A. Anil Kumar, *Polymer Degradation and Stability* **91** (2006) 1097.
9. Ju. Lee, H. Bang, E. Park, C. Baek, B. Rhee and S. Lee, *Synthetic Metals* **144** (2004) 159.
10. T. Chang, C. Liao, K. Wu, H. Chen and J. Yang, *Polymer Degradation and Stability* **66** (1999).

## Chapter 5

### Results and Discussion

The results of experiments carried out to prepare and characterize the urethane macromonomers and the acrylate-urethane graft copolymers, as described in Chapters 3 and 4, are presented here.

#### 5.1. Fourier-transform infrared spectroscopy

FTIR analysis was employed firstly to monitor the isocyanate (NCO-groups) consumption during the UM synthesis, secondly to characterize the UM itself, and thirdly to characterize the acrylate-urethane graft copolymers.

##### 5.1.1 NCO content

The presence of the free –NCO of TDI during the synthesis of the UM pre-polymer is seen in the FTIR spectrum of UM at  $2275\text{ cm}^{-1}$  in Figure 5.1a. The absence of the characteristic NCO-peak at  $2275\text{ cm}^{-1}$  in Figure 5.1.b indicates that all the isocyanate had reacted with EG, isopropanol and HEMA during polymerization. It is very important that no NCO groups remain, because if there is any moisture present, unwanted crosslinked structures will form (especially during the copolymerization stage).

##### 5.1.2 Characterization of the urethane macromonomers

The structure of the UMs was verified by FTIR spectroscopy. The FTIR spectra of the UM of different chain lengths are shown in Figure 5.1b. FTIR spectra of all the UMs show absorption bands between  $2954$  and  $2968\text{ cm}^{-1}$ , due to the asymmetrical and symmetrical C-H stretching of methylene [1]. The absorption band between  $3200$  and  $3350\text{ cm}^{-1}$  in the FTIR spectrum (Figure 5.1.a) represent the OH-groups of the UM prepolymer. These OH- bands disappear in the UMs as seen in the FTIR spectrum (Figure 5.1.b). There is a strong N-H stretching band of the urethane groups at about  $3312$ - $3315\text{ cm}^{-1}$  [2]. The absorption band at  $1532$ - $1545\text{ cm}^{-1}$  is due to the N-H deformation vibration of urethane [1]. The bands around  $1711$ - $1720\text{ cm}^{-1}$  are attributed to the carbonyl stretching of urethane groups [3]. The absorption band at  $1805\text{ cm}^{-1}$  corresponds to C=C, indicating the formation of the urethane macromonomer [4]. UMs

having similar structures have been described in literature [5-7]. A complete list of FTIR groups of UM is given in Table 5.1.

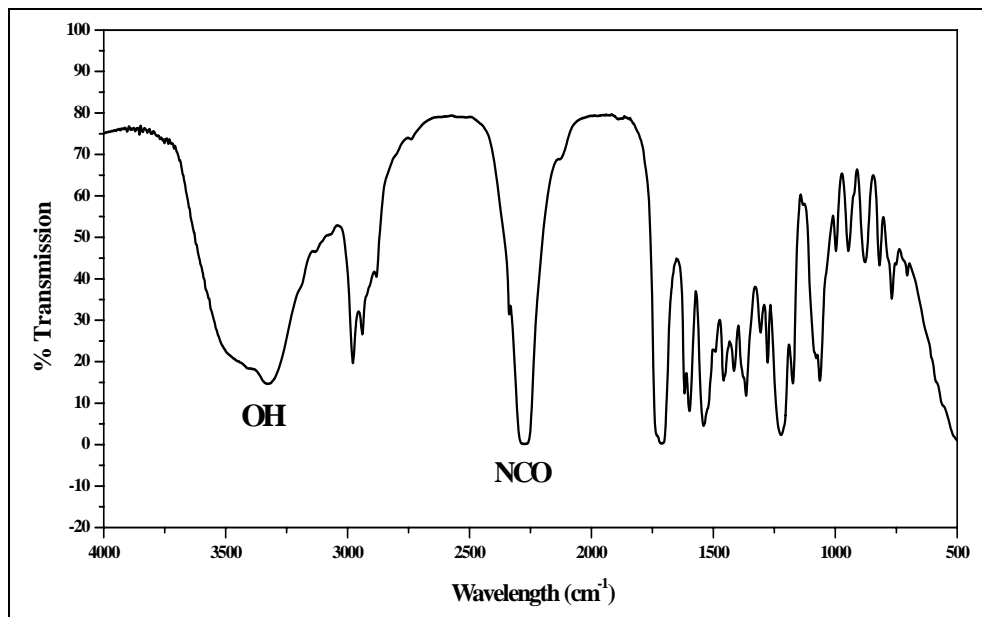


Figure: 5.1 (a) FTIR of UM prepolymer before addition of isopropanol + HEMA

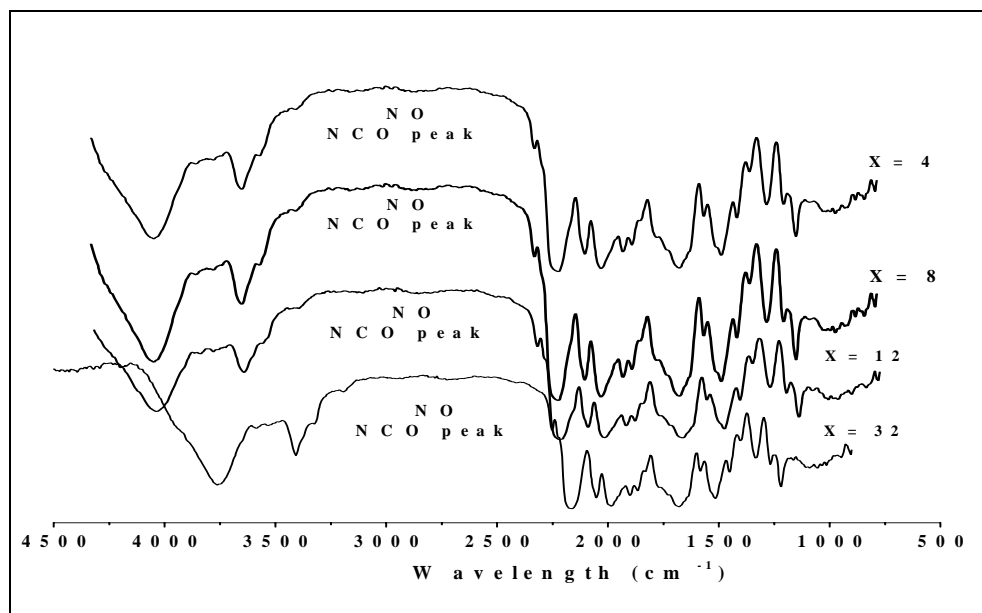


Figure: 5.1 (b) FTIR of UM after addition of isopropanol + HEMA

Figure 5.1: FTIR spectra showing the presence and absence of NCO groups (a) before addition of isopropanol + HEMA, (b) after addition of isopropanol + HEMA.

**Table 5.1: FTIR peak assignment of the UMs [1-6]**

Wavelength number (cm <sup>-1</sup> )	Assignment	Reference
3307-3312	Stretching vibration of the urethane N-H bond	2
2954-2968	Stretching vibration of the aliphatic C-H bond	1
1805-1808	Stretching vibration of C=C in RCH=CH <sub>2</sub> of HEMA	4
2275 -2260	ps isocyanatefree grou	3,4
1711-1720	Amide I, stretching vibration of the of the ester C=O bond	3
1601	Stretching vibration of the aromatic ring C-C	5,6
1532	Amide II, stretching vibration of the benzene ring	1
1450	Bending vibration of the aliphatic C-H bond	1
1414	Stretching vibration of C-C in RCH=CH <sub>2</sub> Stretching vibration of the benzene C-C	1,2
1329	Parallel vibration of C-H bond in CH <sub>2</sub>	1
1180	Twisting vibration of C-H in CH <sub>2</sub>	1
1112	Symmetric stretching vibration of the CO-O-C	1
1060	Symmetric stretching vibration of the CO-O-C	1
882	Out-of-the p Out-of-the plane bending of CH in RCH=CH Out-of-the plane bending of CH in benzene ring	7
816	Vibration of aromatic CH	2
768	Vibration of aromatic CH	2

### 5.1.3 PMMA and n-PBMA homopolymers

The FTIR spectra of PMMA and n-PBMA homopolymers, which will later be used as references for graft copolymerization, are shown in Figures 5.2 and 5.3 respectively.

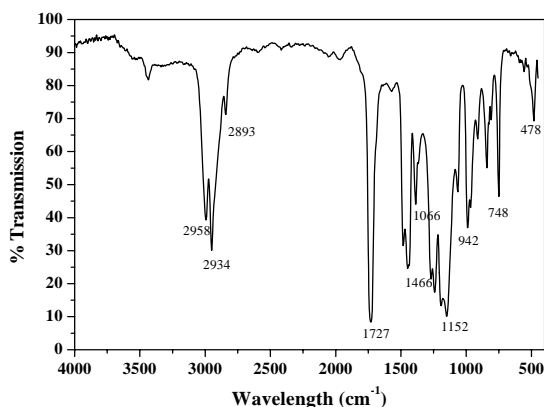


**Figure 5.2: FTIR spectrum of PMMA homopolymer.**

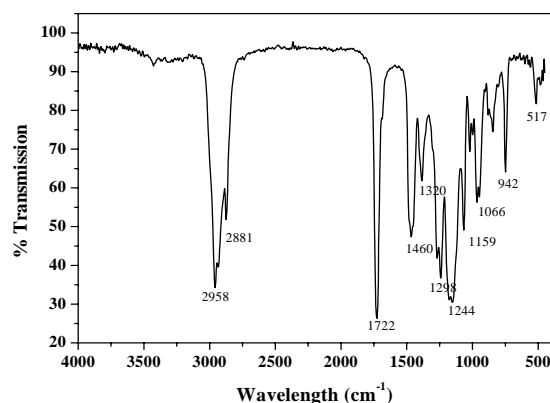


**Figure 5.3: FTIR spectrum of n-PBMA homopolymer.**

A complete list of FTIR peak assignments of the synthesized PMMA and n-PBMA homopolymers is given in Table 5.2.

**Table 5.2: FTIR peak assignments of the PMMA [8] and n-PBMA [9] homopolymers**

PMMA Wavelength (cm <sup>-1</sup> )	Peak assignment	n-PBMA Wavelength (cm <sup>-1</sup> )	Peak assignment
2958	CH <sub>2</sub> symmetric stretching	2958	CH <sub>2</sub> symmetric stretching
2934	CH <sub>2</sub> vibration	2881	-CH <sub>3</sub> symmetric stretching
2893	-CH <sub>3</sub> symmetric stretching	1722	C=O stretching
1727	C=O stretching	1460	-CH deformation
1466	-CH deformation	1320	C-C-C-O stretching
1244	C-O stretching	1298	C-C-C-O stretching
1152	C-(C=O)-O stretching	1244	C-O stretching
1066	O-CH-C symmetric stretching	1159	C-(C=O)-O stretching
942	-CH <sub>2</sub> wag	1066	O-CH-C symmetric stretching
		942	-CH <sub>2</sub> wag

#### 5.1.4 Acrylate-g-urethane copolymers

After all the unreacted and unreactive UMs (UMs with isopropanol in both chain ends) were removed as confirmed by GPC (see Section 5.4), the graft copolymers samples were analyzed by FTIR.

##### 5.1.4.1 PMMA-g-urethane copolymers

Figure 5.4 compares the FTIR spectrum of PMMA-g-urethane copolymer containing 13.7 wt % UM incorporation (as calculated by <sup>1</sup>H NMR) with that of the UM and the PMMA homopolymer. New peaks were observed in the graft copolymer spectrum (compared to the PMMA spectrum). The band at 3313 cm<sup>-1</sup> is assigned to the hydrogen-bonded N-H stretching band of the urethane groups. The amide absorption band appears at 1531 cm<sup>-1</sup> and the aromatic absorption band of the TDI repeat unit appeared at 1601 cm<sup>-1</sup>. These results shows that the UM was successfully incorporated into the PMMA polymer structure, which was confirmed by GPC results.

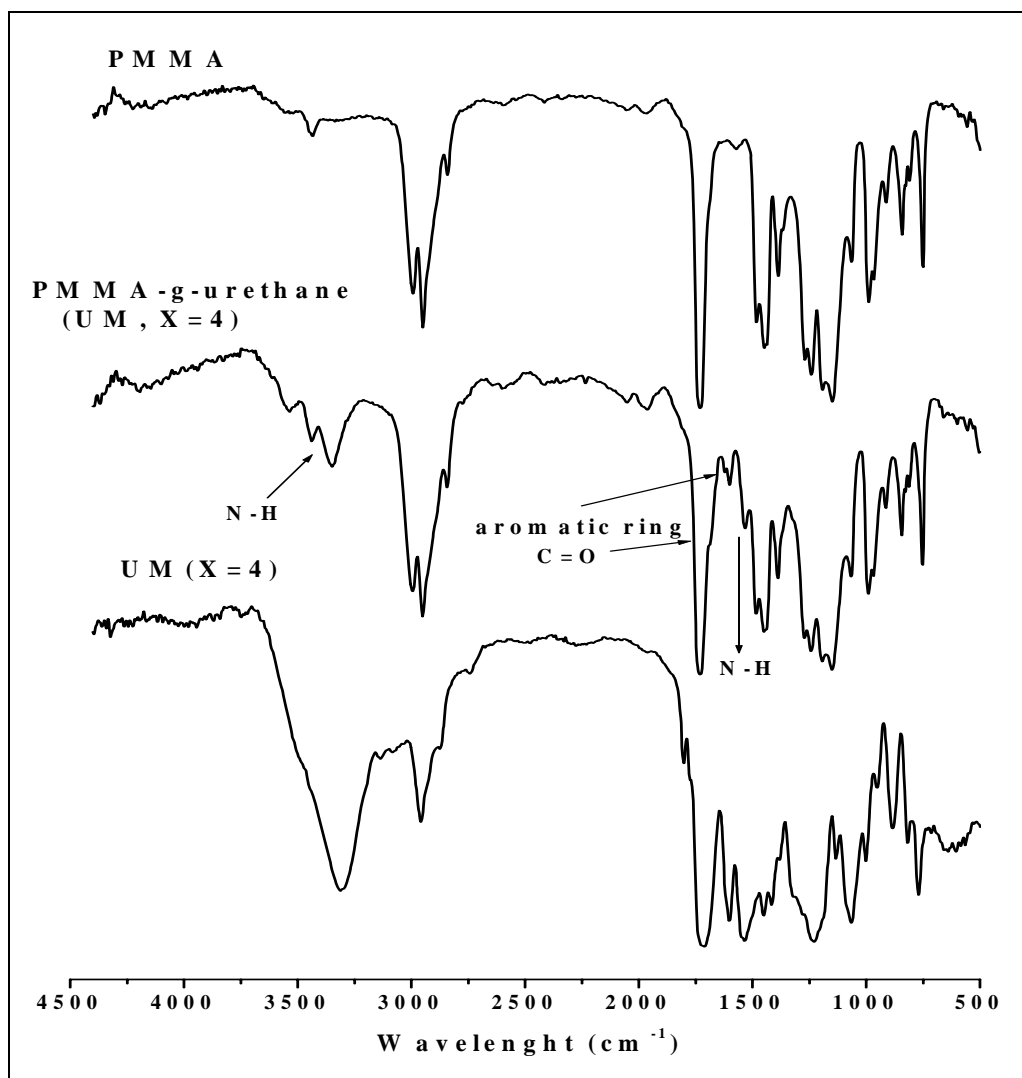
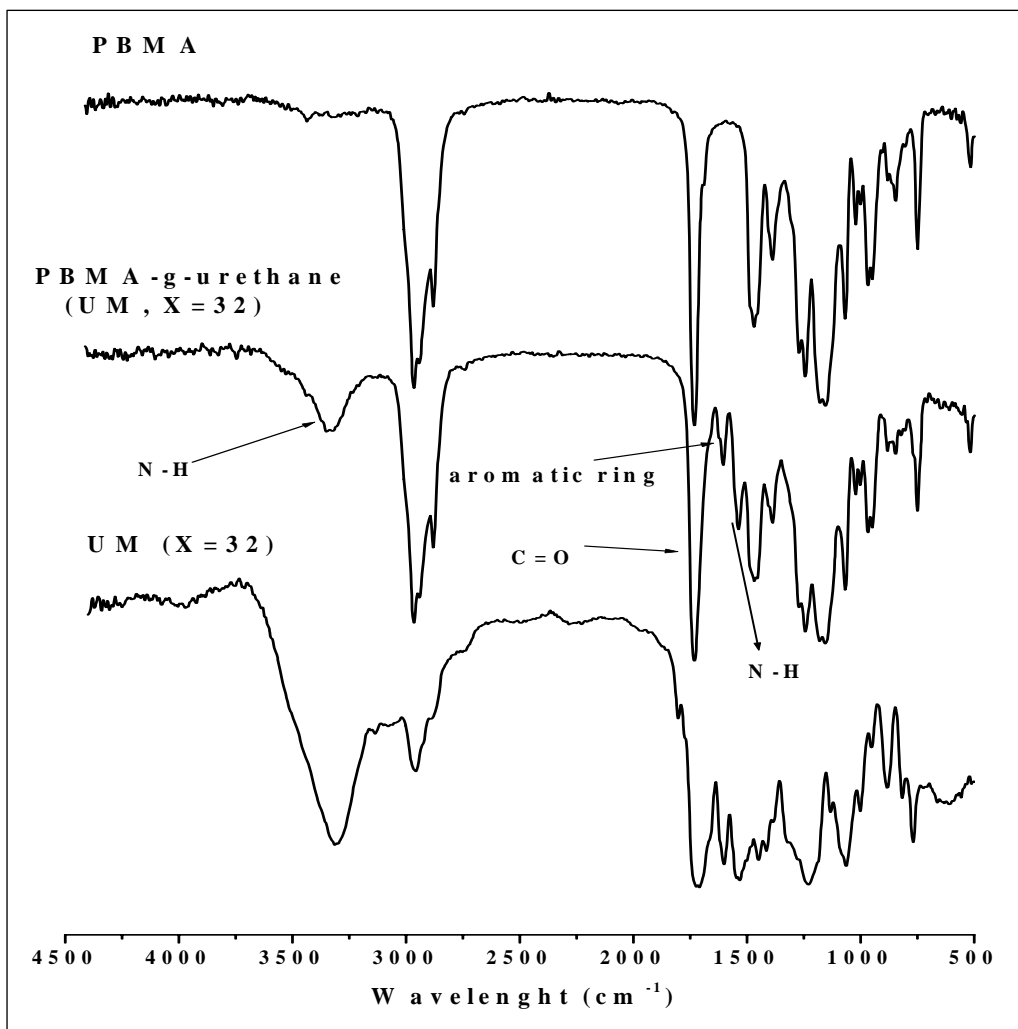


Figure 5.4: FTIR spectra of comparison between PMMA-g-urethane having chain length  $X=4$ , urethane macromonomer, and PMMA homopolymer.

#### 5.1.4.2 n-PBMA-g-urethane copolymers

Figure 5.5 compares the FTIR spectrum of the n-PBMA-g-urethane copolymers containing 11.6 wt% UM incorporation (as calculated by  $^1\text{H}$  NMR) to the spectra of the UM and the n-PBMA homopolymer. New peaks were observed in the graft copolymer spectrum (compared with the n-PBMA spectrum). The absorption band at the  $3334\text{ cm}^{-1}$  is assigned to the N-H stretching band of the urethane group. The amide vibration bands appear at  $1545\text{ cm}^{-1}$  and the aromatic band of the TDI repeat unit appears at  $1605\text{ cm}^{-1}$ . These results shows that the UM was successfully incorporated into the n-PBMA polymer structure, which was confirmed by GPC results.



**Figure 5.5:** FTIR spectra for comparison between n-PBMA-graft-urethane having chain length  $X=32$ , urethane macromonomer, and n-PBMA homopolymer.

### 5.1.5 Effect of the UM content on copolymerization

Figures 5.6 and 5.7 show the FTIR spectra of PMMA and n-PBMA, respectively, when grafted with different amounts of UMs ( $X=12$ ) during free radical copolymerization. These figures clearly show that as the amount of UMs increased during copolymerization, the percentage of UM incorporated into the PMMA-g-urethane and n-PBMA-g-urethane copolymers also increased. This was indicated by an increase in the intensity or the areas of the UM peaks in these spectra, such as NH stretching at  $3330\text{ cm}^{-1}$ , NH absorption at  $1545\text{ cm}^{-1}$ , the aromatic band at  $1605\text{ cm}^{-1}$ , and C=O at  $1732\text{ cm}^{-1}$ .

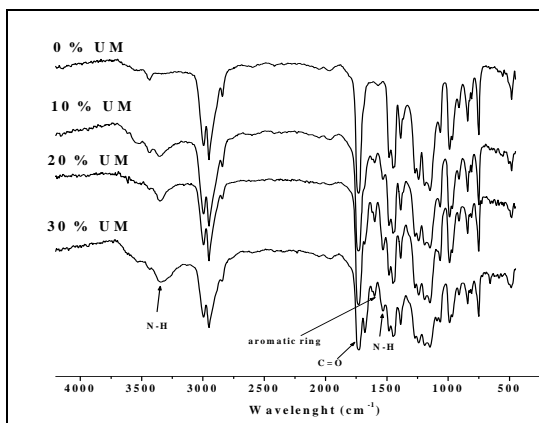


**Figure 5.6: FTIR spectra comparing PMMA copolymerized with different amounts of UM.**

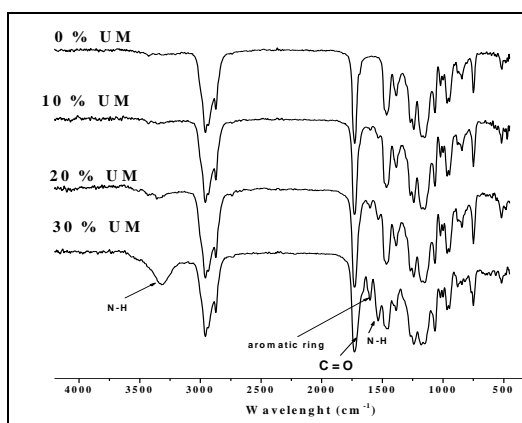


**Figure 5.7: FTIR spectra comparing n-PBMA copolymerized with different amounts of UM.**

## 5.2. $^1\text{H}$ NMR analysis

$^1\text{H}$  NMR analysis was carried out to confirm the structure of the UMs and acrylate-urethane graft copolymers and also to calculate the percentage of UM incorporated into the graft copolymers.

### 5.2.1 $^1\text{H}$ NMR of the urethane macromonomers

The  $^1\text{H}$  NMR spectrum of the UM of chain length  $X=12$  and peak assignments are shown in Figure 5.8 ( $^1\text{H}$  NMR spectra of other UMs of different chain length ( $X$ ) that were synthesized showed similar results). The aromatic ring protons are in the region 7.31-7.56 ppm [10], whereas the resonance signals for the methylene protons of the UM appear in the region 3.12-4.75 ppm [11], depending on the position of the methylene protons with respect to the neighbouring urethane groups. Characteristic bands of urethane N-H protons appear in the region 8.1-9.6 ppm [12]. The signals of the methyl group attached to the aromatic ring appear at 2.15 ppm [8], and the peaks at 1.5-3.53 ppm correspond to the methyl groups of isopropanol and HEMA. The important characteristic signals of the UM are detected in the region 5.7-6.5 ppm, indicating the existence of acrylate groups in the UM structures [13]. UM having a similar structure and showing similar results are reported in literature [14].

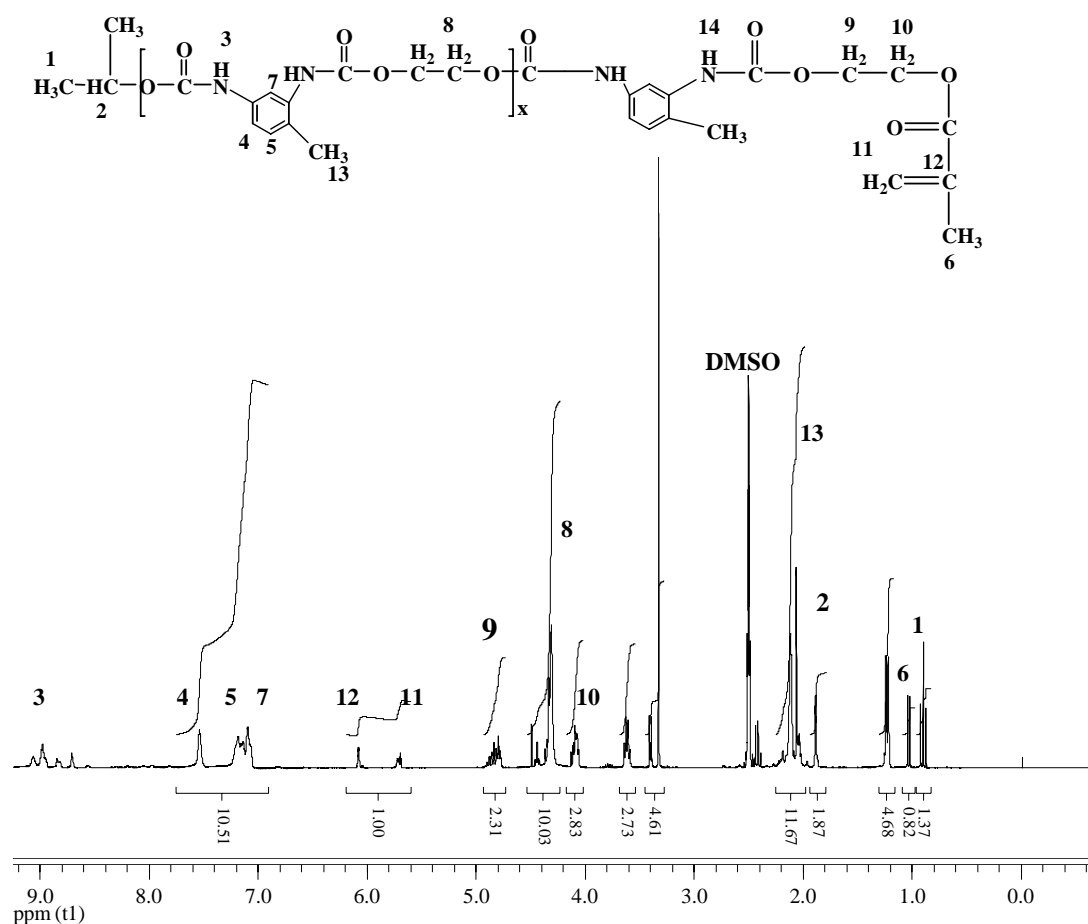


Figure 5.8: <sup>1</sup>H NMR spectrum of urethane macromonomer (X=12) dissolved in DMSO.

### 5.2.2 <sup>1</sup>H NMR of PMMA and n-PBMA homopolymers

<sup>1</sup>H NMR spectra of PMMA and n-PBMA homopolymers are shown in Figures 5.9 and 5.10. These spectra were used as references to determine the incorporation of different amounts of UM into PMMA-g-urethane and n-PBMA-g-urethane copolymers. The spectral data of PMMA and n-PBMA homopolymers are summarized in Table 5.3 [15, 16].

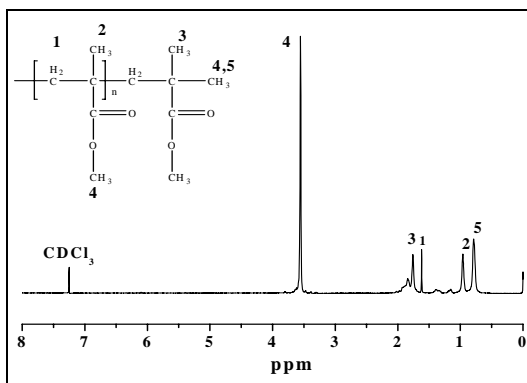


Figure 5.9:  $^1\text{H}$  NMR spectrum of PMMA dissolved in  $\text{CDCl}_3$ .

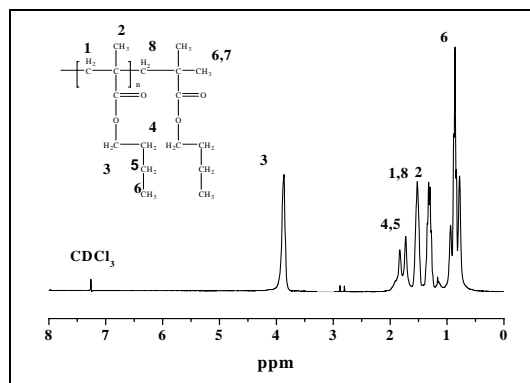


Figure 5.10:  $^1\text{H}$  NMR spectrum of n-PBMA dissolved in  $\text{CDCl}_3$ .

Table 5.3:  $^1\text{H}$  NMR data for PMMA and n-PBMA homopolymers (solvent  $\text{CDCl}_3$ )

$^1\text{H}$ NMR of PMMA	NMR shift (ppm)	$^1\text{H}$ NMR of n-PBMA	NMR shift (ppm)
H(1)	1.62	H(1)	1.48
H(2)	0.95	H(2)	1.32
H(3)	1.81	H(3)	3.84
H(4)	3.57	H(4)	1.84
H(5)	0.78	H(5)	1.73
-	-	H(6)	0.68
-	-	H(7)	1.11
-	-	H(8)	1.5

### 5.2.3 $^1\text{H}$ NMR of acrylate-urethane graft copolymers

After all the unreacted and unreactive UMs (UMs having isopropanol on both chain ends) were removed, which was confirmed by GPC (see section 5.4.2.1), the graft copolymers were analyzed by  $^1\text{H}$  NMR and  $^{13}\text{C}$  NMR.

#### 5.2.3.1 PMMA-g-urethane copolymers

Figure 5.11 compares the  $^1\text{H}$  NMR spectrum of PMMA-g-urethane copolymers containing 13.7 wt% UM incorporation of chain length  $X=4$ , to the spectra of the UM and the PMMA homopolymer, showing the integrated peaks in the graft copolymer spectrum. The two broad peaks in the region 6.5-7.2 ppm of the graft copolymers are mainly attributed to the aromatic protons of the TDI repeat unit in the UMs. The peaks at 4.1-4.7 ppm originate from methylene protons of EG and HEMA in the UMs [17]. In addition, the peaks ascribed to the vinylic protons of the UMs in the region 5.7-6.2 ppm were observed to have completely disappeared upon copolymerization of MMA. These results

shows that the UM was successfully incorporated into the PMMA polymer structure, which was confirmed by GPC results

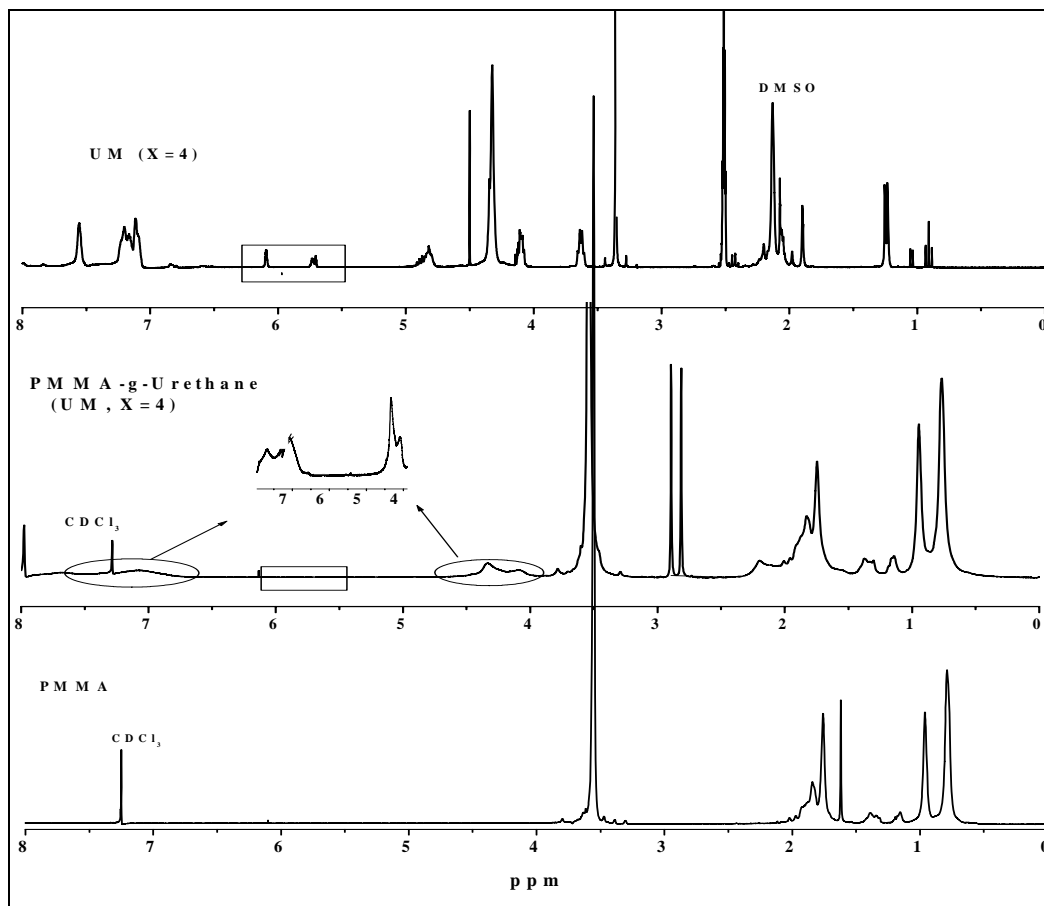


Figure 5.11:  $^1\text{H}$  NMR spectrum of PMMA-g-urethane copolymer, dissolved in  $\text{CDCl}_3$ .

### 5.2.3.2. n-PBMA-g-urethane graft copolymers

Figure 5.12 compares the  $^1\text{H}$  NMR spectra of n-PBMA-g-urethane copolymers containing 11.67% UM incorporation of chain length  $X=32$ , to the spectra of the UM and the n-PBMA homopolymers, showing integration of peaks in the graft copolymer spectrum. The two broad peaks in the region 6.0-7.2 ppm of the graft copolymers are mainly attributed to the aromatic protons of TDI in the UMs. The peaks at 3.7-4.3 ppm originate from methylene protons of EG and HEMA in the UMs [17]. In addition, the peaks ascribed to the vinylic protons of the UMs in the region 5.7-6.2 ppm have completely disappeared upon copolymerization with n-BMA. These results shows that

the UM was successfully incorporated into the n-PBMA polymer structure, which was confirmed by GPC results

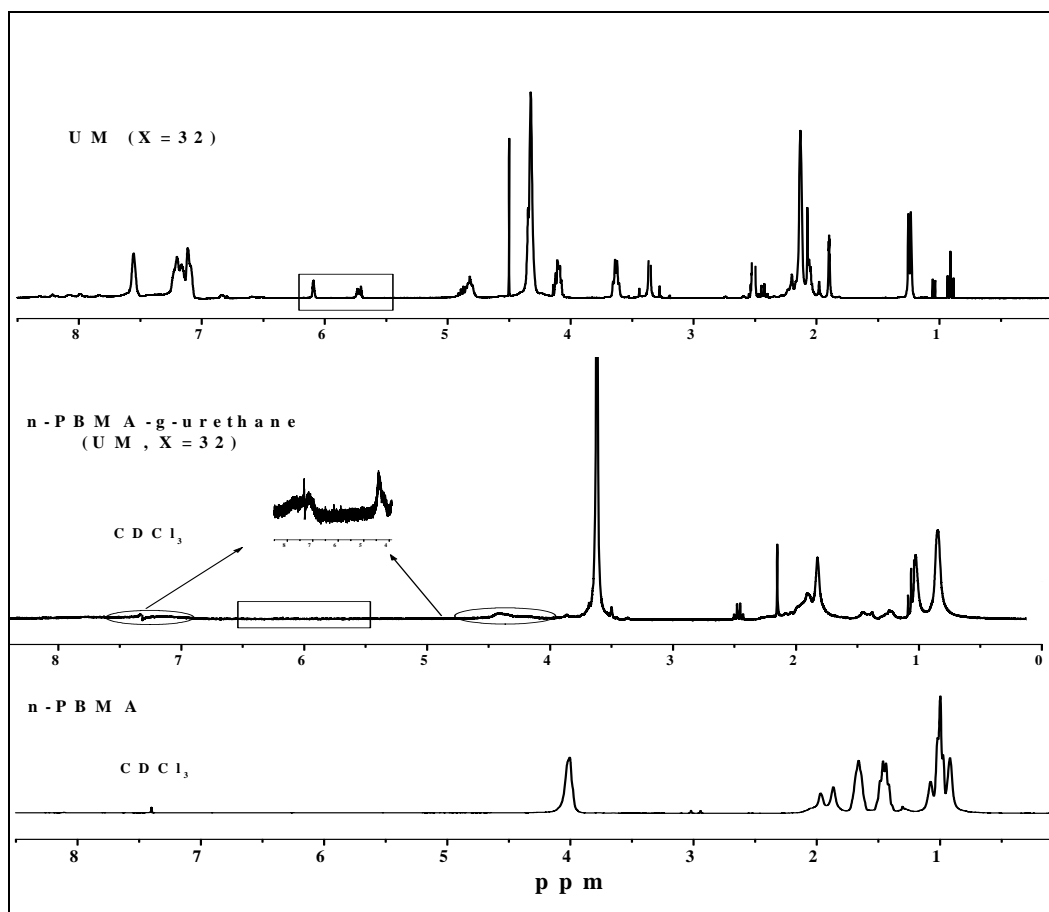


Figure 6.12:  $^1\text{H}$  NMR spectrum of n-PBMA-g-urethane copolymer dissolved in  $\text{CDCl}_3$ .

### 5.2.3.3 Spectroscopic evaluation of the % UM in the graft copolymers

The amount of the UM that was incorporated into the two copolymers was also determined by  $^1\text{H}$  NMR spectroscopy. Calculations were based on the integration of the aromatic ring peak of the UM (6.78-7.55 ppm) in both graft copolymers, the methoxy group of PMMA (6.65 ppm) in the PMMA-g-urethane copolymers, and the methyleneoxy of n-PBMA (3.78 ppm) in the n-PBMA-g-urethane copolymers. These calculations were performed for both graft copolymers by using Equations 5.1 and 5.2 respectively. The results are given in Table 5.4.

$$UM \% = \left[ \frac{Ax / (3 * X)}{Ax / (3 * X) + Ay / 3} \right] \times 100 \quad (5.1)$$

$$UM \% = \left[ \frac{Ax / (3 * X)}{Ax / (3 * X) + Az / 2} \right] \times 100 \quad (5.2)$$

where UM is the mole percentage of UM that was incorporated into the graft copolymers, Ax is the integration area of aromatic group of UM, Ay is the integration area of the methoxy group of PMMA, Az is the integration area of methyleneoxy of n-PBMA and X is the repeat unit of UM i.e X= 4, 8, 12 and 32 .

**Table 5.4: Percentage UM incorporated into the graft copolymers, as determined by FTIR**

UM	Feed ratio by wt%* MMA/UM	Ay	Ax	UM mol %	UM* wt %	Feed ratio by wt%* n-BMA/UM	Az	AX	UM mol %	UM* wt %
X=4	90/10	3.00	0.09	0.7	8	90/10	2.00	0.11	0.9	4
	80/20	3.00	0.15	1.2	13	80/20	2.00	0.18	1.4	7
	70/30	3.00	0.36	2.9	27	70/30	2.00	0.37	2.9	14
X=8	90/10	-	-	-	-	90/10	-	-	-	-
	80/20	3.00	0.17	0.7	9	80/20	2.00	0.15	1.2	7
	70/30	3.00	0.33	1.3	16	70/30	2.00	0.33	2.6	14
X=12	90/10	3.00	0.09	0.3	4	90/10	2.00	0.09	0.2	2
	80/20	3.00	0.13	0.3	6	80/20	2.00	0.17	0.5	3
	70/30	3.00	0.30	0.8	13	70/30	2.00	0.31	0.8	6
X=32	90/10	-	-	-	-	90/10	-	-	-	-
	80/20	3.00	0.16	0.2	10	80/20	2.00	0.12	0.1	4
	70/30	3.00	0.28	0.3	17	70/30	2.00	0.27	0.3	8
	60/40	3.00	0.38	0.4	22	60/40	2.00	0.42	0.4	12

\* The total amounts of UMs and MMA or UMs and n-BMA, in all copolymerization feeds were based on 5.0g, and all calculations were based on assumed molecular weight formula 3.1 (Table 5.7 page 77)

It can be noted from Table 5.4 that as the amount of UMs increased during graft copolymerization so the percentages of UMs incorporated into both PMMA-g-urethane and n-PBMA-g-urethane copolymers also increased. Some of the added UMs were unreactive (i.e. UM with isopropanol additive at both ends), and was solvent extracted. This also contributes to the lower incorporation level of UM into the graft copolymers. The value of 27.74 wt % for the X=4 UM copolymerized with MMA is unreasonably high and must be an experimental error as 24.0 is the theoretical maximum (meaning perfect monomer yield and completed polymerization)

In some cases it was not possible to spectroscopically calculate the percentage UMs that was incorporated into the graft copolymer by  $^1\text{H}$  NMR analysis due to some difficulty in identifying the UM peaks in the spectra. This was caused by too low concentrations of UMs incorporated into PMMA-g-urethane and n-PBMA-g-urethane copolymers. Consequently, their resonance peaks of aromatic ring were too broad to be observed.

### 5.3 $^{13}\text{C}$ NMR analysis

$^{13}\text{C}$  NMR was also carried out to confirm the synthesis of UMs and acrylate urethane graft copolymers.

#### 5.3.1 $^{13}\text{C}$ NMR of urethane macromonomers

The  $^{13}\text{C}$  NMR spectrum of the UM having a urethane chain length  $X=12$  and peak assignments are shown in Figure 5.13. The  $^{13}\text{C}$  NMR spectra of all the UMs show aromatic carbons at 137-113 ppm [18], whereas the resonance signals for the methylene carbons appear in the region 64.41-58.52 ppm [19], depending on the position of the methylene carbon with respect to neighbouring urethane groups. The characteristic signal of the urethane ester appears in the region 166.2-153.4 ppm [20]. The methyl group attached to the aromatic ring of TDI shows a peak at 16.3 ppm [18], whereas the peak at 12.6-18.4 ppm corresponded to the methyl groups of isopropanol and HEMA. The important characteristic signal of the vinyl-terminated group of the UM was detected in the region 126.0-129.6 ppm, which proves the existence of acrylate groups in the UM structure [19].

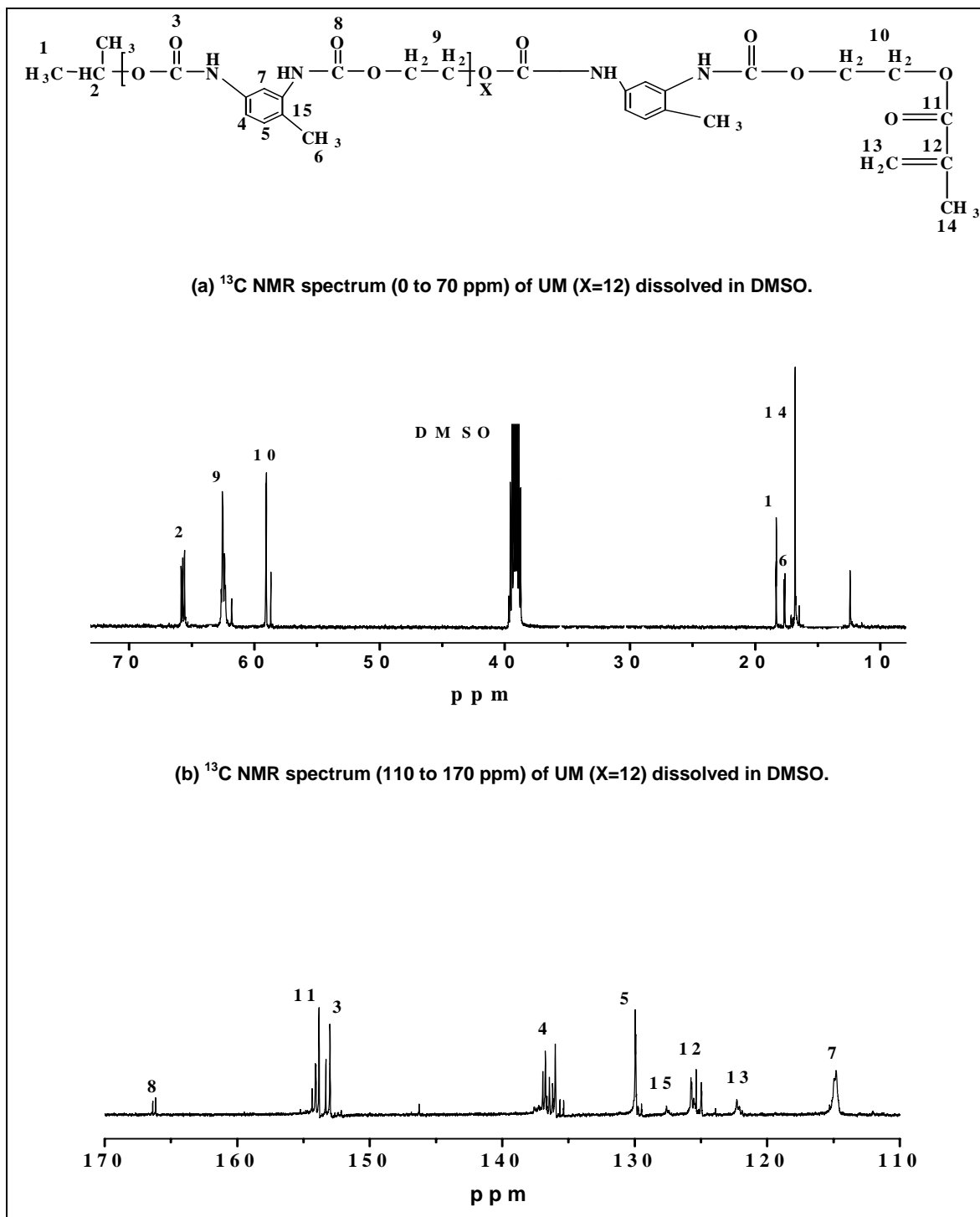


Figure 513:  $^{13}\text{C}$  NMR spectrum of UM of chain length X=12, dissolved in DMSO.

### 5.3.2 $^{13}\text{C}$ NMR of PMMA and n-PBMA homopolymers

$^{13}\text{C}$  NMR spectra of PMMA and n-PBMA homopolymers are shown in Figures 5.14 and 5.15 respectively. These spectra were used as references to determine the incorporation of

different amounts of UM into PMMA-g-urethane and n-PBMA-g-urethane copolymers. The spectral data of PMMA and n-PBMA homopolymers are summarized in Table 5.5 [16].

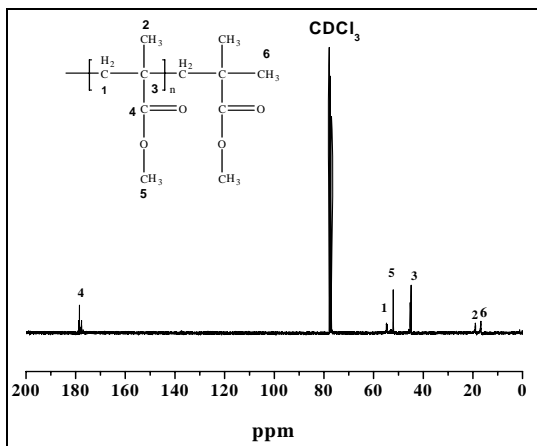


Figure 5.14:  $^{13}\text{C}$  NMR spectrum of PMMA dissolved in  $\text{CDCl}_3$ .

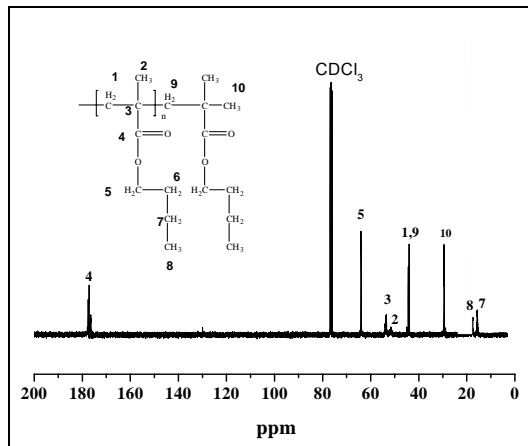


Figure 5.15:  $^{13}\text{C}$  NMR spectrum of n-PBMA dissolved in  $\text{CDCl}_3$ .

Table 5.5:  $^{13}\text{C}$  NMR data for PMMA and n-PBMA homopolymers

$^{13}\text{C}$ NMR of PMMA	NMR shift (ppm)	$^{13}\text{C}$ NMR of n-PBMA	NMR shift (ppm)
C(1)	54.30	C(1)	45.29
C(2)	18.99	C(2)	52.00
C(3)	44.85	C(3)	53.00
C(4)	178.34	C(4)	177.26
C(5)	52.09	C(5)	63.67
C(6)	17.08	C(6)	-
-		C(7)	16.02
-		C(8)	17.42
-		C(9)	43.9
-		C(10)	28.52

### 5.3.3 $^{13}\text{C}$ NMR of acrylate-urethane graft copolymers

NMR was also used to confirm the formation of acrylate-urethane graft copolymer. The graft copolymers (in Scheme 3.2) were successfully synthesized and also characterized with  $^{13}\text{C}$  NMR.

### 5.3.3.1 $^{13}\text{C}$ NMR of PMMA-g-urethane copolymers

Figure 5.16 compares the  $^{13}\text{C}$  NMR spectra of PMMA-g-urethane copolymers containing 13.72 wt% UM (chain length  $X=4$ ), to the spectra of the UM and the PMMA homopolymer. New peaks are evident in the graft copolymer spectrum. The peaks in the region 132-140 ppm are mainly attributed to the aromatic carbons of TDI in the urethane macromonomer. The peaks at 60-68 ppm originate from the methylene carbons of EG and HEMA in the UM [21]. In addition, the  $^{13}\text{C}$  NMR peaks ascribed to the vinylic carbon of the UMs in the region 122-130 ppm were observed to have completely disappeared upon copolymerization with MMA. These results show that the UM was successfully incorporated into the PMMA polymer structure, which was confirmed by GPC results.

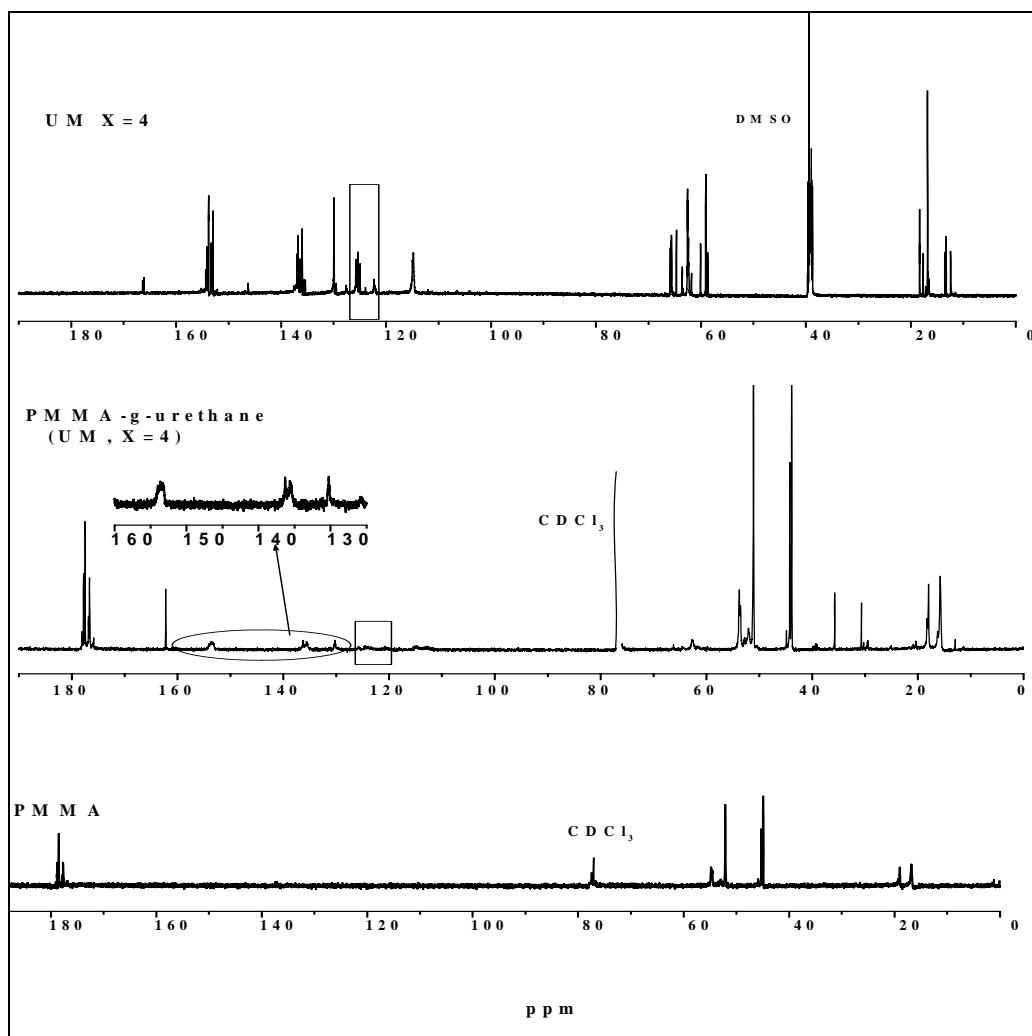


Figure 6.16:  $^{13}\text{C}$  NMR spectrum of PMMA-g-urethane copolymer dissolved in  $\text{CDCl}_3$ .

### 5.3.3.2 $^{13}\text{C}$ NMR of n-PBMA-g-urethane copolymers

Figure 5.17 compares the  $^{13}\text{C}$  NMR spectrum of the n-PBMA-g-urethane copolymer containing 11.67% UM incorporation of chain length  $X=32$  to that of the UM and the n-PBMA homopolymer. New peaks were observed in the graft copolymer spectrum compared with the n-PBMA spectrum. The peaks in the region 130-140 ppm are mainly attributed to the aromatic carbon of TDI in the UM. The peaks at 61-67 ppm originate from methylene carbons of EG and HEMA in the UM [21]. In addition,  $^{13}\text{C}$  NMR peaks ascribed to the vinylic carbon of the UMs in the region 122-128 ppm were observed to have completely disappeared upon copolymerization with n-BMA. These results show that the UM was successfully incorporated into the n-PBMA polymer structure, which was confirmed by GPC results

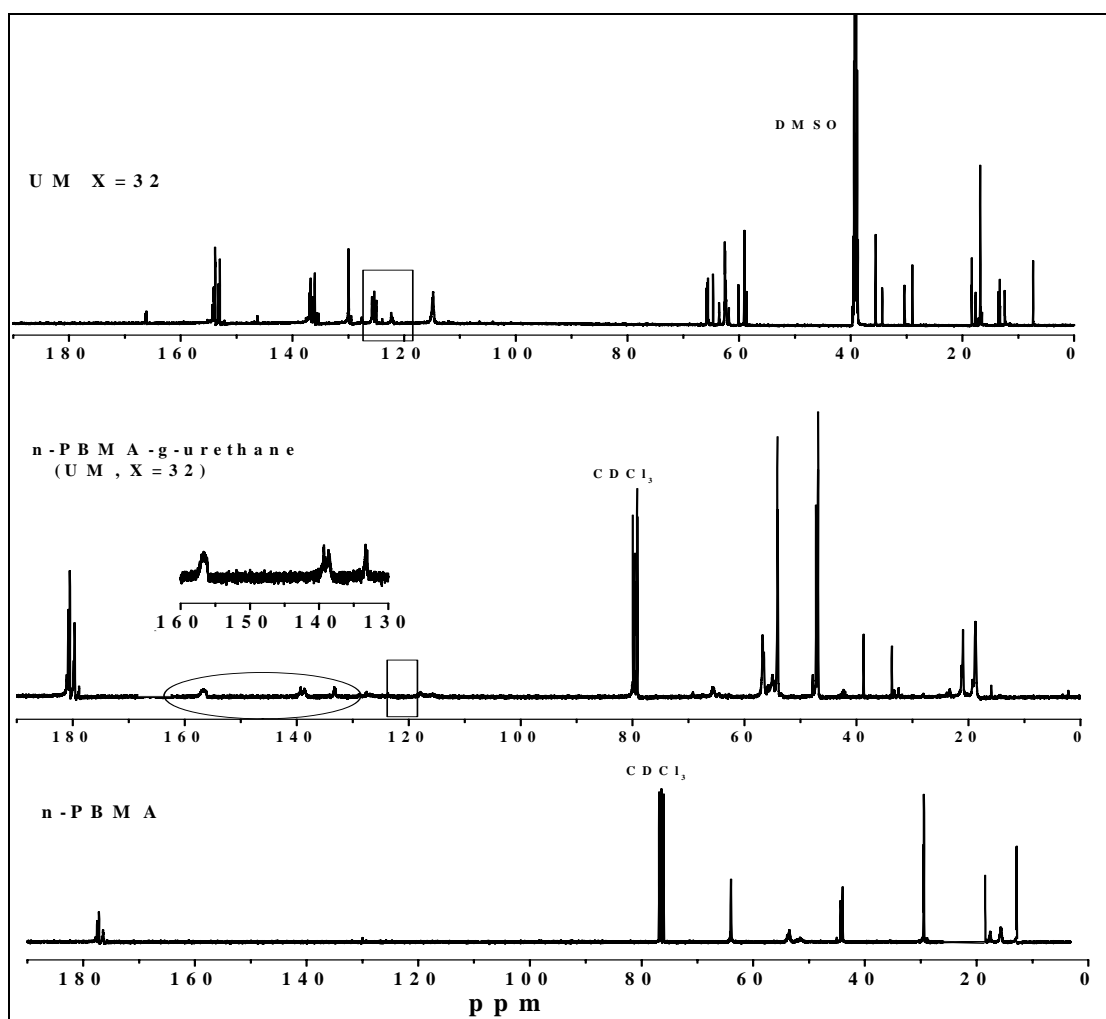


Figure 5.17:  $^{13}\text{C}$  NMR spectrum of n-PBMA-g-urethane copolymer dissolved in  $\text{CDCl}_3$ .

## 5.4 Gel permeation chromatography

GPC analysis was used to characterize the UMs and the acrylate-urethane graft copolymers. The molecular weight, and its distribution, of the UMs and both copolymers (PMMA-g-urethane and n-PBMA-g-urethane) were analyzed by GPC. The GPC instrument was calibrated using linear polystyrene standards. The values of the molecular weights of graft copolymers obtained by GPC measurements are generally lower than the absolute molecular weights because linear polystyrene has a much larger hydrodynamic volume than the corresponding graft copolymers of the same molecular weight [19].

### 5.4.1 Urethane macromonomers

Figure 5.18 shows the GPC traces of the four UMs having different urethane chain lengths; all of which have shoulders. This might be due to high molecular weight fractions; polyaddition polymerization was used to synthesize the UMs which could lead to broad molecular weight distribution and different molecular masses.

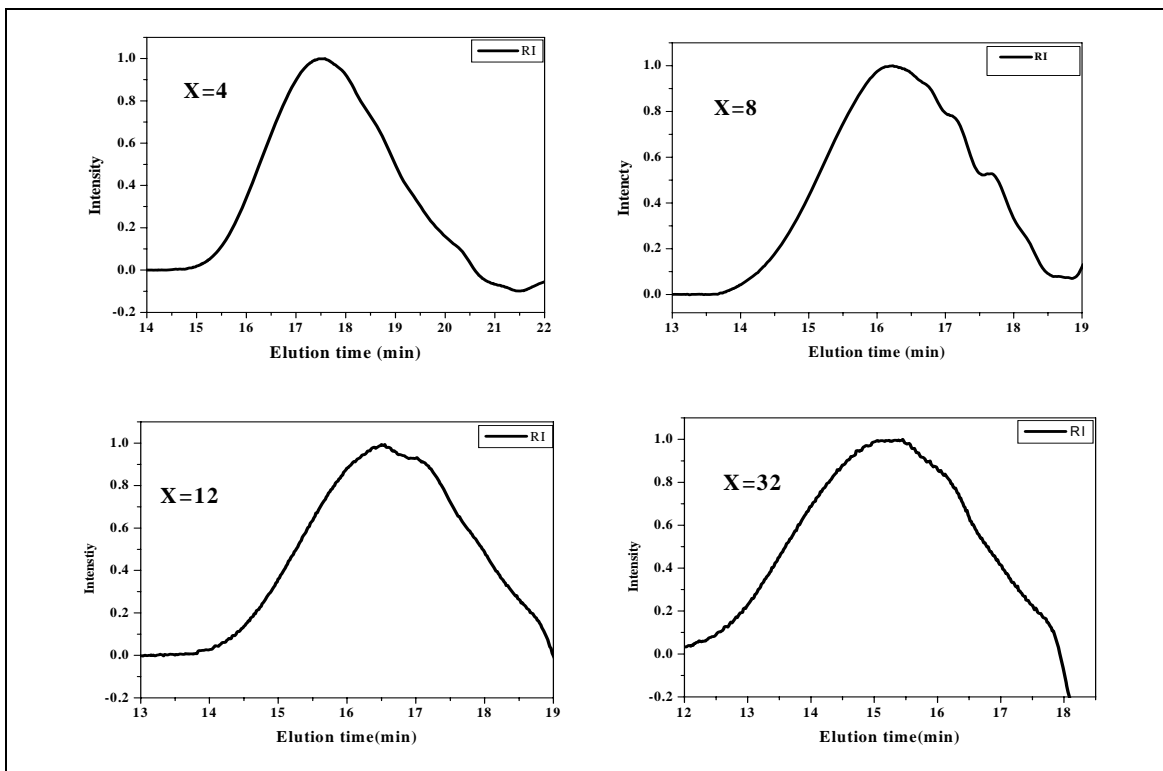


Figure 5.18: GPC chromatograms of UMs having chain lengths (a) X=4, (b) X=8, (c) X=12, (d) X=32.

The number average molecular weights ( $M_n$ ) (experimental and predicted) and polydispersities obtained for all UMs are summarized in Table 5.6. It shows that the synthesized UMs have relatively narrow molecular weight distributions, and also that the actual molecular weights of the UMs are close to the predicted ones, which were calculated based on Equation 3.1. The  $M_n$  and  $M_w$  of the UMs obtained during GPC analysis was done according to polystyrene standards (PS) which does not represent the exact values. However, the values are very close, which indicates that the synthesized UMs were designed and controlled; in other words, all polymerization conditions were controlled during polymerization.

**Table 5.6: Number average molecular weight ( $M_n$ ), and polydispersity ( $M_w/M_n$ ) of the UMs of different chain lengths, as determined by GPC**

Urethane length (X)	Predicted molecular weight*	$M_n$	Polydispersity
4	1280	1255	1.64
8	1480	1811	1.85
12	1810	2100	2.16
32	7310	7840	2.32

Theoretical molecular weight was calculated by formula 1

#### 5.4.2 Synthesis of acrylate-g-urethane copolymers

The PMMA-g-urethane and n-PBMA-g-urethane copolymers were synthesized by solution free radical polymerization, as described in Section 3.3.4.2. The molecular structures were confirmed using GPC, with UV and IR detectors.

The ability of UMs to undergo copolymerization was determined using MMA and n-BMA as comonomers. Four different UMs (see Table 3.2) were copolymerized with different amounts of MMA and n-BMA under free radical copolymerization conditions (see Table 3.3). The resulting graft copolymers were isolated by precipitation from DMF solution into methanol. Methanol was a solvent for UM and a non-solvent for PMMA, n-PBMA and the corresponding acrylate-g-urethane copolymers.

The graft copolymers were characterized by GPC (using a double detector system of UV (254 nm) and RI). The UV detector detected the UMs, but not the PMMA and n-PBMA (absorptions of the latter were too small to detect at this wavelength). Figure 5.19 shows GPC traces for UM, PMMA and n-PBMA (using the UV detector), and that the UM has a

strong UV absorption due to the aromatic ring in the polymer chain, whereas no UV absorption is detected for PMMA or n-PBMA.

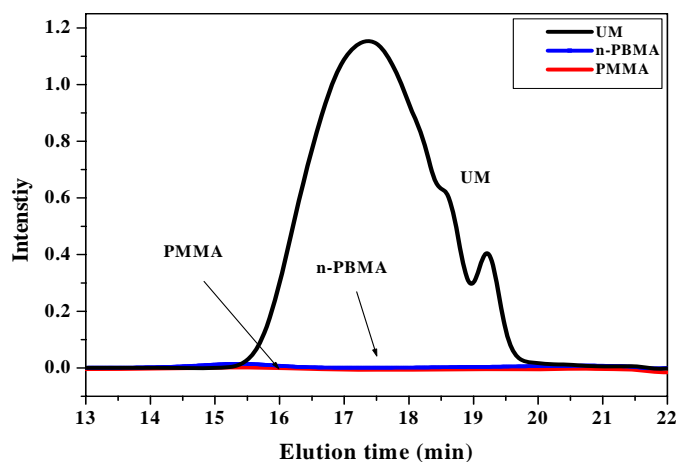


Figure 5.19: GPC traces of UMs, n-PBMA and PMMA (UV detector).

#### 5.4.2.1 Extraction of unreacted and unreactive UMs

The UMs were soluble in methanol but PMMA and n-PBMA were not, so that the unreactive UMs (UMs containing both isopropanol end groups which cannot react during graft copolymerization) and unreacted UMs (UMs containing at least one HEMA end group, which did not react during graft copolymerization) were extracted by precipitation in methanol. However, it was expected that some unreactive and unreacted UMs might precipitate along with the graft copolymer, as shown in Figure 5.20a by a small shoulder at low molecular weight. Attempts to separate unreacted and unreactive UMs from the copolymers were made by repeated precipitation in methanol (methanol dissolves unreacted and unreactive UMs and not the copolymers). Figure 5.20b shows that the unreacted and unreactive UMs (in the low molecular weight region) are still present after two precipitations in methanol at room temperature, whereas these unreacted and unreactive UMs were completely removed after three precipitations in methanol, as shown in Figure 5.20c.

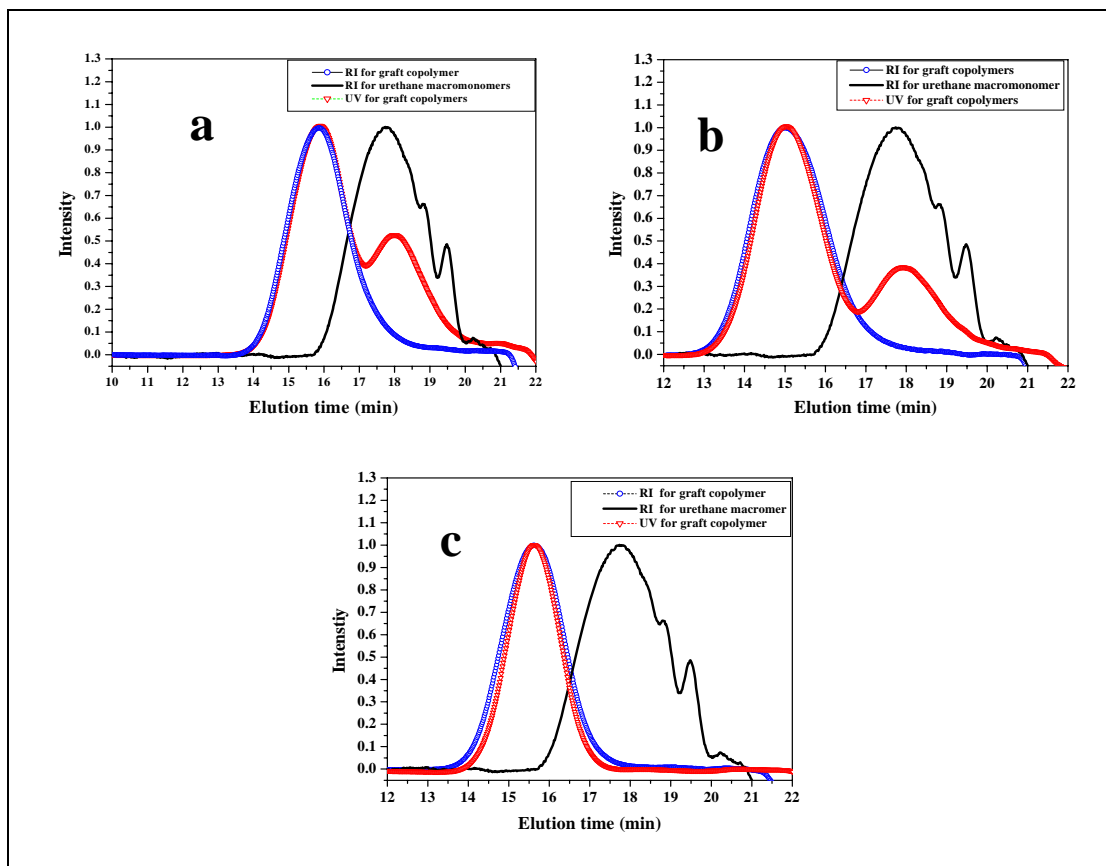
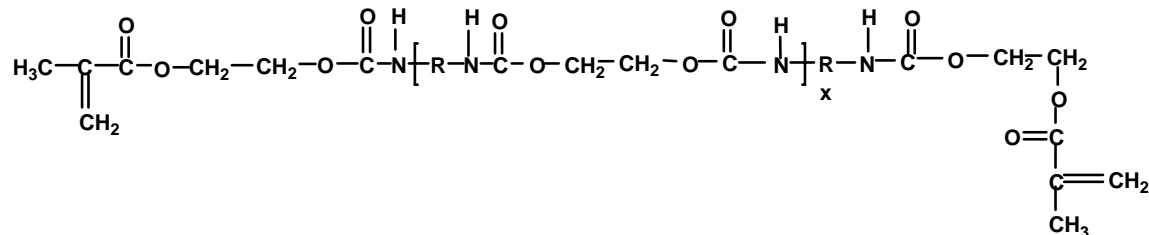


Figure 5.20: GPC traces of MMA copolymerization with 5% UM ( $X=32$ ) after: (a) one, (b) two, (c) three precipitations in methanol.

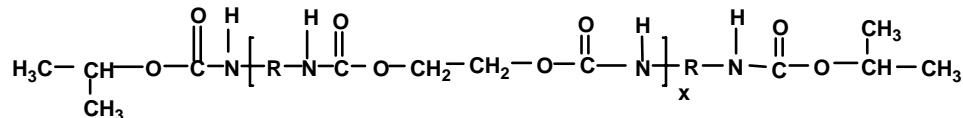
#### 5.4.2.2 Different methods used to optimize the structure of UMs

The obtained UMs which were synthesized as described in sections 3.2.4 and 3.2.5 (experimental work) can have another two possible chemical structures, because the reagents are stoichiometric and the reactivity parameters and the reaction conversion will limit the chemical homogeneity of macromonomers. One of these other possible structures of UMs that could form when HEMA reacts on both sides of the urethane pre-polymers (urethane chain with excess isocyanate) is shown in Scheme 5.1. This structure is considered undesirable, as it will lead to the formation of crosslinked polymers when copolymerized further with acrylic monomers due to double bonds being present on chain ends.



**Scheme 5.1: Reaction products when HEMA reacts on both sides of the UM.**

The other possible structure that could form when isopropanol reacts on both chain ends of the urethane pre-polymers, as shown in Scheme 5.2 This structure is also considered to be undesirable, as it will render the UM unreactive for further copolymerization with acrylic monomers due to no double bonds being present on either of the chain ends.



**Scheme 5.2: Reaction product when isopropanol reacts on both sides of the UM, to form unreactive urethane macromonomers.**

Three different synthesis methods were used to optimize the desired structure of UMs as discussed in Section 3.2.4 (where HEMA is on the one chain end and isopropanol on the other). These were as follows:

- 1- HEMA added all at once followed by the addition of isopropanol
- 2- HEMA added dropwise, followed by isopropanol
- 3- HEMA and isopropanol added together, in fractions.

Table 5.7 compares the three results of different methods that were used to obtain the desired UMs structures. It shows that the first method gave the highest yields of both PMMA-g-urethane and n-PBMA-g-urethane copolymers under similar copolymerization conditions. These comparisons were done after all the unreacted and unreactive UMs were removed, as confirmed by GPC. The first method gave the highest % of UMs containing HEMA on only one chain end (an increase in UMs containing HEMA on both chain ends would result in an increase in UMs containing isopropanol on both chain ends, thereby decreasing the yield of graft copolymers). Method 1 was therefore

considered to be best method, and was thus used to synthesize all of the UMs in this study.

**Table 5.7: Yield comparisons between the three different methods used to synthesize UMs**

Method	Feed polymerization (g)			graft yield of PMMA-g-urethane (g)	graft yield of PBMA-g-urethane (g)
	UM (X=8)	MMA	n-BMA		
1	0.25	4.75	4.75	*3.79	*3.86
2	0.25	4.75	4.75	*3.65	*3.75
3	0.25	4.75	4.75	*3.59	*3.64
1	0.50	4.50	4.50	*3.75	*3.89
2	0.50	4.50	4.50	*3.62	*3.80
3	0.50	4.50	4.50	*3.54	*3.66

\*The total amount of UM and MMA, or UM and n-BMA, in all copolymerization feeds were based on 5.00 g

#### 5.4.2.3 GPC analysis of acrylate-g-urethane copolymers

As it was mentioned previously in Section 5.4.2, the UV detector only detects the UM at 254nm due to the absorption by the aromatic ring in the polymer chain, hence GPC with double detectors was used to prove the syntheses of PMMA-g-urethane and n-PBMA-g-urethane copolymers. Figures 5.21 and 5.22 are examples of GPC traces showing the extracted graft copolymers of PMMA-g-urethane and n-PBMA-g-urethane copolymers respectively after all the unreacted and unreactive UM was removed. They showed that no UV peaks for unreacted UM were observed at high retention time and also that the retention times of the graft copolymer samples were shifted to lower time compared to the retention time of the starting materials (i.e. retention time of UMs). This result indicates that the molecular weights of the graft copolymer samples were increased due to the grafting reaction, and also that no homopolymers of PMMA or n-PBMA, or UMs, were present. In the absence of unreacted UMs, the UV response almost mirrors the RI response in all graft copolymers, which indicated the compositional homogeneity of UM grafts onto the graft copolymers.

Chapter 5: Results and discussion

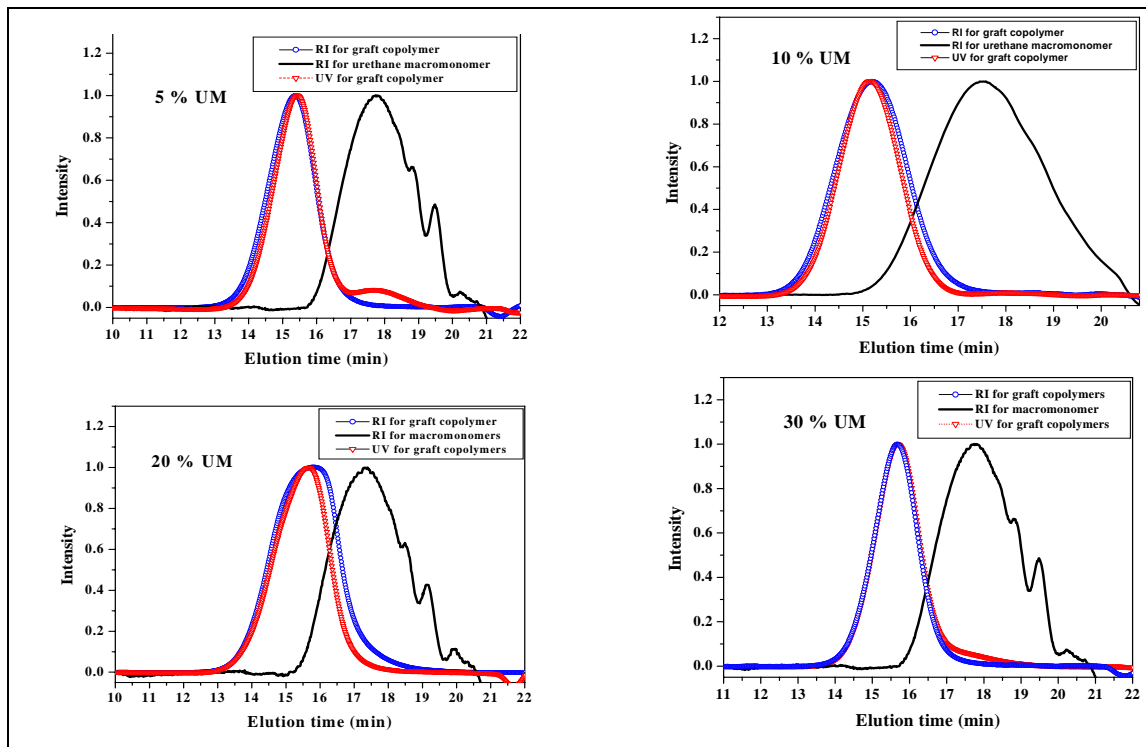


Figure 5.21: GPC traces of MMA copolymerization with various amounts of UM (5, 10, 20, 30%) of chain length  $X=12$ .

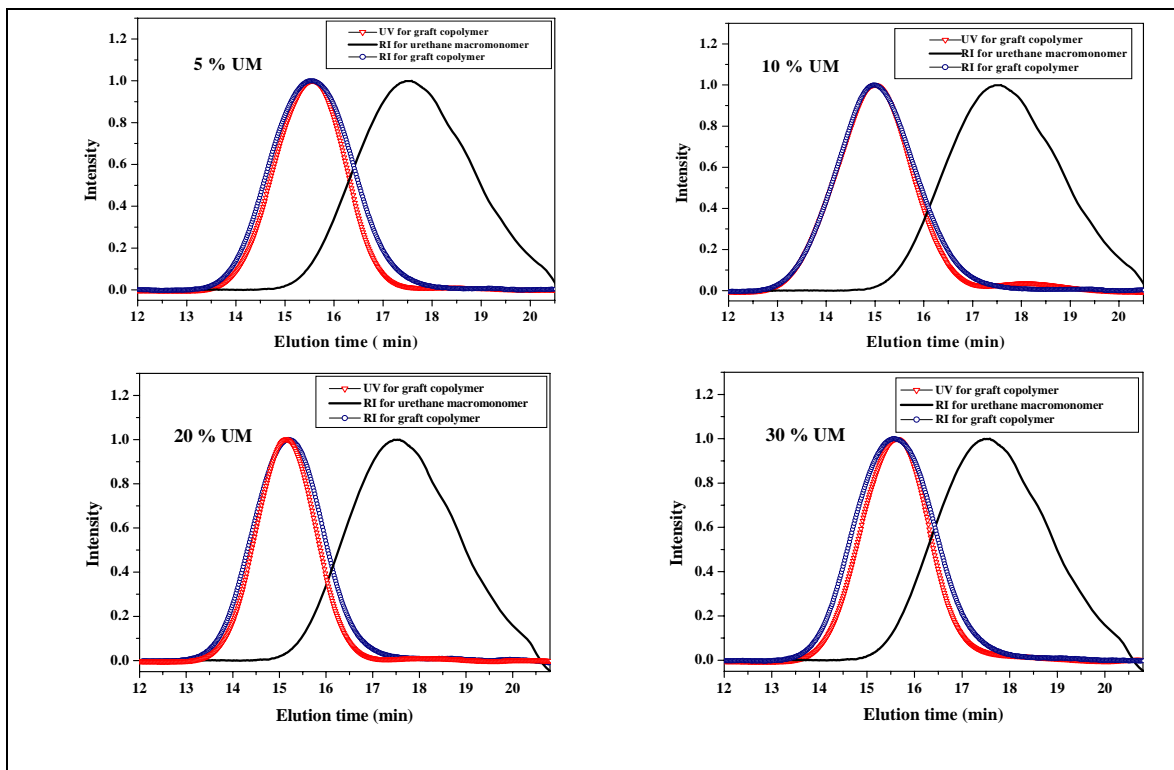


Figure 5.22: GPC traces of n-BMA copolymerization with various amounts of UM (0, 10, 20, 30%) of chain length  $X=4$ .

#### **5.4.2.4 Number average molecular weight, weight average molecular weight and polydispersity of the graft copolymers**

The number average molecular weights, the weight average molecular weights and polydispersities (PD) obtained for both PMMA-g-urethane and n-PBMA-g-urethane copolymers are summarized in Tables 5.8 and 5.9 respectively. All PMMA-g-urethane and n-PBMA-g-urethane copolymers had molecular weights of about 30000, which was higher than the starting UMs. However, the molecular weights of synthesized graft copolymers are considered slightly low. This was expected due to the fact that DMF has a high chain transfer constant for MMA and n-BMA respectively ( $5.01 \times 10^{-4}$  and  $4.38 \times 10^{-4}$ )[22]. An example of the calculations of expected molecular weights is shown in Appendix A. In addition, the molecular weight values of the graft copolymers obtained by GPC measurements were generally much lower than the absolute molecular weights because linear polystyrene has a much larger hydrodynamic volume than the corresponding graft copolymers of the same molecular weight [19]. Tables 5.8 and 5.9 also show that the molecular weight distributions of all graft copolymers were close to that of the PMMA and n-PBMA homopolymers, which means that all polymerization conditions were controlled during the free radical copolymerization.

Chapter 5: Results and discussion

**Table 5.8: Number average molecular weight ( $M_n$ ), weight average molecular weight ( $M_w$ ) and polydispersity ( $M_w/M_n$ ) for PMMA-g-urethane copolymers**

UMs	Feed ratio by wt%* MMA/Macromonomer	$M_n \cdot 10^{-3}$	$M_w \cdot 10^{-3}$	PD ( $M_w/M_n$ )	Yield of product PMMA-g-urethane (g)	% Yield
X=4	100/0	35.88	55.27	1.54	3.98	79.6
	95/5	27.97	44.48	1.59	3.65	73.0
	90/10	25.56	42.29	1.66	3.55	71.0
	85/15	34.47	46.89	1.36	3.32	64.4
	80/20	26.43	40.45	1.53	3.12	62.4
	75/25	35.08	48.42	1.38	3.06	61.2
	70/30	19.98	33.98	1.70	3.01	60.2
X=8	95/5	24.55	48.13	1.96	3.53	70.6
	90/10	29.11	44.55	1.53	3.38	67.6
	85/15	29.65	47.15	1.59	3.20	64.0
	80/20	28.22	41.21	1.46	3.11	62.2
	75/25	22.16	39.45	1.78	3.04	60.1
	70/30	24.75	34.65	1.40	2.99	59.8
X=12	95/5	26.95	52.30	1.94	3.42	68.4
	90/10	25.71	45.78	1.78	3.22	64.4
	85/15	20.22	41.25	2.04	3.13	62.6
	80/20	25.57	47.32	1.85	3.01	60.2
	75/25	19.58	42.17	2.11	2.98	59.6
	70/30	16.57	35.47	2.14	2.85	57.0
X=32	90/10	20.94	44.47	2.17	3.28	65.4
	80/20	22.59	41.58	1.84	3.09	60.4
	70/30	25.11	42.45	1.69	2.92	58.8
	60/40	22.95	34.21	1.49	2.61	51.4

\*The total amounts of UM and MMA in all copolymerization feeds were based on 5.00 g.

**Table 5.9: Number average molecular weight ( $M_n$ ), weight average molecular weight ( $M_w$ ) and polydispersity ( $M_w/M_n$ ) for n-PBMA-g-urethane copolymers**

UMs	Feed ratio by wt%* BMA/Macromonomer	$M_n \cdot 10^{-3}$	$M_w \cdot 10^{-3}$	PD $M_w/M_n$	Yield of product PBMA-g-Urethane (g)	% Yield
X=4	100/0	38.52	68.26	1.77	3.85	77.0
	95/5	26.59	52.12	1.96	3.63	72.6
	90/10	33.49	51.24	1.53	3.51	70.2
	85/15	28.63	47.24	1.65	3.33	66.6
	80/20	28.86	48.21	1.67	3.11	62.6
	75/25	22.05	41.24	1.87	3.07	61.4
	70/30	17.84	37.12	2.08	3.01	60.2
X=8	95/5	28.56	51.13	1.79	3.55	71.0
	90/10	21.50	49.47	2.30	3.33	66.6
	85/15	20.40	45.29	2.22	3.21	64.2
	80/20	27.66	48.13	1.74	3.11	62.6
	75/25	28.13	43.61	1.55	3.04	60.8
	70/30	17.07	39.14	2.30	2.98	59.6
X=12	95/5	19.84	55.17	2.78	3.45	69.0
	90/10	33.93	51.24	1.51	3.27	65.4
	85/15	30.66	48.15	1.57	3.19	63.8
	80/20	29.62	49.18	1.66	3.11	62.6
	75/25	20.80	47.44	2.28	3.01	60.2
	70/30	16.87	38.14	2.26	2.99	59.8
	60/40	17.70	37.54	2.12	2.91	58.2
X=32	90/10	20.94	44.47	2.17	3.32	66.4
	80/20	22.59	41.58	1.84	3.12	62.4
	70/30	25.11	42.45	1.69	2.94	58.8
	60/40	22.95	34.21	1.49	2.67	53.4

\*The total amounts of UM and n-BMA in all copolymerization feeds were based on 5.00 g.

#### 5.4.2.5 Yield of graft copolymers

The yields of the copolymerization reactions for both PMMA-g-urethane and n-PBMA-g-urethane copolymers are included in Table 6.9 and Table 6.10. The UM consists of three possible structures (see also Section 4.2.6)

- (a) isopropanol-(TDI-EG)<sub>x</sub>-TDI-isopropanol
- (b) isopropanol-(TDI-EG)<sub>x</sub>-TDI-HEMA
- (c) HEMA-(TDI-EG)<sub>x</sub>-TDI-HEMA

Due to the UM being end-capped with 60:40 mole ratio of isopropanol to HEMA, the UM will consist of an unreactive fraction (structure (a) above). This unreactive UM fraction is the primary cause of the reduced percentage yield with an increased weight fraction and chain length during copolymerization.

Firstly, the yields of both PMMA-g-urethane and n-PBMA-g-urethane copolymers decreased as the amounts of the UM is increased. This is because as the weight fraction increases, so too does the weight fraction of the unreactive UM increase, which, after removal with methanol, decreases the percentage yield of the graft copolymers.

Secondly, the yields of the graft copolymers decreased as the chain length of UM increased. This is because as the chain length of the UM increases, so too does the chain length and the weight fraction of the unreactive fraction increase, which, after removal with methanol, decreases the percentage yield of the graft copolymers.

## **5.5 Thermogravimetric analysis (TGA)**

Many techniques have been used to study the thermal degradation of polymers, including pyrolysis mass spectroscopy, thermal volatilization analysis, etc. [23]. However, TGA analysis is the technique most widely used to investigate the thermal decomposition of a polymer [24, 25]. TGA analysis was done on dried samples of UMs and acrylate urethane graft copolymers to investigate their thermal stability

### **5.5.1 Thermal stability of urethane macromonomers**

In complex compounds like polyurethanes, the onset of degradation is governed by the weakest link in the chain, whereas the most frequent chain and the environment of the given groups are the dominant factors for overall thermal stability. Polyurethanes with different backbones have different thermal stabilities [26].

Segmented polyurethane materials are generally not very thermally stable, especially above their softening temperatures. Generally the ester-based polyurethanes exhibit better thermal and oxidative stabilities than ether-based polyurethanes do. Several studies have reported the results of the thermal degradation of ester- and ether-based thermoplastic polyurethanes (TPUs) which have been performed under vacuum, in air and nitrogen [27-29]. The thermal degradation of polyurethanes is very complicated, and has been suggested that polyurethanes break down by a combination of three

independent pathways: (1) dissociation to the original diol and isocyanate; (2) formation of a primary amine, an alkene, and carbon dioxide in the reaction; (3) formation of a secondary amine and carbon dioxide [30-32].

The thermal decomposition patterns of the UMs were determined by TGA. Typical thermograms of the UMs having different chain lengths were recorded in a nitrogen atmosphere. Typical TGA curves of these UMs are shown in Figure 5.23.

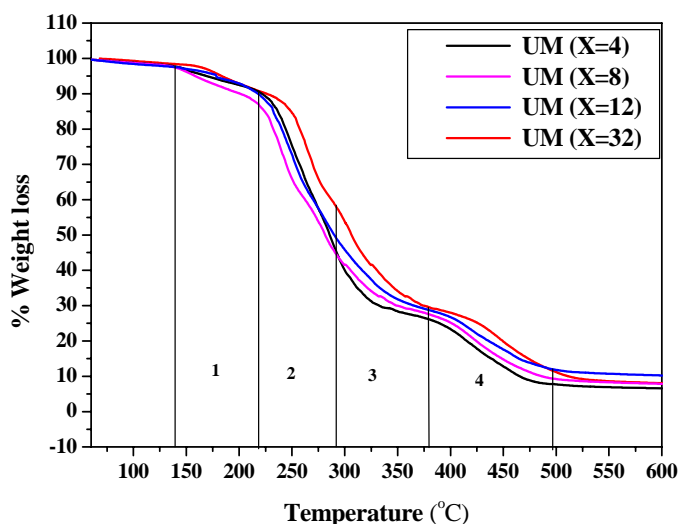


**Figure 5.23: TGA curves of UMs having different urethane chain lengths.**

The decomposition patterns of all the UMs samples are very similar. There is a slight improvement in thermal stability as the chain length of the UMs increases. Four stages of degradation were observed in Figure 5.24. The first stage of degradation occurs in the temperature range 150–225 °C and presents a maximal rate of weight loss at 190 °C. The second step of the degradation takes place in the temperature range 225–275 °C. The third step of the degradation takes place in the temperature range 275–380 °C. The fourth stage of degradation takes place in the temperature range 380–500 °C, and may be attributed to the oxidation of the residual material. This stage ends with the loss of all volatile fractions and a mass loss that does not change much after 500 °C.

### 5.5.2 Thermal stability of acrylate-urethane graft copolymers

Polyacrylates are extremely resistant to oxygen, and only decompose very slowly under extreme conditions such as high temperature and in an oxygen-rich atmosphere. When

heated, polyacrylate depolymerizes to monomers much less readily than the corresponding polymethacrylates do [33]. Polymethylacrylate decomposes at 290-400 °C to produce methanol and carbon dioxide. Volatile decomposition products of polybutylacrylate at 300-500 °C are butene, butanol and carbon dioxide [34].

#### **6.5.2.1 Thermal stability for PMMA-g-urethane copolymers**

Primary TGA curves for MMA copolymerized with different amounts of UMs ranging from 0-30% by weight (according to MMA), from UMs having different chain lengths (X= 4, 8, 12 and 32) are shown in Figure 5.24. The decomposition patterns for all the graft copolymer samples were similar. There was a slight improvement in thermal stability as the amount of UMs increased, which might be due to optimum morphological interaction between PMMA and the urethane segments. There was also a slight improvement in thermal stability as the chain length (X) of the UM increases.

The TGA curves of PMMA-g-urethane copolymers under nitrogen compared with PMMA homopolymers are shown in Figure 5.24. PMMA is degraded in three steps, and is virtually completely destroyed at 450 °C. The first stage of degradation occurs in the temperature range 205-290 °C. The second stage of the degradation takes place in the temperature range 290-390 °C. The third stage of degradation occurs in range 390-450 °C, and possibly attributed to the oxidation of the residual material. However, the graft copolymers degrade less as the UM content in the graft copolymers increases. From these results it can also be concluded that the thermal stability increased as the amount and chain length (X) of the UMs increased. Thus the best thermal stability was found when MMA was copolymerized with 30 wt % of UM of chain length X=32

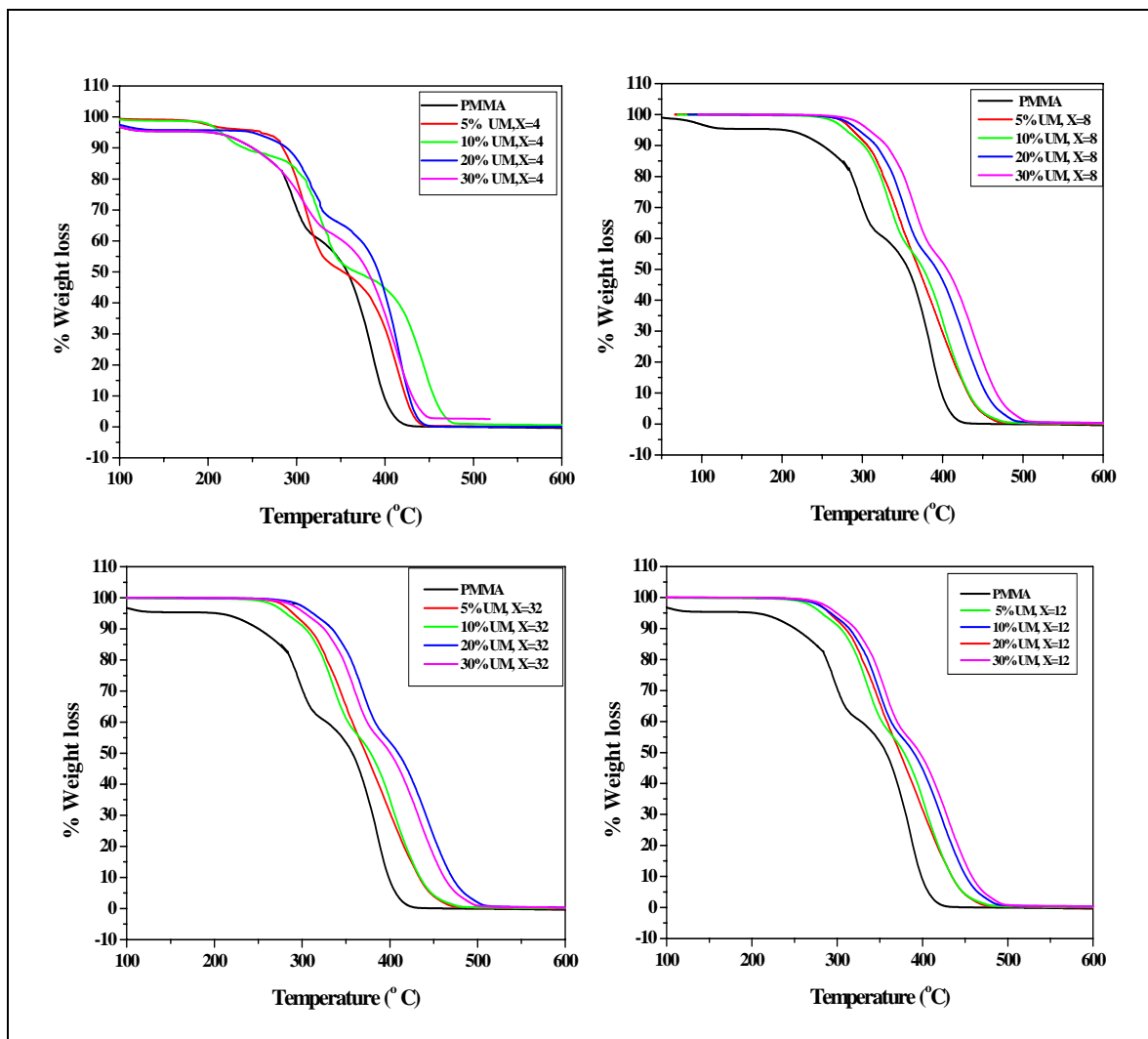


Figure 5.24: TGA curves of MMA copolymerized with different amounts of UMs of various chain lengths.

### 5.5.2.2 Thermal stability of n-PBMA-g-urethane copolymers

Primary TGA curves for n-BMA copolymerized with different amount of UMs of various chain lengths (X) are shown in Figure 5.25. The decomposition patterns for all graft copolymers samples were similar. There was however a slight improvement in thermal stability as the amount of UMs in the graft copolymer is increased, which might be due to better morphological interaction between n-PBMA and UM segments. There is also a slight improvement in thermal stability as the chain length of UMs is increased.

The TGA curves of n-PBMA-g-urethane copolymers under nitrogen compared with n-PBMA homopolymers are shown in Figure 5.25. n-PBMA is degraded in three steps, and

Chapter 5: Results and discussion

is virtually completely destroyed at 450 °C. The first stage of degradation occurs in the temperature range 175-250 °C. The second step of the degradation occurs in the temperature range 250-350 °C. The third step of the degradation takes place in the temperature range 350-500 °C, and is possibly attributed to the oxidation of the residual material. However, the graft copolymers degrade less as the UM content in the graft copolymers increased. From these results it can be concluded that the best thermal stability was found as the amount and chain length (X) of the UMs increased. Thus the best thermal stability was found when n-BMA was copolymerized with 40 wt % of UM of chain length X=32.

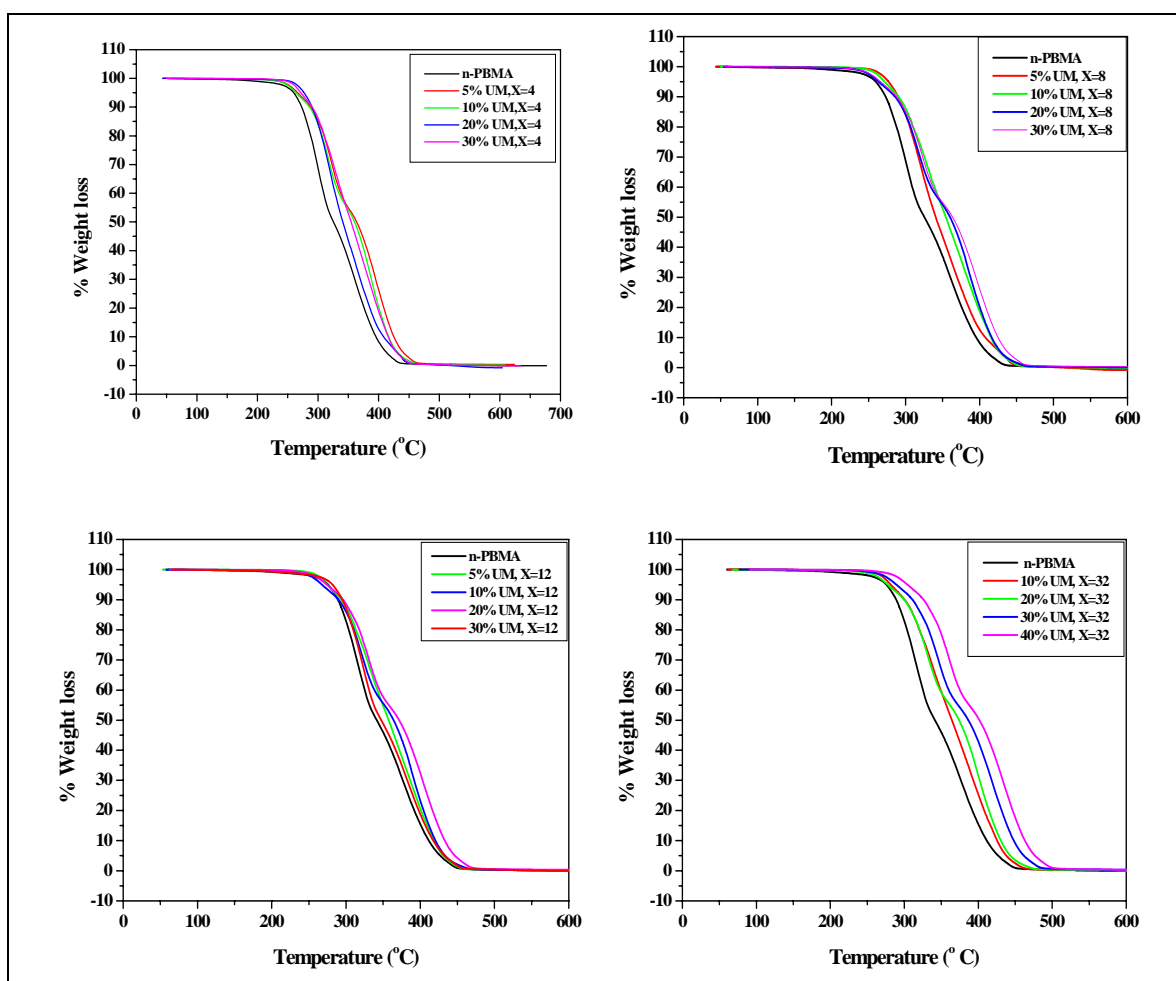


Figure 5.26: TGA curves of n-BMA copolymerized with different amounts of UMs of various chain lengths.

## 5.5.2. Dynamic mechanical analysis

### 5.5.2.1. Introduction

The mechanical and physical properties of polyurethanes are dependent on factors such as: (i) the ratio of the soft to hard segments; (ii) the lengths of the soft and hard segments; (iii) the compositions of the soft and hard segment; (iv) anomalous linkages; and (v) molecular mass [35-43].

The structural differences between the soft and hard blocks normally result in phase separation. The degree of phase separation affects the properties of the polymer [3, 44-47]. Phase separated domains can be decreased by increasing the compatibility between the hard and soft segments. In this study, different UMs were incorporated into the acrylate backbone. The dynamic mechanical behaviour of copolymers depends on the miscibility of a polymer pair. The compatibility between pairs of polymers can be characterized by dynamic mechanical analysis. For incompatible copolymers the damping ( $\tan\delta$ ) temperature curve shows the presence of two ( $\tan\delta$ ) peaks corresponding to the glass transitions of the individual polymers, whereas in highly compatible copolymers only a single peak that is located in between the transition temperatures of the pure polymers is observed [48]. In the case of partially compatible copolymers, two broad separate peaks corresponding to the individual polymer components or one broad peak are observed but with their positions shifted closer to the single (compatible) peak, depending on the copolymers composition and the influence of their microstructures [49-51].

From a molecular standpoint, the glass transition temperature is viewed as the temperature above which large-scale chain segments develop mobility that permits conformational rearrangements of the chain backbones [25]. There are several factors that affect the mobility of a polymer chain: backbone flexibility, pendent groups like “fish hooks”, “boat anchors” and pendent groups like “elbow room” [52]. The more flexible the backbone chain, the lower its T<sub>g</sub> value will be.

DMA offers the possibility to follow the change in both elastic and viscous properties of a material as a function of temperature and morphology of the polymers [53]. DMA-analysis was used firstly to determine the T<sub>g</sub> for UMs and graft copolymer samples, and

secondly to investigate the phase separation between urethane and acrylate segments of the synthesized acrylate-g-urethane copolymers.

### 5.5.2.2. Urethane macromonomers

Figure 5.26 shows the ( $\tan\delta$ ) spectra of UMs, having different chain lengths, as detected by DMA.

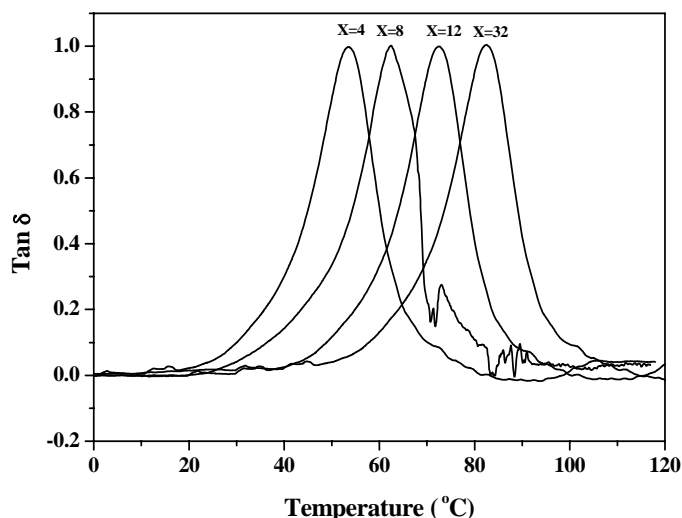


**Figure 5.26: Tan  $\delta$  curves of UM of different chain lengths.**

The  $\tan \delta$  peak is associated with the loosening in polymer structure, so that the functional groups and the small chain segment can move [8]. The  $\tan \delta$  traces of the UMs show only  $\alpha$  relaxation  $T_g$  (i.e. the onset of the long-range, coordinated molecular motion) and show absence of heterogeneous mixing of EG and TDI segments in the urethane polymer matrix, which may lead to more than one  $T_g$  value. This result confirms results that were obtained in previous work [13, 54-56]. On the other hand, the  $T_g$  increased with increasing the chain length of UM. This will be the result of decreasing the free volume as the length of the chain increases making fewer highly mobile chain ends available. Table 5.10 gives the  $T_g$  data for UMs, having different chain lengths, as determined by DMA.

**Table 5. 10: T<sub>g</sub> values of UMs of different chain lengths, as determined by DMA.**

UM	T <sub>g</sub> (°C) at onset*	T (°C) at max peak height
X=4	38	53
X=8	45	62
X=12	57	72
X=32	63	80

### 5.5.2.3. PMMA-g-urethane copolymers

In the PMMA-g-urethane copolymers, PMMA is the more abundant than UM. PMMA homopolymer has a glass transition temperature of  $\pm 115$  °C [57]. When MMA is copolymerized, molecular chain packing is disturbed, shifting the T<sub>g</sub> of the copolymer to a lower temperature, in between that of the two polymer components UM and PMMA. The tan  $\delta$  traces of the UMs show only a single peak between the PMMA and UM peaks, which suggests a homogeneous (i.e not phase separated material). Figure 5.27 shows tan  $\delta$  spectra of PMMA-g-urethane copolymers containing different amount of UMs, with chain length X=12. The T<sub>g</sub> values was measured as the onset temperature, and the T<sub>g</sub> values of the PMMA-g-urethane copolymers varied between 76-115 °C. The T<sub>g</sub> values of all the synthesized PMMA-g-urethane copolymers are tabulated in Table 5.11

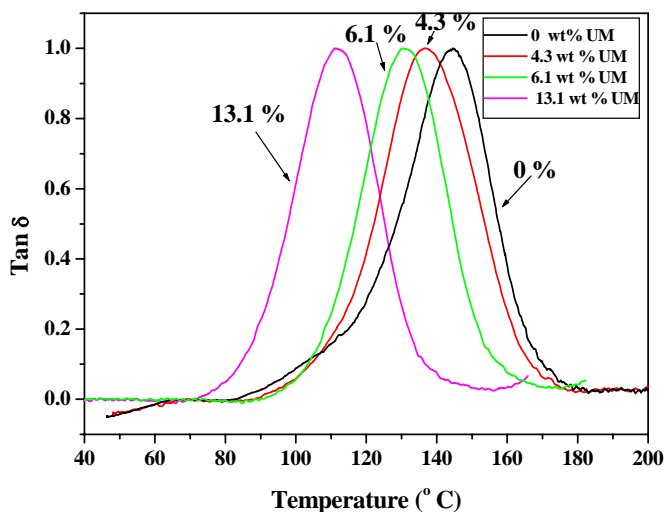


**Figure 5.27: Tan  $\delta$  curves of PMMA-g-urethane copolymers containing different amounts of UM of chain length X=12.**

**Table 5.11: Tg values of PMMA-g-urethane copolymers as determined by DMA.**

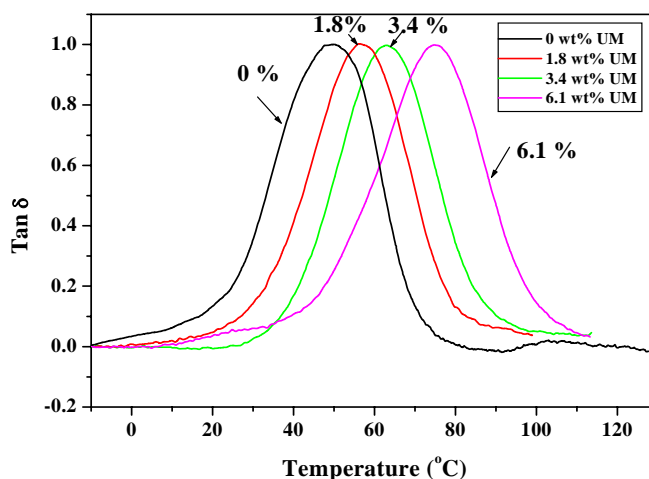
UM	Feed ratio by wt% MMA/UM	Tg (°C) at Onset	T (°C) at max peak height
X=4	100/0	115	144
	90/10	110	137
	80/20	104	131
	70/30	95	122
X=8	90/10	108	133
	80/20	100	127
	70/30	93	117
X=12	90/10	106	129
	80/20	95	121
	70/30	88	113
X=32	90/10	102	125
	80/20	96	118
	70/30	85	108
	60/40	76	100

From Table 5.11 it can be noted that the single Tg values of PMMA-g-urethane graft copolymers decreases with an increase in the amount of UM content incorporated into the graft copolymers. This confirms that the UMs and PMMA segments in the PMMA-g-urethane copolymer are (completely compatible or that there is no large scale phase separation). In addition to that, the Tg values of graft copolymers are shifted to lower temperatures because of the presence of the pendent groups of UM (graft chain) which limits polymer chain packing and adds many loose chain ends. Therefore the distance between the chains is increased, and they can move around more easily. This lowers the Tg due to the more free volume in the polymer. As free volume increases, the glass transition temperature tends to decrease. It is further noted from Figure 5.27 that the Tg values of PMMA-g-urethane copolymers decreased as the amount of UM incorporated into graft copolymers increased. On the other hand, the Tg values is also observed to decrease with increasing urethane chain length(X). This is contrary to the freedom of chain ends concept, but is in itself very understandable because the compatibility must worsen as the UM chain length increases and this creates a dropping of Tg values on the UM side or low temperature side. If the UM length is increases far enough, the Tg values on the low side would drop until that the Tg values of the pure UM is reached at full incompatibility.

### 5.3.2.4. n-PBMA-g-urethane copolymers

In the n-PBMA-g-urethane copolymers, the n-PBMA segment is the more abundant and flexible chain in the copolymer. n-PBMA homopolymer has a glass transition temperature of  $\pm 25^\circ\text{C}$  [57]. Here the  $T_g$  of n-PBMA is lower than that of the  $T_g$  of UMs, compared to the  $T_g$  of PMMA which is higher than that of the UMs.

Figure 5.28 is an example of a  $\tan \delta$  spectrum of a n-PBMA-g-urethane copolymers containing different amounts of UMs of chain length  $X=12$  (calculated by  $^1\text{H}$  NMR). It shows that the copolymers have only one  $T_g$  (measured as the onset temperature), which varied between  $19\text{--}45^\circ\text{C}$ , confirming that the UM and n-PBMA segments are largely compatible in the n-PBMA-g-urethane copolymer system. The  $T_g$  values of all the synthesized n-PBMA-g-urethane copolymers are summarized in Table 5.12.



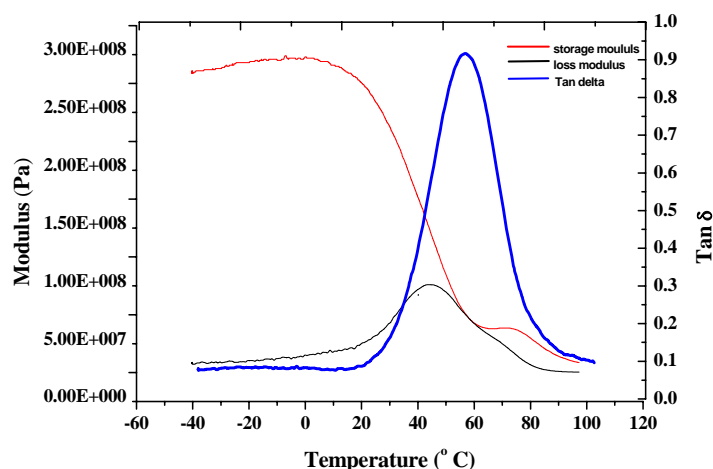
**Figure 5.28:**  $\tan \delta$  curve of n-PBMA-g-urethane copolymers containing different amounts of UM of chain length  $X=12$ .

Table 5.12 shows that the  $T_g$  values of n-PBMA-g-urethane copolymers increased as the amount of UM incorporated into the graft copolymers increased. It is obvious that when harder segments are introduced into the softer n-PBMA segment, the  $T_g$  will increase. On the other hand, lower  $T_g$  values are observed with increasing the chain length of UM. Increasing the chain length forces demixing even on the nanoscale. This means the n-PBMA domains are purer and the  $T_g$  value will drop to be closer to the purer  $T_g$  value of n-PBMA (instead of one homogeneous peak, two peaks are close together to form the peak envelope). So also will the higher damping temperature tend to higher values as the chain length of the UM is increased.

**Table 5.12: Tg value of n-PBMA-g-urethane copolymers as determined by DMA.**

UM	Feed ratio by wt% BMA/Macromonomer	Tg (°C) at onset	T (°C) at max peak height
X=4	100/0	19	49
	90/10	30	61
	80/20	37	68
	70/30	42	80
X=8	90/10	28	59
	80/20	36	65
	70/30	40	78
X=12	90/10	25	58
	80/20	34	64
	70/30	41	77
X=32	90/10	22	53
	80/20	30	58
	70/30	38	70

Thus, when the chain length of UM was increased to X=32 and the amount of UM increased to 40% during copolymerization, microphase separation occurs, as shown by the loss and storage modulus in Figure 5.29.



**Figure 5.29: Tan  $\delta$ , loss and storage modulus curves of n-BMA copolymerized with 40% UM of chain length X=32.**

The Tan  $\delta$  curve shows only one peak, as it is less sensitive to incompatibilities, but the loss and storage modulus curves show two peaks at different temperatures (19.0 and 76.0 °C), which are due to softer n-PBMA and harder UM segments respectively. This means that there are some degrees of micro-phase separation. Detection of glass

transition temperatures associated with each of the respective homopolymers indicates that the UM segments and n-PBMA segments in the above case are locally separated (microphase separation) into distinct regions. This result is supported by the TEM image presented in Figure 5.30, which shows nanosegregated regions of darker UM segment and lighter n-PBMA.

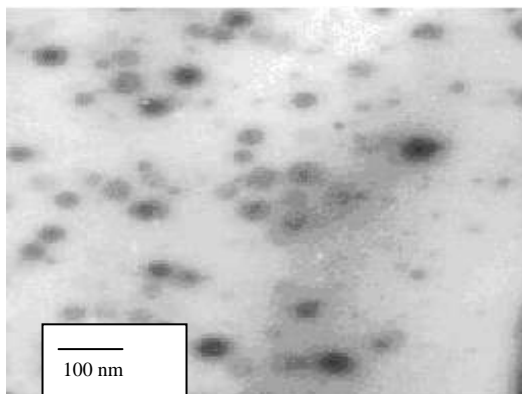


**Figure 5.30: Transmission electron microscope (TEM) image of n-PBMA-g-urethane copolymer tinted with Osmium Tetroxide. (The light regions are soft n-PBMA domains and the dark regions are hard urethane domains).**

## 5.6 References

1. J. Garrett, R. Xu, J. Cho and J. Runt, *Polymer* **44** (2003) 2711.
2. D. Otts, S. Dutta, P. Zhang, O. Smith, S. Thames and M. Urban, *Polymer* **45** (2004) 6235.
3. W. Kuran, M. Sobczak, T. Listos, C. Debek and Z. Florjanczyk, *Polymer* **41** (2000) 8531.
4. S. Dutta, and N. Karak, *Progress in Organic Coating* **53** (2005) 147.
5. R. Jayakumer and S. Nanjundan, *European Polymer Journal* **41** (2005) 1623.
6. S. Guelcher, K. Gallagher, J. Didicr and D. Klinedinst, *Acta/ Biomaterialia* **1** (2005) 471.
7. G. Xu and W. Shi, *Progress in Organic Coating* **52** (2005) 110.
8. E. Tang, G. Cheng and X. Ma, *Powder Technology* **161** (2005) 209.
9. K. Ouzineb, H. Hua, R. Jovanovic, M. Dube and T. Mckenna, *C.R. Chimie* **6** (2003)
10. C. Ma, Y. Du, F. Wang, H. Wang and J. Yang, *Journal of Applied Polymer Science* **83** (2002) 1875.
11. Y. Kim, H. Kim, J. Yoo and J. Hong, *Surface and Coatings Technology* **157**

- (2002) 40.
12. S. Shim, H. Jung, K. Lee, J. Lee and S. Choe, *Journal of Colloid and Interface Science* **279** (2004) 464.
  13. P. Zhou and H. Frisch, *Journal of Polymer Science: Part A: Polymer Chemistry* **30** (1992) 2577.
  14. C. Ma, Y. Du, F. Wang, H. Wang and J. Yang, *Journal of Applied Polymer Science* **83** (2002) 962.
  15. Z. Yin, C. Koulic, C. Pagnouille and R. Je, *Macromolecules* **34** (2001) 5132.
  16. A. Vries, MSc thesis, University of Stellenbosch, Dec. 2001.
  17. Y. Jin, Y. Hahn, K. Nahm, Y. Lee, *Polymer* **46** (2005) 11294.
  18. R. Arun, S. Nanjundan, T. Pakula and M. Klapper, *European Polymer Journal* **40** (2004)1767.
  19. E. Dzunuzovic, S. Tasic, B. Bozic, D. Babic and B. Dunjic, *Progress in Organic Coating* **52** (2005) 136.
  20. S. Asha, M. Thirumal, A. Kavitha and C. Pillai, *European Polymer Journal* **41** (2005) 1343.
  21. S. Kim, K. Lee, H. Jung and S. Shim, *Polymer* **46** (2005) 7974.
  22. C. Boyer, C. Loubat, J. Jacques and B. Boutevin, *Journal of Polymer Science: Part A: Polymer Chemistry* **42** (2004) 5146.
  23. C. Wilkie, *Polymer Degradation and Stability* **66** (1999) 301.
  24. T. Chang, Y. Shen, S. Chiu and H. SY, *Polymer Degradation and Stability* **49** (1995) 353.
  25. A. Pticek, Z. Hrnjak-Murgic, J. Jelencic and T. Kovacic, *Polymer Degradation and Stability* **90** (2005) 319.
  26. T. Chang, Y. Shen, S. Chiu and H. Sy, *Polymer Degradation and Stability* **57** (1997) 7.
  27. Z. Petrovic, Z. Zavargo and J. Flynn, *Journal of Applied Polymer Science* **51** (1994) 1087.
  28. Y. Shieh, H. Chen, K. Liu and Y. Twu, *Journal of Polymer Science: Part A: Polymer Chemistry* **37** (1999) 4126.
  29. A. Pattanayak and S. Jana, *Polymer* **46** (2005) 5183.
  30. F. Wang, PhD thesis, Virginia Polytechnic Institute and State University, April 1998.
  31. B. Elvers, S. Hawkins and W. Russey, *Ullmann's Encyclopedia of Industrial*

- Chemistry, VCH Publishers, New York, **Vol. B6** (1993) 4.
32. E. Wilks, *Industrial Polymer Handbook*, John Wiley and sons, New York **1** (1988) 578.
  33. M. Zeng, L. Zhang, J. Kennedy, *Carbohydrate Polymer* **60** (2005) 399.
  34. B. Elvers, S. Hawkins, G. Schulz, *Ullmann's Encyclopedia of Industrial Chemistry*, John Wiley and sons, New York **21A** (1992) 158.
  35. S. Giraud, S. Bourbigot, M. Rochery, I. Vroman, L. Tighzert and R. Delobel, *Polymer Degradation and Stability* **77** (2002) 285.
  36. K. Mequanint, MSc Thesis, University of Stellenbosch, South Africa, Dec. 1997.
  37. G. Hundiwale, R. Kapadi and V. Pandya, *Journal of Applied Polymer Science* **55** (1995) 1329.
  38. I. Corniglion and B. Pascanlt, *Journal of Polymer Science; Polymer Physics* **34** (1996) 401.
  39. S. Sanchez-Adsuar, M. Pastor-Blas, M. Martin-Martinez, *Journal Adhesion* **67** (1998) 327.
  40. R. Lin and W. Chen, *Journal of Polymer Science* **69** (1998) 1563.
  41. R. Lin and W. Chen, *Journal of Polymer Science* **69** (1998) 1575.
  42. S. Velankar and S. Cooper, *Macromolecules* **31** (1998) 9181.
  43. S. Velankar and S. Cooper, *Macromolecules* **33** (2000) 382.
  44. J. Sheth, A. Aneja, G. Wilkes, E. Yilgor, G. Atilla, I. Yilgor and F. Beye, *Polymer* **45** (2004) 6919.
  45. G. Zhu and Tao Li, *European Polymer Journal* **41** (2005)1090.
  46. J. Garrett and J. Runt, *Macromolecules* **33** (2000) 6353.
  47. A. Hq, H. Liu, D. Huang and S. Guo, *European Polymer Journal* **37** (2001) 497.
  48. S. Thomas and A. George, *European Polymer Journal* **28** (1992) 145.
  49. S. Malaika and W. Kong, *Polymer* **46** (2005) 209.
  50. S. George, N. Neelakantan, K. Varughese and S. Thomas, *Journal of Polymer Science; Polymer Physics* **35** (1997) 2309.
  51. D. Singh, V. Malhotra, J. Vats, *Journal of Applied Polymer Science* **71** (1999) 1959.
  52. [www.psrc.usm.edu/macrog/tq.htm](http://www.psrc.usm.edu/macrog/tq.htm) (accessed22/03/2006).
  53. S. Ioan, G. Grigorescu, A. Stanciu, *European Polymer Journal* **38** (2002) 2295.
  54. R. Jayakumar, Y. Lee and S. Nanjundan, *Polymer Science; Polymer Chemistry* **41** (2003) 2865.

*Chapter 5: Results and discussion*

---

55. R. Jayakumar, Y. Lee and S. Nanjundan, *Journal of Applied Polymer Science* **92** (2004) 710.
56. R. Arun, S. Nanjundan, T. Pakula and M. Klapper, *Polymer Degradation and Stability* **85** (2004) 11.
57. B. Elvers, S. Hawkins and G. Schulz, *Ullmann's Encyclopedia of Industrial Chemistry*, John Wiley and sons, New York, **21A** (1992) 45.

## Chapter 6

### Conclusions and Recommendations

#### 6.1 Conclusions

- Urethane macromonomers were successfully synthesized by the polyaddition of toluene diisocyanate (TDI) and ethylene glycol (EG) by the pre-polymer method, and successfully terminated by 2-hydroxy ethyl methacrylate (HEMA) and isopropanol to yield UMs having different urethane chain lengths (X) of X= 4, 8, 12 and 32, and predominantly monofunctional (using 0.4 to 0.6 HEMA/isopropanol) .
- The unreacted UM could be easily removed in three precipitations from methanol.
- Three different synthesis methods were used to obtain the desired structure of urethane macromonomers (where HEMA reacts from one side and isopropanol reacts from the other side). In the first method HEMA was added to urethane prepolymer all at once, followed by the addition of isopropanol. In the second method HEMA was added dropwise to the urethane prepolymer, followed by isopropanol. In the third method HEMA and isopropanol were added together to urethane prepolymer, in fractions. The first method was considered the best method; it gave the highest yield of both graft copolymers: PMMA-g-urethane and PBMA-g-urethane.
- The molecular structures of the urethane macromonomers were confirmed by FTIR, <sup>1</sup>H NMR, <sup>13</sup>C NMR and GPC.

The thermal stability of the urethane macromonomer improved slightly as the urethane chain length (X) increased, as confirmed by the TGA technique.

Compatibility between segments of the urethane macromonomers was detected by DMA. All urethane macromonomer samples showed a single T<sub>g</sub>, which indicated that segments of UM were completely compatible. It was also found

that as the urethane chain length increased the T<sub>g</sub> of the urethane macromonomer increased as expected.

- The PMMA-g-urethane and n-PBMA-g-urethane copolymers were successfully synthesized by the macromonomer technique in solution free radical polymerization (in which AIBN was used as initiator and DMF as solvent). The obtained graft copolymer molecular structures were fully characterized by GPC with double detectors (UV and RI), <sup>1</sup>H NMR, <sup>13</sup>C NMR and FTIR, after removing nonfunctional as well as unreacted UM.

It was found that as the concentration of the urethane macromonomers in the free radical copolymerization feed increased, the yield was lower (as more nonfunctional UM can be extracted). On the other hand, it was also found that as the concentration of urethane macromonomer in free radical copolymerization feed increased more urethane was incorporated into the PMMA and PBMA backbone. It was also found that as the chain length of urethane macromonomer increased the yields of both graft copolymers PMMA-g-urethane and PBMA-g-urethane were lower. This result was confirmed by GPC with UV detectors, <sup>1</sup>H NMR, <sup>13</sup>C NMR, and FTIR after removal of nonfunctional or unreacted UM after polymerization.

In most of the graft copolymers PMMA-g-urethane and PBMA-g-urethane it was possible to determine the percentage of UM that was incorporated into the acrylate backbone quantitatively by <sup>1</sup>H NMR spectroscopy. The results showed that as the concentration of UM increased in the solution free radical polymerization feed, a higher percentage of UM were incorporated in both graft copolymers, PMMA-g-urethane and PBMA-g-urethane.

It was found that the thermal stability of PMMA-g-urethane and PBMA-g-urethane copolymers improved, as the amounts of urethane macromonomer increased in the polymerization feed. Also, the better thermal stability was found in both PMMA-g-urethane and n-PBMA-g-urethane as the chain length of the UM increased.

## *Chapter 6: Conclusions and recommendations*

---

- In most of the PMMA-g-urethane and n-PBMA-g-urethane copolymers a large measure of compatibility was observed. This result was confirmed by the DMA technique. In the PMMA-g-urethane the  $T_g$  values decreased as the concentration of urethane macromonomer increased in the copolymerization feed. In contrast, the  $T_g$  increased as the concentration of urethane macromonomer increased in n-PBMA-g-urethane copolymer.
- In the case of one n-PBMA-g-urethane copolymer, two glass transitions at temperatures of 22.0 and 76.0 °C were observed, corresponding to the n-PBMA and urethane fractions, respectively. The result also indicates that PBMA and urethane moieties exhibit microphase separation. This result was found when the chain length of the urethane macromonomer was increased from  $X=4$  to  $X=32$ , and the amount of this UM used in the copolymerization feed was increased from 0% to 40%. This result was confirmed by DMA and TEM images.
- This work showed that even incompatibility phases will mix or only show nanophases separation when chain lengths are shortened.

### **6.2. Recommendation and future work**

- To improve the desired properties obtained from the synthesized urethane macromonomers especially in terms the monomers used to make urethane less compatible.
- Investigate possible applications for PMMA-g-urethane and PBMA-g-urethane products both in compatible and incompatible forms.
- Find another way to optimize desired structure from urethane macromonomer.
- Synthesize the graft copolymers in emulsion for use as coating and glues.

***Appendix A: Calculation of the molecular weight of PMMA and n-PBMA homopolymers***

The molecular weight of PMMA and n-PBMA was calculated by using equation A.1

$$M_w = M_{w_0} \cdot DP_n \quad (A.1)$$

Where:

$M_w$  = molecular weight of PMMA or n-PBMA homopolymer

$M_{w_0}$  = molecular weight of MMA (100) or n-BMA (143)

$DP_n$  = average degree of polymerization

The average degree of polymerization ( $DP_n$ ) in solution free radical polymerization can be expressed as:

$$1/DP_n = C_s[S] / [M]$$

Where

$C_s$  = solvent transfer constant (DMF),  $C_s$  at 70 °C =  $5 \cdot 10^{-4}$  and  $4.38 \cdot 10^{-4}$  for PMMA and n-PBMA respectively

[S] = concentration of solvent (DMF: 35g/ml).

[M] = concentration of monomers (MMA or n-BMA: 5g/l).

From equation A.1 the theoretical molecular weight of PMMA = 28532g/mol and the theoretical molecular weight of n-PBMA = 32165 g/mol

***Appendix B: Article Submitted To POLYMER JOURNAL***